1-1-1996

Multiple forms of carboxylesterase from Leptinotarsa decemlineata hemolymph associated with permethrin resistance.

Sihyeock Lee
University of Massachusetts Amherst

MULTIPLE FORMS OF CARBOXYLESTERASE FROM *LEPTINOTARSA DECEMLINEATA* HEMOLYMPH ASSOCIATED WITH PERMETHRIN RESISTANCE

A Dissertation Presented
by

SIHYEOCK LEE

Submitted to the Graduate School of the
University of Massachusetts Amherst in partial fulfillment
of the requirements for the degree of

DOCTOR OF PHILOSOPHY

February 1996

Entomology

MULTIPLE FORMS OF CARBOXYLESTERASE FROM *LEPTINOTARSA DECEMLINEATA* HEMOLYMPH ASSOCIATED WITH PERMETHRIN RESISTANCE

A Dissertation Presented
by

SIHYEOCK LEE

Approved as to style and content by:

J. Marshall Clark, Chair

Chih-Ming Yin, Member

John H. Nordin, Member

Robert E. Levin, Member

T. Michael Peters, Department Head
Entomology

DEDICATION

To my parents, and to my wife and daughter, for their love, support, and patience.

ACKNOWLEDGEMENT

First of all, I would like to express my deep thanks to my supervisor, Dr. John M. Clark, for his continuous guidance, advice, encouragement, and support. I would also like to thank my dissertation committee members, Drs. Chih-Ming Yin, John. H. Nordin, and Robert E. Levin for their valuable inputs and discussions. I would specially like to thank Dr. Kunyan Zhu, Daniel Tessier, and Andy Curtis for their help in experiments and valuable discussion. I would like to thank Steve Symington for his assistance in computer graphics, etc. I would also like to thank Maggie Malone, Amity Lee-Bradley, and Julia Connelly, Liz Chapin, and Stephen Marvell for the assitance with the paper works over the years. Finally, I would like to wish Dan Tessier, Raymond Putnam, Gerard Roy, Steve Symington, and Jessica Dunn the best luck in their ongoing projects.

ABSTRACT

MULTIPLE FORMS OF CARBOXYLESTERASE FROM *LEPTINOTARSA DECEMLINEATA* HEMOLYMPH ASSOCIATED WITH PERMETHRIN RESISTANCE

FEBRUARY 1996

SIHYEOCK LEE, B.S., SEOUL NATIONAL UNIVERSITY, KOREA

M.S., SEOUL NATIONAL UNIVERSITY, KOREA

Ph.D., UNIVERSITY OF MASSACHUSETTS AMHERST

Directed by: Professor J. Marshall Clark

The purpose of this dissertation is to purify and characterize the carboxylesterase(s) associated with permethrin resistance in the permethrin-resistant (PE-R) strain of Colorado potato beetle (CPB), *Leptinotarsa decemlineata*, and to develop an immunoassay system for the detection of resistance in field populations of CPB.

Most carboxylesterase (CbE) activity is found in the hemolymph and the soluble fraction of body tissue. Among a number of charged forms of CbE identified from hemolymph, the p*I* 4.5-4.8 CbEs are quantitatively elevated and are most responsible for permethrin resistance in the PE-R strain.

Permethrin CbEs (i.e., p*I* 4.2-4.8 CbEs) have been purified from the hemolymph of the PE-R strain through several chromatographic procedures. The p*I* 4.8 CbE is a 46-48 kDa monomeric protein. The p*I* 4.5 CbE is likely a 57-59 kDa dimeric protein. All p*I* 4.5-4.8 forms are glycoproteins but the charge heterogeneity is not associated with *N*-glycan moieties. Biochemical properties of the p*I* 4.2-4.5 CbEs have been comparatively characterized through substrate kinetic analyses, specific inhibition studies, and pH-temperature experiments. The p*I* 4.8 and 4.5 CbEs share a number of

similarities in their biochemical properties and functional role in resistance despite of their distinct molecular properties.

The kinetics of inhibition of the p*I* 4.5-4.8 CbEs by permethrin and DDT are best described by a mixed-noncompetitive type and a noncompetitive type inhibition, respectively. The kinetic analyses indicate the presence of hydrophobic non-catalytic site(s) as well as hydrophobic catalytic site(s) that are available for the binding to hydrophobic insecticides. Along with a low level of permethrin hydrolysis, the hydrophobic binding nature of the p*I* 4.5-4.8 CbEs suggests that permethrin resistance is mainly conferred by sequestration rather than rapid hydrolysis of permethrin. The nonspecific sequestration by the p*I* 4.5-4.8 CbEs appears to be associated with the cross-resistance of the PE-R strain to other hydrophobic insecticides such as other pyrethroids, DDT, and abamectin.

Polyclonal antisera have been generated against the 30, 48, and 60 kDa denatured CbE immunogens. A high degree of cross-reactivities of the antisera to different immunogens indicate that all CbE immunogens share a high level of structural similarity. An antibody capture immunoassay using denatured CPB hemolymph is shown to be effective in detecting the different levels of permethrin CbE in permethrin-resistant and -susceptible populations of CPB.

TABLE OF CONTENTS

LIST OF FIGURES

CHAPTER I

INTRODUCTION

A. Objectives

The objectives of this dissertation are twofold. The first objective is the isolation, purification, and characterization of the permethrin-sequestrating and hydrolyzing carboxylesterases (CbE) associated with permethrin resistance in a nearly isogenic permethrin-resistant (PE-R) strain of Colorado potato beetle (CPB). The second objective is the development of an immunoassay system for the detection and validation of permethrin resistance in field populations of CPB using polyclonal antibodies raised against the purified CbE.

B. Colorado Potato Beetle

The Colorado potato beetle, *Leptinotarsa decemlineata* (Say), is one of the most harmful pest of solanaceous crops including potatoes, tomatoes, and eggplant. Since it has rapidly developed resistance to all major classes of insecticides, control failure of CPB has been a main limiting factor in solanaceous crop production (1). Although CPB resistance has been a particularly serious problem in the northeastern United States, it is now widespread in the midwest (2) and western United States (3).

In the late 1970s, pyrethroids were used widely in the control of CPB, particularly in the Northeast where resistance to organochlorine, organophosphate, and carbamate insecticides was wide spread and severe (4, 5). Extensive use, however, resulted again in high levels of resistance in CPB populations to pyrethroids (6). Although CPB

populations are highly resistant to fenvalerate in New York and some other eastern states, resistance to permethrin and other pyrethroids is still moderate in Massachusetts (7), most western states, and world-wide (8). To utilize this valuable group of insecticides to their full potential, it is necessary to establish efficient resistance management programs for CPB based on rapid, accurate, and sensitive resistance detection methods when the frequencies of resistance genes are still low in the field population. In order to develop an effective resistance detection system, a complete understanding of overall resistance mechanisms is necessary both at the biochemical and molecular basis.

Despite the significance and ramification of pyrethroid resistance of CPB, little information exists on the biochemical and molecular genetic factors that resulted in its development. Permethrin resistance in field and laboratory populations (MA-R and PE-R strains, respectively) of CPB was determined to be sex-linked and incompletely recessive (7). Permethrin resistance in the near isogenic PE-R strain was determined to be due principally to increased esterase activity (i.e., permethrin carboxylesterase) and possibly site insensitivity (e.g., cross-resistance to DDT)(9,10). Sex-linkage of resistant traits is very important in resistance development because it creates a situation where recessive alleles can be functionally dominant, leading to an accelerated resistance development. In both field and computer simulation studies, resistance to permethrin evolved in only 4 generations because of sex-linkage even though the resistant factor was determined previously to be incompletely recessive (11, 12).

A considerable amount of information on the biochemical and molecular mechanisms of resistance exists for dipterans because of their medical importance, convenience of rearing, and the large volume of background information on genetics (13). However, information on resistance mechanisms in dipterans may not be a suitable model for herbivorous insects such as CPB because overall aspects in the metabolism and detoxification of xenobiotics in herbivorous insects are greatly different

from non-herbivorous insects (14). Under the constant selection pressure by toxic secondary compounds, herbivorous coleopterans have been shown to evolve unique digestive enzyme systems that may play a crucial role in detoxification of insecticides and in insecticide resistance (15). This may be particularly true in CPB because solanaceous plants, the host cultivar for CPB, contain highly toxic secondary compounds such as steroidal glycoalkaloids (e.g., solanine, chaconine, tomatine) etc.

CPB has successfully evolved specific enzymes, including carboxylesterases, for the endogenous detoxification of these plant toxins. Recently, CPB has apparently employed them as resistance mechanisms against the toxic action of insecticides. From this point of view, information obtained from the studies of resistance mechanism in CPB would be much more valuable in predicting resistance mechanisms in other herbivorous pests, especially coleopterans.

CPB has not been proven to be a particularly efficient molecular genetic model in studying resistance because of its relatively long generation time, complex dietary needs, and relatively large genome size (approx. 13-times larger than *Drosophila,* personal communication J. Stewart, Purdue University). Nevertheless, biochemical and molecular genetic studies with CPB are justified due to its status as one of the most insecticide-resistant pests identified to date. CPB has shown multiple and cross-resistance to all five major groups of insecticides and most recently to *Bacillus thuringiensis* and abamectin, two of the most promising new insecticidal compounds. Thus, investigations on the insecticide resistance mechanisms of CPB are necessary and meaningful, despite their relative difficulty.

C. Esterases Involved in Insecticide Resistance

Esterases are involved in a variety of endogenous metabolic reactions in insects including degradation of neurotransmitters (e.g., acetylcholinesterase), endocrine control (e.g., juvenile hormone esterase), and detoxification of foreign compounds (e.g., serum, fat body, and midgut esterases) (16-18).

Insecticide detoxification and sequestration mechanisms by esterases are perhaps the best understood means by which insects become resistant. Enhanced esterase activity has been reported to be strongly associated with organophosphate (OP) resistance in many insect species. Early studies by Welling and Blaakmeer (19) on OP-resistant strains of housefly, *Musca domestica*, revealed that a microsomal CbE was associated with malathion-resistance. This CbE was susceptible to metal ion inhibition and to many oxon-analogues of OP insecticides. Needham and Sawicki (20) found that OP resistance in the peach-potato aphid, *Myzus persicae,* was associated with an increase in the level of total CbEs. Electrophoretic analysis of several resistant strains of *M. persicae* revealed that this increase was solely attributed by a single CbE (21). This CbE was demonstrated later to function as an OP-hydrolyzing enzyme (22). High levels of α-naphthyl acetate (αNA) hydrolysis found in OP-resistant strain of *M. persicae* were also reported to be associated with resistance and to be due to the enhanced activity of a single esterase (i.e., E4). The identical kinetic properties of purified E4 from both resistant and susceptible strains implied that an overproduction of E4 was responsible for the resistance rather than any structural alteration of enzyme itself (23). Studies on the biochemical mechanisms of malathion resistance in two mosquito species, *Anopheles stephensi* and *A. arabiensis*, showed that increased levels of malathion hydrolysis were associated with resistance in spite of no differences in the rate of hydrolysis of αNA and β-naphthyl acetate (βNA) between the resistant and susceptible strains (24, 25). Similarly, a malathion-resistant strain of *Culex tarsalis*

showed greatly elevated malathion hydrolysis but little increase in the hydrolysis of α NA (26). Ashour *et al.* (27) reported on a CbE from a malathion-resistant strain of *Drosophila* that was involved in malathion resistance. A 120 kDa soluble esterase from parathion-resistant *Heliothis virescens* was demonstrated to efficiently hydrolyze paraoxon (28). Resistance to malathion in a strain of the Australian sheep blow fly, *Lucilia cuprina,* was reported to be due to the higher level of malathion hydrolysis activity by a quantitatively increased CbE (29).

Esterase-mediated resistance mechanisms are also well documented in pyrethroid resistance in a variety of arthropod species. An esterase hydrolyzing two enantiomer of permethrin was found in crude homogenates of southern armyworm, *Spodoptera eridania* (30). Devonshire and Moores (31) reported that a CbE (i.e., E4) with broad substrate specificity caused OP, carbamate, and pyrethroid resistance in *M. persicae*. A pyrethroid-resistant strain of the Egyptian cotton leafworm, *Spodoptera littoralis,* was found to possess 3-6.5 times higher levels of pyrethroid hydrolytic activity compared to the susceptible strain (32). De Jersey *et al.* (33) isolated a 67 kDa esterase from *Boophilus microplus* that hydrolyzed cypermethrin, an α-cyano-containing pyrethroid. Chang and Whalon (34) reported that CbE-type detoxification system played an important role in pyrethroid resistance of a resistant strain of predacious mite, *Amblyseius fallacis*. Delorme *et al.* (35) found that the hydrolysis of deltamethrin in a deltamethrin-resistant strain of *Spodoptera exigua* was 17 times higher than in the susceptible strain. An elevated level of esterase in the mosquito, *Anopheles albimanus*, was shown to confer cross-resistance between fenitrothion, an organophosphate, and deltamethrin, a pyrethroid (36). Enhanced CbE activity was also determined to be primarily associated with permethrin resistance in the permethrin-resistant strain of CPB (i.e., PE-R strain, 9). Although most pyrethroid-hydrolyzing esterases have been categorized as carboxylesterases, a permethrin hydrolase from soybean looper, *Pseudoplusia includens*, was suggested to be a possible aminopeptidase

because it required both metal ion and free sulfhydryl groups for catalysis but was still inhibited by typical serine hydrolase inhibitors (e.g., DFP, paraoxon, etc.)(37).

Enhanced esterase activity is generally associated with an overproduction of the enzyme, itself. However, any qualitative change within the structure of the enzyme may result in more efficient insecticide-hydrolyzing activity by improving its kinetics. Kao et al. (38) reported that enhanced malathion hydrolysis found in a resistant strain of house fly, *M. domestica*, was primarily due to a structurally-modified esterase. A qualitatively altered esterase capable of hydrolyzing malathion more rapidly was also reported in a resistant strain of predacious mites, *amblyseius pontentillae* (39).

In addition to enhanced hydrolysis of insecticides, overproduced esterases have been reported to function as sequestration enzymes in some insects such as the OP-resistant aphid *M. persicae* (31), the mosquito *Culex quinquefasciatus* (40), and *Culex pipiens* (41). These overproduced esterases were demonstrated to protect the insects by sequestering insecticides. Sequestration was accomplished by having an esterase with very low turnover rate rather than rapidly hydrolyzing them. The overproduced CbE in *M. persicae* was also suggested to confer cross-resistance to pyrethroids through sequestration by a reversible binding to the catalytic site. The mechanisms for esterase overproduction in these three insect species (i.e., *M. persicae, C. quinquefasciatus, and C. pipiens*) have been determined to be due to gene amplification (42-44). However, the only actual mechanistic information on how insecticide-resistant genes are regulated is the report of changes in methylation levels on the E4 gene amplification unit of peach-potato aphid, *M. persicae* (45).

D. Significance

A number potential benefits can be obtained from understanding the biochemical and molecular genetic mechanisms of insecticide resistance in CPB. Information gained from this dissertation will allow: 1) the development of efficient resistance detection methods; 2) the determination of possible fitness disadvantage, and eventually; 3) establishment of an effective resistance management system for CPB that will result in the extended use of pyrethroids, a particularly effective and environmentally-sound group of insecticidal products.

To effectively prevent the development of resistance in CPB, rapid, accurate, and sensitive monitoring methods are necessary to detect resistance genes at low frequency in field populations. Traditional bioassay techniques require large numbers of individuals to detect resistance in field populations. Moreover, bioassay is often impossible because of sampling constraints and the expense involved in terms of time and energy (46).

An enzyme assay has been developed recently to detect the field resistance of *M. persicae*. Detection of resistant individuals of *M. persicae* by enzyme assay is possible because the E4 esterase can efficiently hydrolyze general naphthyl substrates such as α NA. This assay was useful because the E4 esterase was overexpressed to the extent that it make up 3% of the total protein of the insect. Generally, assessment of the activity of esterase using general substrates has the disadvantages of relatively low selectivity and sensitivity because the activity of esterases associated with resistance is often overwhelmed by the activity of other more abundant esterases. Furthermore, since general CbE activities often do not correlate directly with the level of resistance in many cases (24, 25), enzyme assays using general substrates can only be developed for the situations where resistance is positively correlated with enzyme activity.

In contrast, immunoassays based on antibodies raised against esterases associated with resistance have been considered to be more efficient because of their higher sensitivity and specificity (47, 48). An additional benefit of monitoring the level of the overproduced esterase involved in resistance by immunoassay was that the antibodies raised against the organophosphate-resistant CbE extended detection to carbamate- and pyrethroid-resistant aphids due to the broad substrate specificity of this esterase (31). If this is generally the case, antibodies generated against the CbEs responsible for permethrin resistance in CPB would not only insure the rapid and accurate detection of permethrin resistance in field populations but they could also be used to detect cross-resistance associated with other pyrethroids and perhaps other carboxylester-containing insecticides. Moreover, esterases can be easily purified and kinetically characterized, making them particularly suited to serve as immunogens for the production of antibodies.

Understanding of resistance mechanism may also enable us to elucidate the biochemical nature of fitness disadvantages often associated with insecticide resistance. Fitness disadvantage associated with resistance can delay the development of resistance significantly when insecticide mixtures or rotation strategies are employed (49). Although permethrin resistance was determined not to cause any significant fitness disadvantage when evaluated by some parameters such as fecundity, fertility, development time, etc., certain meaningful fitness differences may not be easily identified with these parameters (50). By evaluating the endogenous function of the esterase and understanding the biochemical and molecular nature of resistance, a more complete assessment of the fitness disadvantage associated with the resistant esterase can be made and ways to exploit it as an efficient resistance management strategy can be implemented.

Once the CbE associated with permethrin resistance (i.e., permethrin CbE) is isolated, purified, and amino acid-sequenced, identification of the esterase gene through

molecular cloning and sequencing technologies could be attempted using standard techniques. Two CbEs associated with insecticide resistance in *Culex* and *Myzus*, respectively, have been isolated, amino acid-sequenced and the genes cloned (51, 52). Along with the amino acid sequence of the permethrin CbE from CPB, nucleic acid sequence information on the amplified CbE genes from *Culex* and *Myzus* will be quite useful in the molecular cloning and sequencing of the permethrin CbE gene of CPB. The availability of a molecular clone of the permethrin CbE gene and its regulatory sequences would enable to analyze the basic molecular processes resulting in resistance mechanisms such as gene amplification, allelic selection, and enzyme induction. If gene amplification is determined to be involved in permethrin resistance in CPB and to be unstable as in the case of *Myzus*, it will provide valuable information for understanding resistance development in CPB. Since gene amplification and its associated instability can occur at very high frequency, it could not only enable resistance to arise quickly but also to show flexibility in response to selection pressure. This basic information is absolutely necessary when constructing a resistance management strategy since alternate use of insecticides may efficiently suppress the esterase gene amplification associated with permethrin resistance, etc.

CHAPTER II

MATERIALS AND METHODS

A. Materials

1. Insect Strains

The susceptible (SS) strain of Colorado potato beetle (CPB, *Leptinotarsa decemlineata* Say) was originally provided by Dr. G. G. Kennedy (North Carolina State University, Raleigh, NC) and has been maintained in our laboratory for the past 7 years. The near isogenic permethrin-resistant (PE-R) strain (7) has been continuously selected every 3-4 month by topically applying permethrin to 4th instars or by immersing adults in a permethrin solution. In the case of selection by topical application, 200-300 4th instars (average body weight ca. 100 mg) were treated with a discriminating dose of permethrin (i.e., 1.0 μg/larva). The survival rate after 24 hrs was 30-50%. For the selection of adults by immersion, 50-150 adults (2-3 day-old) were immersed in 500 ppm permethrin solution [1 part acetone : 9 parts 0.1% Triton X-100 (reagent grade I) in double distilled water (ddH_2O)] for 1 min. The resulting survival rate after 24 hrs was 20-30%. In both cases, individuals that were alive 24 hrs post-treatment were collected and allowed to reproduce. A permethrin-resistant field resistant strain from Maryland (Mar-R) was provided by Dr. G. P. Dively (University of Maryland, College Park, MD). A field susceptible strain from Maine (Mai-S) was provided by Dr. R. A. Alford (University of Maine, Orono, ME). All strains were reared in aluminum and fiberglass screen cages (66 × 91 × 50 cm) and fed with yellow potato plants (Superior, Katahdin or Russet, *Solanum tuberosum* L.). The rearing conditions were 27 ± 2°C, 50-85% RH, and a photoperiod of 16:8 (L:D).

2. Chemicals

[^{14}C]*trans*-permethrin (methylene-labeled, specific activity 57 μCi/μmole) and cypermethrin (95% > purity) were gifts from FMC, Princeton, NJ. Permethrin (93% purity) was obtained from ICI, Goldsboro, NC. DDT (99% purity), *S*,*S*,*S*-tributyl phosphorotrithioate (DEF, 98% purity), azinphos-methyl (96% purity), and piperonyl butoxide (PBO, 99.2% purity) were purchased from Chem Services, West Chester, PA. Parathion (99.9% purity) was obtained from EPA, Research Triangle Park, NC. Abamectin was a gift from Merck Sharp & Dohme Research Lab, Rahway, NJ. [^{3}H]diisopropylfluorophosphate (DFP, specific activity 6.0 mCi/μmole) was purchased from New England Nuclear, Boston, MA. All chromatographic media were purchased either from Sigma Chem. Co., St. Louis, MO, Bio-Rad, Hercules, CA, or Pierce, Rockford, IL. Additional biochemicals were purchased from Sigma Chem. Co., except when stated otherwise.

B. Methods for Identification and Distribution of Permethrin Carboxylesterase

1. Preparation of Tissue Fractions

Four tissue fractions (i.e., hemolymph, nucleolar-mitochondrial fraction, microsomal fraction, and soluble fraction) from 4th instars of the SS or PE-R strains of CPB were examined as possible sources of permethrin CbE. For large scale hemolymph collection, twenty-five 4th instars (body weight ca. 150 mg) were placed into a 25 ml disposable syringe barrel that was placed into a 50 ml plastic centrifuge tube. The larvae were centrifuged at 1,500 × g for 5 min at 4°C to remove gut content and saliva. The centrifuged larvae were rinsed with ice-chilled isolation buffer (50 m*M* imidazole containing 0.05% phenylthiourea, pH 7.4) and a longitudinal cut (i.e., 3-4 mm) was made on the lateral cuticle of larva using dissecting scissors. The larvae were

placed into a clean 25 ml disposable syringe barrel with glass wool, presoaked with isolation buffer, packed into the bottom. The syringe barrel with larvae was subsequently placed into a 50 ml centrifuge tube and centrifuged at 3,000 × g for 10 min at 4°C. Following centrifugation, the hemolymph was collected from the bottom of the centrifuge tube, placed into a clean centrifuge tube, and centrifuged at 10,000 × g for 10 min at 4°C to precipitate haemocytes and other debris. The supernatant was carefully decanted and used as the hemolymph (HAE) tissue fraction.

The nucleolar-mitochondrial (NMT), microsomal (MIC), and soluble (SOL) fractions were prepared by differential centrifugation of the hemolymph-depleted bodies. The hemolymph-depleted bodies were rinsed twice with ice-chilled isolation buffer to remove any remaining hemolymph and homogenized in isolation buffer (i.e., 25 bodies per 5 ml buffer) on ice using a motor-driven Potter-Elvehjem homogenizer (50 strokes at 600 rpm). The homogenate was filtered through glass wool, centrifuged at 10,000 × g for 10 min at 4°C, and the supernatant (S1) and pellet (P1) collected. The P1 pellet was re-homogenized in 2 ml of isolation buffer containing 0.5% Triton X-100. Following a 40 min interval, the resuspended pellet was centrifuged again at 10,000 × g for 10 min, and the supernatant collected as the NMT tissue fraction. The S1 supernatant was centrifuged at 105,000 × g for 40 min. The resulting supernatant (S2) was designated as the SOL tissue fraction. The pellet (P2) was re-homogenized in 1 ml of isolation buffer containing 0.5% Triton X-100. Following a 40 min interval, the resuspended P2 pellet was centrifuged at 105,000 × g for 40 min. The resulting supernatant (S3) was used as the MIC tissue fraction.

2. Evaluation of α-Naphthyl Butyrate (αNB) and Permethrin Hydrolysis Associated with the HAE, NMT, MIC, and SOL Tissue Fractions

The assay procedure for αNB hydrolysis (53) was modified for a microtiter plate format. Each tissue fraction was appropriately diluted (e.g., 40-fold dilution for HAE,

4-fold for NMT and MIC, and 10-fold for SOL) so that the final optical density (OD) was in the range of 0.1 to 1.0 absorbance unit. Five µl of each diluted sample was preincubated with 100 µl of inhibitor solution [0.25 m*M* ρ-hydroxymercuribenzoate (PHMB) and 0.25 m*M* eserine dissolved in reaction buffer (50 m*M* sodium phosphate, pH 7.2)] at 32°C for 10 min in each well of a 96-well microtiter plate. A 100 µl aliquot of substrate solution (0.25 m*M* αNB in reaction buffer) was added and the reaction mixture was further incubated for 3 min. Fifty µl of stop solution (3.4% SDS/4% dianisidine in ddH_2O) was added to stop the reaction. After 10 min, OD_{600} was measured using a microplate reader (UV-Max, Molecular Devices Co., Palo Alto, CA). The hydrolysis rate was calculated using a six-point naphthol calibration curve (e.g., 40, 50, 75, 125, 250, and 500 µ*M* α-naphthol).

Permethrin hydrolysis was assessed using the method of Argentine *et al.* (9) with a slight modification. Two µl of a piperonyl butoxide solution (PBO, 20 m*M* in acetone) was added to 400 µl of each diluted sample fraction (i.e., 7-fold dilution for HAE, 3-fold for NMT, 2-fold for MIC and 4-fold in SOL) held in an 1.5 ml microfuge tube and the mixture incubated at 32°C for 7 min. Four µl of [^{14}C]*trans*-permethrin (4.6 nCi, 0.2 µM final assay conc.) was added to the reaction mixture and incubated for an additional 60 min. The reaction was terminated by mixing with 100 µl of a 20% trichloroacetic acid (TCA) solution. The resulting assay mixture was centrifuged at 12,590 × g for 5 min and the supernatant transferred to a clean 1.5 ml microfuge tube. The supernatant was extracted sequentially with three 1 ml aliquots of chloroform. The pellet was extracted sequentially with 0.5 ml of hexane and 0.5 ml of methanol. The extracts were combined into a 10 ml glass tube and reduced just to dryness under a stream of N_2 (N-Evap Model 111, Organomation Associate Inc., South Berlin, MA). The residues were resolubilized in 200 µl of methanol-acetone mixture (1:1) and a 50 µ l aliquot was applied onto a K5F silica TLC plate (20 × 20 cm, Whatman Inc., Clifton, NJ). The TLC plate was developed in a solvent system of benzene : ethyl acetate

(6:1) until the solvent front reach to within 1 cm from the top of the plate (ca. 40 min). The radioactivity associated with various metabolites was detected and quantified using Berthold Model LB2820-1 linear analyzer/TLC scanner (Berthold Instruments Inc., Nashua, NH).

3. Inhibition of Hemolymph Esterases by Permethrin

Solutions containing permethrin plus substrate (i.e., αNB) were prepared by mixing one part of the serially-diluted permethrin stock solutions (0, 1.6, 3.2, 6.3, 12.5, 25, 50 and 100 m*M* in acetone) with 99 parts of αNB solutions [0.125 or 0.25 m*M* in reaction buffer (50 m*M* sodium phosphate containing 0.05% Triton X-100, pH 7.2)]. After vigorous vortexing to disperse permethrin evenly, a 100 µl aliquot of the mixture was transferred into each well of a 96 well-microtiter plate. High concentrations of permethrin (e.g., when the 100, 50, and 25 m*M* stock solutions were used), however, resulted in milky emulsions. The hemolymphs from the SS and PE-R strains were diluted 30-fold with reaction buffer. At this dilution, the control levels of αNB hydrolysis activities in the PE-R and SS hemolymphs were ca. 0.65 and 0.26 OD_{600}, respectively. To equalize the final levels of αNB hydrolysis activity, each hemolymph sample was diluted appropriately (i.e., 75-fold for PE-R *vs*. 30-fold for SS to adjust the final levels of activity to ca. 0.26 OD_{600} or 33-fold for PE-R *vs*. 13-fold for SS to adjust the final levels of activity to ca. 0.65 OD_{600}). One part of the appropriately diluted hemolymph was mixed with 9 parts of inhibitor solution (0.25 m*M* PHMB and 0.25 m*M* eserine in reaction buffer) and preincubated at 32°C for 10 min. After preincubation, 100 µl of the reaction mixture was immediately transferred to each well of the microtiter plate containing various concentrations of permethrin-αNB solutions and incubated at 32°C for 5 min. After terminating the reaction by the addition of 50 µl of stop solution (3.4% SDS/4% dianisidine in ddH_2O), the level of αNB hydrolysis was measured as described previously.

4. Polyacrylamide Gel Electrophoresis (PAGE) of Hemolymph

Hemolymphs from the SS and PE-R strains were electrophoresed on a 1.0 mm-thick native polyacrylamide gel (7.5% separating gel in 0.375 *M* Tris-HCl, pH 8.8; 4% stacking gel in 0.125 *M* Tris-HCl, pH 6.8) using the Mini-Protein II system (Bio-Rad, Hercules, CA). Hemolymph was centrifuged in a 1.5 ml microfuge tube at 12,590 × g for 5 min at 4°C to remove any insoluble particulate. One part of the hemolymph supernatant was mixed with four parts of the sample buffer (62.5 m*M* Tris-HCl, 10% glycerol, 125 ppm bromophenol blue, pH 6.8). Paired hemolymph samples of the SS and PE-R strains (i.e., 25 µl each, ca. 100 µg total protein) were electrophoresed at 200 V constant voltage for 45 min at 4°C side by side on the gel using Tris-glycine running buffer system. Following electrophoresis, the gel was cut longitudinally so that each section contained one pair of samples (i.e., SS and PE-R). In this way, each section could be stained with Coomassie brilliant blue for protein determination and the other identical section could be stained for CbE hydrolytic activity. In CbE activity staining, the gel was equilibrated in ice-chilled 40 m*M* Tris-HCl buffer (pH 6.6) for 10 min and then preincubated in the inhibitor solution (40 m*M* Tris-HCl containing 0.1 m*M* PHMB and 0.1 m*M* eserine, pH 6.6) for 10 min prior to incubating in the substrate-staining solution (40 m*M* Tris-HCl containing 0.1% dianisidine and 0.05% α NB or αNC, pH 6.6) for 10-20 min. After staining, the background was removed by destaining the gel with 10% acetic acid solution for 30 min. The gel was then dried between two sheets of cellulose membrane (Promega, Madison, WI). The band intensities of the gel were analyzed using a scanning densitometer (Model GS300, Hoefer Scientific Instruments, San Francisco, CA).

5. Isoelectricfocusing (IEF) Gel Electrophoresis of Hemolymph

Hemolymph CbEs were separated by non-denaturing IEF [6.5% polyacrylamide, 10% glycerol, 2.4% Bio-Lyte 3/10 (Bio-Rad)] using a vertical slab gel (Mini-Protein

II, Bio-Rad). Each hemolymph sample was mixed with one volume of sample buffer (15% glycerol, 6% Bio-Lyte 3/10, 2% glycine) and applied to a prefocused gel (5 W for 30 min). Hemolymph samples were electrophoresed at 10 W for 90 min in a buffer system of 20 m*M* NaOH (i.e., catholyte) and 20 m*M* acetic acid (i.e., anolyte). Following IEF, the gel was stained and processed in the same manner as for native PAGE.

6. Chromatofocusing of Hemolymph

Aliquots of the SS and PE-R hemolymph, each containing 21 mg of total protein, were separated using a chromatofocusing column (PBE94 ion exchanger, Pharmacia, Uppsala, Sweden). Hemolymph (i.e., 1.5 ml of the SS hemolymph; 1.59 ml of the PE-R hemolymph) was applied to a chromatofocusing column (1.0 x 30 cm, V_t = 24 ml) that had been equilibrated with 25 m*M* imidazole buffer (pH 7.4) containing 5% glycerol. The sample was eluted with 320 ml of 8-fold diluted Polybuffer74 (Pharmacia, pH 4.0, adjusted with HCl) containing 5% glycerol at a flow rate of 0.5 ml/min. The resulting pH gradient was pH 7-4. After completion of the elution with Polybuffer74, the column was washed with 100 ml of 25 m*M* *l*-histidine buffer (pH 4.0) containing 0.5 *M* NaCl at the same flow rate. The protein profile was determined at 280 nm using a UV monitor (Spectra/Chrom, Spectrum, Houston, TX). Eighty fractions (i.e., 4.5 ml each) were collected and the pH of each fraction was measured. The hydrolysis activities towards three naphthyl substrates [i.e., α-naphthyl acetate (α NA), αNB, α-naphthyl caproate (αNC)] were evaluated for each fraction without preincubation with PHMB or eserine. To determine αNC hydrolytic activity, the reaction buffer was supplemented with Triton X-100 (0.05% final) to overcome the low water-solubility of αNC. Fractions showing CbE activity were then evaluated for [^{14}C]*trans*-permethrin hydrolysis as described previously. Kinetic analyses using αNC as a substrate were performed for the each representative p*I* fractions that showed the

highest CbE activities (e.g., p*I* 4.2, 4.5, and 4.8 fraction). Selected fractions of the pI 3.8-4.8 chromatofocused hemolymph (i.e., fraction # 44-59 from the SS hemolymph and fraction # 43-58 from the PE-R hemolymph) were pooled and concentrated to 70 µl by sequential uses of a Centriprep30 concentrator (Amicon, Beverly, MA) and a Ultrafree-MC10 concentrator (Milipore, Bedford, MA) for the native PAGE analysis,. The concentrated SS and PE-R samples were electrophoresed on a 7.5% native polyacrylamide gel. One section of the gel was substrate-stained using αNB or αNC while the other section was protein-stained as described previously. The protein band intensities were analyzed using a scanning densitometer (Model SM3, Howtek Inc., Hudson, NH).

7. Protein Assay

Protein concentrations were determined using the bicinchoninic acid (BCA) method (54) modified for a microplate format. For protein determinations of samples containing ampholites, UV absorption at 280 nm was used because the presence of ampholites resulted in strong background color with the BCA method.

C. Methods for Purification of Permethrin CbE

1. Ammonium Sulfate Fractionation

Hemolymph was collected from 100-150 individual 4th instars (average body weight 133 mg) of the PE-R strain in the same manner as described previously except that the glass wool in the syringe barrel was presoaked with 1.5 ml of isolation buffer (see Preparation of Tissue Fractions). Initial fractionation (i.e., 40% saturation) of hemolymph was accomplished by slowly dissolving finely ground ammonium sulfate (2.9 - 3.6 g) into 12-15 ml of the hemolymph solution (i.e., hemolymph plus isolation

buffer) and stirring for 1 hr on ice. The 40%-saturated sample was centrifuged at 20,000 × g for 10 min at 4°C and the supernatant decanted. For the second fractionation (i.e., 40 to 80%-saturation), 3.4-4.3 g of ammonium sulfate was further added to the supernatant and stirred slowly for 1 hr on ice. Following centrifugation (20,000 × g, 10 min, 4°C), the supernatant was discarded and the pellet re-dissolved into 2 ml of 0.1 *M* sodium phosphate buffer (pH 7.0). The proteins in the dissolved pellet were further separated by hydrophobic interaction chromatography.

2. Hydrophobic Interaction Chromatography (HIC)

The ammonium sulfate-precipitated sample (i.e., 3-4 ml) was applied to a methyl HIC column (Bio-Rad, 1.5 × 25 cm, Vt = 44 ml) previously equilibrated with 0.1 M sodium phosphate buffer (pH 7.0) containing 1.7 *M* ammonium sulfate (i.e., 40% saturation concentration). The sample was eluted with 240 ml of 0.1 *M* sodium phosphate buffer (pH 7.0) in the presence of a decreasing linear gradient of ammonium sulfate (i.e., 1.7 to 0 *M*) at a flow rate of 2.0 ml/min. Forty fractions (i.e., 6 ml each) were collected and the protein profile monitored continuously at 280 nm using a UV monitor. A 10 µl aliquot of each fraction was taken for the determination of αNC hydrolysis. Fractions with relatively high levels of αNC hydrolysis were subsequently evaluated for [^{14}C]*trans*-permethrin hydrolysis activity. Fractions containing high levels of [^{14}C]*trans*-permethrin hydrolysis were pooled and concentrated to ca. 10 ml with a stirred cell concentrator (Model 8200, Amicon, Beverly, MA). The concentrated sample was dialyzed against 1 L of ion exchange buffer [10 m*M* imidazole, 10 m*M* NaCl, 1 m*M* dithioerythritol (DTE), pH 7.2] at 4°C overnight to remove ammonium sulfate. If the dialyzed sample remained turbid, it was centrifuged at 10,000 × g for 10 min at 4°C to remove precipitate.

3. Diethylaminoethyl-Anionic Exchange (DEAE-Ion Exchange) Chromatography

The dialyzed HIC sample (ca. 15 ml) was loaded onto a DEAE Bio-Gel A column (Bio-Rad, 2.5 × 13 cm, Vt = 63 ml) previously equilibrated with low salt buffer (10 m*M* imidazole, 10 m*M* NaCl, 1 m*M* DTE, pH 7.2) at a flow rate of 1.0 ml/min. The applied sample was eluted by a linear NaCl gradient (i.e., 10 - 500 m*M*) formed in 480 ml of 10 m*M* imidazole buffer containing 1 m*M* DTE (pH 7.2) at a flow rate of 2.5 ml/min. The protein profile of each fraction was continuously measured at 280 nm with a UV monitor. Forty fractions were collected and a 50 μl aliquot from each fraction was evaluated for the hydrolysis of αNC as detailed previously. Fractions with high CbE activities as judged by αNC hydrolysis were combined and sequentially concentrated to ca. 2.5 ml using the Model 8200 stirred cell and Centriprep30 concentrators (Amicon), respectively.

4. Gel Filtration Chromatography

The CbE sample from the DEAE-ion exchange (ca. 2.5 ml) was applied onto a Sephacryl S-200-HR column (Pharmacia, 1.5 × 97 cm, Vt = 171 ml) and eluted with 150 ml of elution buffer (10 m*M* imidazole, 50 m*M* NaCl, 1 m*M* DTE, 4% glycerol, pH 7.2) at a flow rate of 0.5 ml/min. Thirty-five fractions (i.e., 4.5 ml each) were collected and a 30 μl aliquot from each fraction was used for CbE activity assay using αNC as a substrate. The fractions with high CbE activities were pooled and concentrated to ca. 10 ml using a Model 8200 stirred cell concentrator. The molecular weights (MW) of CbEs were estimated using a calibration curve generated from a set of MW standard proteins (MW-GF-200, Sigma Chem. Co.): cytochrome c (12.3 kDa), carbonic anhydrase (29 kDa), bovine serum albumin (66 kDa), alcohol dehydrogenase (150 kDa), and β-amylase (200 kDa).

5. Chromatofocusing

The sample from the gel filtration chromatography (ca. 10 ml) was loaded onto a PBE94 chromatofocusing column (Pharmacia, 1.0 x 30 cm, Vt = 24 ml) equilibrated with 25 m*M* imidazole buffer (pH 7.4) containing 5% glycerol. The elution, evaluation of hydrolysis activity, and other procedures were the same as described previously (i.e., see *Chromatofocusing of hemolymph*). Three representative p*I* fractions (i.e., p*I* 4.2, 4.5, and 4.8 fractions) were used for the kinetic analyses of multiple charged forms of the CbEs. To obtain better separation of p*I* 4.2-4.8 CbE, the combined p*I* 4.2-4.8 fractions were re-chromatofocused using a narrower pH gradient (i.e., pH 4-5). In the chromatofocusing with a pH 4-5 gradient, the PBE94 column was initially equilibrated with 25 m*M* piperazine-HCl buffer (pH 5.5) containing 5% glycerol and sample eluted with 10-fold diluted Polybuffer-HCl (pH 4.0) containing 5% glycerol. For long-term storage, the pH of chromatofocused fractions was raised to pH 6.6-6.8 by adding 1/20 volume of 1 *M* sodium phosphate buffer (pH 7.2). The pH-adjusted samples could be stored at 4°C for 2-3 weeks without a significant loss of activity (unpublished observation). For further purification using preparative native PAGE, p*I* 4.2 - 4.8 fractions with CbE activity were combined, concentrated to ca. 10 ml, and dialyzed against 1 L of electrophoresis sample buffer (60 m*M* Tris-HCl, 5% glycerol, pH 6.8) overnight at 4°C to remove ampholytes. After dialysis, the CbE preparation was concentrated to the final volume of ca. 1.5 ml with a Centrprep30 concentrator.

6. Preparative Native PAGE

A 1.5 mm-thick slab gel (7.5% separating gel and 4.0% stacking gel with plain edge on the top, Bio-Rad Mini-Protein II) was used for preparative gel electrophoresis. The concentrated CbE sample from chromatofocusing (ca. 700-800 μl of sample containing 2-3 mg total protein) was mixed with 1/100 volume of 0.05% bromophenol

blue and applied onto top surface of stacking gel. Electrophoresis was carried out at 200 V for 45-50 min. The temperature of gel was controlled at ca. 10°C by circulating chilled upper chamber buffer via a peristaltic pump. Following preparative electrophoresis, the gels were stained with αNB or αNC as described previously, CbE bands cut out, and finely diced for the electro-elution.

7. Electro-Elution

Electro-elution was performed using the Bio-Rad electro-eluter (Model 422, Hercules, CA) according to the manufacturer's manual. The diced gel from the preparative PAGE was loaded into the elution module with a dialysis membrane cap placed on the bottom. The elution was done at 9 mA constant current/elution module for 3-5 hrs using Tris-glycine buffer (25 mM Tris, 192 mM glycine, pH 8.3-8.7). Following elution, the protein was gently collected from the dialysis membrane cap. In the case of electro-elution of protein from SDS-polyacrylamide gels, the same procedures were used except a modified elution buffer (25 mM Tris, 192 mM glycine, 0.1% SDS, pH 8.3-8.7) was included.

D. Methods for Characterization of Purified Permethrin CbE

1. Two-Dimensional Gel Electrophoresis (2-DGE)

The overall procedure for 2-DGE was based on the manufacturer's instruction manual of the Bio-Rad Mini-Protein II 2-D Cell System, which was modified from the methods of O'Farrell (55). Purified permethrin CbE sample was first isoelectricfocused in 1 mm (i.d.)-capillary tube gels (4% acrylamide, 9.2 *M* urea, 4% Bio-Lyte 4-6, and 1% Bio-Lyte 3-10). After prerunning the gel at 300 V for 30 min, the sample in one volume of sample buffer (9.5 *M* urea, 5% β-mercaptoethanol, 1.6%

Bio-Lyte 4-6, 0.4% Bio-Lyte 3-10) and p*I* markers (IEF Mix 3.6-9.3, Sigma Chem. Co.) were loaded onto the gel. Isoelectricfocusing (IEF) was performed at 750 V for 3 hrs in a running buffer system of 20 m*M* NaOH (i.e., catholyte) and 100 mM phosphoric acid (i.e., anolyte). After IEF in the first dimension, the gel was removed from the capillary tube and placed longitudinally into the slot of the second dimensional 1 mm-thick slab gel (i.e., 10% SDS-PAGE). The SDS-PAGE was run at 200 V for 50 min and the gel silver-stained (56). For non-denaturing 2-DGE, a native IEF gel, in which urea was replaced with glycerol (7.5% final conc.), was used in the first dimension and a 7.5% native polyacrylamide gel was used for the second dimension. Samples were electrophoresed in duplicate in the non-denaturing 2-DGE format. One gel was silver-stained for protein determination and the other activity-stained with αNC as substrate using the same method detailed previously but without preincubation with PHMB and eserine (see Polyacrylamide Gel Electrophoresis of Hemolymph).

2. Determination of Molecular Mass (*Mr*)

Sephadex G-100 gel filtration chromatography (Pharmacia, 1.0 × 50 cm, Vt = 39 ml) and Bio-Sil SEC 250 HPLC (Bio-Rad) were employed for the determination of native *Mr* of purified permethrin CbE. For Sephadex G-100 gel filtration, 300 µl of purified CbE (ca. 100 µg) was loaded onto the column and eluted with 20 m*M* Tris-HCl buffer (pH 7.2) containing 0.1 *M* NaCl at a flow rate of 0.12 ml/min. Eighty-five fractions (i.e., 0.48 ml each) were collected and the CbE activity of each fraction was determined by αNB or αNC hydrolysis in the presence or absence of specific inhibitors, PHMB and phenylmethylsulfonyl fluoride (PMSF)(see Inhibition Studies). Protein concentration of each fraction was monitored at 280 nm by UV absorption. *Mr*s were estimated using a calibration curve (Molecular weight *vs.* elution volume) generated from a set of molecular weight (MW) standard proteins (MW-GF-200, Sigma

Chem. Co.): cytochrome c (12,300), carbonic anhydrase (29,000), bovine serum albumin (66,000), alcohol dehydrogenase (150,000), and β-amylase (200,000).

For HPLC, 10 µl of purified CbE was injected onto the Bio-Sil column and eluted with elution buffer (50 m*M* sodium phosphate, pH 6.8) at the flow rate of 1 ml/min. Forty-five fractions (i.e., 0.25 ml each) were collected and CbE activity of each fraction as judged by αNC hydrolysis was measured. *Mr*s were estimated using a calibration curve generated from a set of molecular weight standard proteins (Bio-Rad gel filtration MW markers): vitamin B-12 (1,350), myoglobulin (17,000), ovalbumin (44,000), immunoglobulin G (158,000), and thyroglobulin (670,000).

The *Mr* of denatured CbE was determined by SDS-PAGE (10% separating gel). The purified CbE sample was mixed with 4 volumes of SDS-sample buffer (62.5 m*M* Tris-HCl, 2% SDS, 5% 2-β mercaptoethanol, 10% glycerol, 125 ppm bromophenol blue, pH 6.8) and boiled for 5 min. The denatured CbE sample and standard MW marker proteins (SDS-6H, Sigma Chem Co.) were loaded onto the gel and electrophoresed at 200 V under constant voltage conditions for 45-50 min. The gel was stained with Coomassie brilliant blue and then the *Mr* of CbE estimated from a standard curve of MW marker proteins (i.e., MW *vs.* relative mobility).

In order to determine the *Mr*s of multiple charged forms of the CbE, the purified permethrin CbE was analyzed by 2-DGE (i.e., 1st dimension-denatured IEF *vs*. 2nd dimension-SDS-PAGE) as described previously. The gel was silver-stained and the *Mr* of each charged form of protein estimated from the standard curve of MW marker proteins.

3. Renaturation of CbEs Separated on SDS-Polyacrylamide Gel

To identify the permethrin CbE following SDS-PAGE by detecting hydrolytic activity *in situ*, the proteins in the gel were renatured based on the methods of Lacks and Springhorn (57). One volume of the permethrin CbE sample were mixed with 4

volumes of SDS-sample buffer (62.5 m*M* Tris-HCl, 2% SDS, 5% 2-β mercaptoethanol, 10% glycerol, 125 ppm bromophenol blue, pH 6.8), and incubated for 1-30 hrs or boiled for 5 min. The denatured samples were electrophoresed on a 10% SDS-polyacrylamide gel containing bovine serum albumin (BSA, 10 μg protein/ml of separating gel) at 200 V for 50 min. Following electrophoresis, the gel was rinsed with ddH_2O and then washed three times (i.e., 1 hr per washing) with 100 ml of 40 m*M* Tris buffer (pH 7.6) at room temperature to remove SDS. The washed gel was activity-stained with αNB-dianisidine and the stained bands were marked by punching a hole at the edge of each band. The activity-stained gel was further stained with Coomassie brilliant blue for the determination of protein bands.

4. Determination of Optimum pH and Temperature Conditions for Hydrolytic Activity of Permethrin CbE

Representative charged forms of CbE (i.e., p*I* 4.8, 4.5, and 4.2 CbEs from chromatofocusing) were used to determine optimum temperature and pH conditions for hydrolytic activity. In pH experiments, several types of reaction buffer were used to ensure maximum buffer capacity for each pH condition. The CbE sample (i.e., 10 μl) was mixed with substrate solutions (i.e., 190 μl) prepared by dissolving αNB or αNC (i.e., 125 μ*M* final conc.) in different pH reaction buffers (0.1 *M* glycine-HCl, pH 3.0; 0.1 *M* citric acid-NaOH, pH 4.0 & 5.0; 0.1 *M* sodium phosphate, pH 6.0 & 7.0; 0.1 *M* Tris-HCl, pH 8.0 & 9.0; 0.1 *M* glycine-NaOH, pH 10.0) and incubated at 37°C for 10 min. Since high levels of non-enzymatic hydrolysis were observed at high pH (e.g., pH 8.0-10.0), control reactions without CbE at each pH condition were carried out at the same time to subtract the non-enzymatic hydrolysis. In temperature experiments, a 10 μl aliquot of the CbE sample was mixed with 190 μl of αNB or αNC substrate solution (each 125 μ*M* in 50 m*M* sodium phosphate, pH 7.2) and incubated at 10, 20, 30, 40, 50, and 60°C for 10 min. Each reaction was terminated by adding 50 μl stop

solution (3.4% SDS/4% dianisidine in ddH_20) and the absorbance (i.e., OD_{600}) was measured as described previously.

5. Kinetic Analyses of Naphthyl Substrates

Three naphthyl substrates were selected to investigate relationships between increasing substrate hydrophobicity (i.e., αNC > αNB > αNA) and the affinity (i.e., $1/K_m$) and catalytic (i.e., V_{max}) constants of three charged forms of CbE (i.e., p*I* 4.8, 4.5 and 4.2 CbEs from chromatofocusing). For each CbE sample, a 40 µl aliquot was mixed with a set of serially-diluted substrate solutions (i.e., 50, 75, 125, 250 and 500 µ *M* in 50 m*M* sodium phosphate containing 0.05% Triton X-100, pH 7.2) and incubated for 3 min at 32°C. Other procedures were the same as described in previous section (see Evaluation of α-Naphthyl Butyrate and Permethrin Hydrolysis Associated with the HAE, NMT, MIC, and SOL Tissue Fractions). The data were analyzed by construction of Lineweaver-Burk double reciprocal plots and the K_m and V_{max} kinetic constants calculated graphically.

6. Inhibition Studies

All inhibition studies were performed using the purified p*I* 4.8 and 4.5 forms of CbE unless stated otherwise. Appropriately diluted CbE sample (i.e., 30 µl, 0.4-0.9 OD_{600} level of αNC hydrolysis in control reaction) was preincubated with various concentrations of inhibitors (i.e., 70 µl each, final concentrations: 0.005-500 µ*M* DFP; 1-625 µ*M* PMSF, PHMB, and parathion; 0.2-625 µ*M* DEF; 20-2500 µ*M* eserine; 0.5-1000 µ*M* $HgCl_2$; 100 µ*M* NaCN) for 10 min at 37°C prior to the addition of αNC (i.e., 100 µl, 125 µ*M* final) as substrate. The reaction was terminated after 5 min and the level of αNC hydrolysis measured as described previously. To determine the I_{50} value of inhibitor, percent inhibition was calculated over a range of inhibitor concentrations and I_{50} value determined by logit analysis. Inhibition of p*I* 4.2-4.8

CbEs by several protease inhibitors such as EDTA, *trans*-epoxysuccinyl-*l*-leucylamido-(4-guanidino)butane (E-64), PMSF, and pepstatin A (i.e., final concentrations: 890 μ *M*, 20 μ*M*, 200 μ*M*, and 10 μ*M*, respectively) were also performed in the same manner except that preincubations were for 30 min at 37°C. To identify the PHMB-sensitive or PMSF-sensitive fractions during various chromatographic procedures (e.g., re-chromatofocusing, gel filtration, SE-HPLC, etc.), a 10-20 μl aliquot of each fraction was preincubated individually with PHMB or PMSF (i.e., 125 μ*M* final) for 10 min and then incubated with αNC (i.e., 125 μ*M* final) for 10 min at 37°C. In experiments with insecticides, a 30 μl aliquot of the permethrin CbE samples (i.e., p*I* 4.8 and 4.5 CbEs from re-chromatofocusing) was preincubated with various concentrations of insecticides (i.e., 70 μl, final concentrations: 20-80 μ*M* permethrin, cypermethrin, abamectin, and azinphos-methyl; 5-80 μ*M* DDT; 80-320 μ*M* eserine; prepared with reaction buffer containing 0.05% Triton X-100) at 37°C for 10 min prior to the addition of αNC solution (125 μ*M* final). Other procedures were the same as above.

7. Inhibition Kinetics of Permethrin and DDT on Permethrin CbE

One part of a serially-diluted inhibitor stock solution (i.e., 4-16 m*M* permethrin and 1-16 m*M* DDT in acetone) was mixed with 99 parts of a range of αNC substrate solutions (i.e., 40, 70, 100, 150, 250, and 500 μ*M* αNC in reaction buffer containing 0.05% Triton X-100). A 100 μl aliquot of the mixture was transferred into each well of a 96 well-microtiter plate. The purified p*I* 4.5-4.8 CbE sample was appropriately diluted with reaction buffer to obtain a final control hydrolysis activity level of 0.1-0.6 OD_{600} depending on substrate concentrations. The reaction was initiated by transferring 100 μl of the diluted CbE solution into each well of microtiter plate containing the inhibitor-αNC solution. After incubating at 37°C for 3 min, the reaction was terminated by adding 50 μl of stop solution (3.4% SDS/4% dianisidine in ddH_2O). The αNC hydrolysis activity was measured as described previously. The data were

initially analyzed by Lineweaver-Burk double reciprocal plots and then replots (i.e., slopes *vs*. inhibitor concentrations and intercepts *vs*. inhibitor concentrations) constructed. The substrate dissociation constant (K_s) was estimated from the x-axis intercept of control regression line (i.e., in the absence of permethrin or DDT) in the initial double reciprocal plot. The inhibitor dissociation constant (K_i) from enzyme-inhibitor (i.e., EI) complex was estimated from the x-axis intercept of the regression line of the slopes *vs*. inhibitor concentrations. The inhibitor dissociation constant (αK_i) from enzyme-substrate-inhibitor (i.e., ESI) complex was estimated from the x-axis intercept of the regression line of the intercepts *vs*. inhibitor concentrations.

8. *p*-Chloromercuribenzoate (PCMB)-Agarose Affinity Chromatography

PCMB-agarose chromatography was employed to separate the PHMB-sensitive CbE from the PMSF-sensitive CbE. Purified p*I* 4.2-4.8 CbE sample was buffer-exchanged with binding buffer (100 m*M* sodium phosphate, 10 m*M* EDTA, pH 7.6) and concentrated to ca. 5 ml using a Centriprep30 concentrator. The sample was applied to a PCMB-agarose column (Pierce, Rockford, IL, Vt = 5 ml) previously equilibrated with binding buffer. The column was washed with 30 ml of binding buffer at a flow rate of 0.5 ml/min. After washing, the column was eluted first by 0-1.0 *M* NaCl gradient formed in 60 ml of elution buffer A (20 m*M* sodium phosphate, pH 6.8). Since no CbE was eluted by elution buffer A, the column was further eluted with 30 ml of elution buffer B (20 m*M* sodium phosphate, 50 m*M* DTE, pH 6.8). A 5 μl aliquot from each fraction was evaluated for αNC hydrolysis activity in the presence or absence of PHMB and PMSF (i.e., final 125 μ*M* each).

9. Concanavalin A (ConA)-Sepharose Affinity Chromatography

The p*I* 4.2-4.8 CbE sample from chromatofocusing was concentrated to ca. 21 ml using the model 8200 stirred cell concentrator. The concentrated sample was buffer-

exchanged by mixing with 40 ml of ConA binding buffer (50 m*M* Tris-HCl, 0.1 *M* NaCl, 1 m*M* $CaCl_2$, 1 m*M* $MnCl_2$, 5% glycerol, pH 7.1) and then concentrating again to ca. 21 ml. The sample was applied onto the ConA-sepharose column (Sigma Chem. Co., Vt = 5 ml) previously equilibrated with binding buffer and then the column washed with 50 ml of binding buffer at a flow rate of 0.5 ml/min. The proteins bound to ConA-sepharose were eluted with 70 ml of elution buffer (i.e., binding buffer containing 0.5 M mannopyranoside) at a flow rate of 0.5 ml/min. Protein profile was continuously monitored at 280 nm with a UV monitor. A 5 μl aliquot was taken from each fraction for the evaluation of αNC hydrolysis.

The p*I* < 4.0 CbE sample from chromatofocusing was also separated by ConA-Sepharose affinity chromatography for comparison purposes. The p*I* < 4.0 CbE sample (ca. 24 ml) was buffer-exchanged by mixing with 50 ml of ConA binding buffer and then concentrating to ca. 21 ml using the Model 8200 stirred cell concentrator. Other procedures were the same as above except the elution step, where the column was left at 4°C for 24 hrs and then elution resumed with an additional 70 ml of elution buffer. This was necessary because no proteins were eluted by the initial elution procedure using ca. 53 ml of elution buffer.

10. *N*-Deglycosylation of Permethrin CbE

The pI 4.2-4.8 CbE sample from chromatofocusing (i.e., 940 μl, ca. 70 μg protein) was mixed with 14 ml of digestion buffer (50 m*M* potassium phosphate, 20 m*M* EDTA, pH 7.5) and then concentrated to ca. 1 ml using a Centriprep30 concentrator. The 1 ml sample was further concentrated to ca. 20 μl using a Ultrafree-MC10 concentrator. The buffer-exchanged CbE sample was mixed with 20 μl of the endoglycosidase F/*N*-glycosidase F (20-30 U *N*-glycosidase F in 20 m*M* potassium phosphate, 20 m*M* EDTA, pH 7.5; Boeringer Mannheim Biochemicals, Indianapolis, IN) and incubated at 37°C for 20 hrs. For a control sample, CbE was incubated at 37°

C for 16 hrs without the *N*-glycosidase F. After deglycosylation, the CbE samples were analyzed by native IEF followed by αNB/αNC-dianisidine staining and by SDS-PAGE followed by Coomassie brilliant blue staining as described previously.

11. Labeling of Permethrin CbE with [^{3}H]DFP

A 6-30 µl aliquot of [^{3}H]DFP (6.0-30 µCi, specific activity 6.0 mCi/µmole) was mixed with 30-50 µl of CbE sample (i.e., 37-200 µg protein) and incubated at room temperature for 20 hrs. The unbound [^{3}H]DFP was removed from the labeling reaction mixture using a Bio-Spin 6 desalting column (Bio-Rad) previously equilibrated with PAGE sample buffer (60 mM Tris-HCl, pH 6.8) according to the manufacturer's instruction. The [^{3}H]DFP-labeled CbE sample and unlabeled CbE sample were electrophoresed side by side on a 12% SDS-polyacrylamide gel at 200 V for 50 min. The gel lane with the [^{3}H]DFP-labeled CbE sample was cut out longitudinally and diced laterally into ca. 1.5 mm-wide pieces. Each piece of gel was placed into a scintillation vial containing 200 µl of 1 N NaOH and incubated at room temperature overnight. The NaOH-treated gel was neutralized by mixing with 200 µl of 1 N HCl and then 5 ml of scintillation solution (Universal Cocktail, ICN Radiochemicals, Irvine, CA) was added to the vial. The radioactivity of each vial was measured with a scintillation counter (1209 Rackbeta, LKB Wallac, Turku, Finland). The gel lane containing unlabeled sample was stained with Coomassie brilliant blue to determine the location of CbE band.

E. Methods for Immunological Studies

1. Purification of the 30, 48, and 60 kDa Immunogens

Hemolymph from the PE-R strain (i.e., total protein ca. 100-200 mg) was chromatofocused as described previously (see Chromatofocusing of Hemolymph). The pH 4.2-4.8 fractions were pooled and concentrated to ca. 5-15 ml by using the Model 8200 stirred cell concentrator. The concentrated sample was dialyzed against 1 L of electrophoresis sample buffer (60 mM Tris-HCl, 5% glycerol, pH 6.8) or buffer-exchanged by passing through a Bio-6DG desalting column (Bio-Rad, 2.5 × 12 cm, Vt = 59 ml) previously equilibrated with the electrophoresis sample buffer. The sample was concentrated again to ca. 0.5-1 ml using a Centriprep30 concentrator. Appropriate amounts of SDS, β-mercaptoethanol, glycerol, and 0.05% bromophenol blue (i.e., final conc. 2%, 5%, 10%, and 125 ppm, respectively) were added to the concentrated sample and the sample boiled for 5 min. The denatured CbE sample (i.e., total protein ca. 2-10 mg) was electrophoresed on a SDS-polyacrylamide gel (10% total acrylamide, 1.5 mm-thick, 20 × 20 cm, Bio-Rad Model SE 600) at 30 mA constant current for 4-5 hrs. The gel was visualized by copper staining (58), briefly washed with ddH_2O, and then the desired protein bands (i.e., ca. 30, 48, and 60 kDa protein) were cut out. Each strip of gel was placed into a 1.5 ml microcentrifuge tube and stored at -20°C until use. For the purpose of electro-elution, the gel strip was destained by incubating in 10 ml of destaining buffer (0.25 M Tris-HCl, 0.25 M EDTA, pH 9.0) with three solution changes of 5 min each. The destained gel strip was electro-eluted using an electro-eluter (Bio-Rad Model 422) according to the manufacturer's instruction.

2. Immunization

The gel strips were disrupted by injecting the gel strips back and forth between two syringes (59) and then mixed well with one volume of Freund's complete adjuvant.

Each fragmented immunogen (i.e., 30, 48, and 60 kDa denatured CbE proteins, 5-7 ml, ca. 200-500 μg) was injected intradermally into individual female New Zealand white rabbits on 15-20 spots that encompassed the hind back area. Rabbits were given booster injections by using Freund's incomplete adjuvant 6 weeks after the first injection. Two additional booster injections of the 30 kDa immunogen and 6 additional booster injections of the 48 and 60 kDa immunogens were given over 4-6 weeks-interval following the first booster injections. Blood samples (i.e., 5-20 ml) were collected 2 weeks after final injections. Blood sera were separated and stored at -20°C until use. Nonspecific sera were obtained from blood collected prior to immunization for control purposes.

3. Purification of Immunoglobulin G (IgG) Using Protein A-Agarose

Purification of IgG from each antiserum was performed using the Affi-Gel Protein A MAPS II kit (Bio-Rad). A 2.5-7.5 ml aliquot of each serum sample was processed in a single purification using protein A-agarose column (i.e., 2.5 ml bed volume) following the manufacturer's instruction manual. Purified IgG was aliquoted and stored at -20°C until use.

4. Titration of Antibody

Purified immunogens (i.e., electro-eluted 30, 48, and 60 kDa CbE proteins) were diluted with 50 m*M* carbonate buffer (pH 9.0) to a protein concentration of 10 μg/ml. The diluted immunogen (i.e., 50 μl) was transferred into each well of a 96-well microtiter plate (High Binding ELISA Plate, Corning Inc. Corning, NY) and incubated at 4°C overnight or 2-4 hrs at room temperature. After incubation, the diluted immunogen was removed and the plate washed twice with phosphate buffered saline (PBS, pH 7.2). The plate was blocked with PBS containing 2% BSA by incubating 2-4 hrs and then washed twice with PBS. A 50 μl aliquot of diluted crude antiserum or

purified IgG (i.e., 10^1 to 10^7-fold dilution with PBS containing 1% BSA) was added into each well and incubated for 1 hr, followed by two rounds of washing with PBS. The plate was incubated with anti-rabbit IgG peroxidase conjugate (i.e., 2,500-fold diluted, 50 µl/well, Sigma Chem. Co) for 1 hr and washed with PBS 4-5 times. Substrate solution [0.003% H_2O_2, 0.42 m*M* tetramethylbenzidine (TMB) in 0.1 *M* sodium citrate buffer, pH 6.0] was freshly prepared, transferred to the plate (i.e., 50 µl/well), and incubated for 20-30 min until color developed. The reaction was stopped by adding 50 µl of 2 *M* H_2SO_4 per well and OD_{450} determined. All procedures were carried out at room temperature except when stated otherwise.

5. Antibody Capture Immunoassay

Hemolymph (i.e., 5-20 µl) was collected from individual 4th instars (i.e., 120-140 mg body weight) using a pipetter with disposable tip after making a tiny incision on doso-lateral cuticle using a razor blade. A 2 µl aliquot of individual hemolymph was diluted 10-fold with PBS containing 1% SDS and boiled for 5 min to denature proteins. The denatured hemolymph was further diluted 20-fold with PBS and used as the antigen solution. A 50 µl aliquot of the antigen solution was transferred into each well of a 96-well microtiter plate and incubated for 2 hrs in a humid container. The plate was washed twice with PBS and blocked by PBS containing 3% BSA and 0.02% sodium azide for 2 hrs. The plate was washed twice with PBS and a 50 µl aliquot of the diluted 30 kDa IgG (i.e., IgG purified from the antiserum generated against 30 kDa CbE protein, 8 ng/µl in PBS containing 3% BSA and 0.02% sodium azide) was transferred into each well. The plate was incubated for 2 hrs in a humid container and then washed twice with PBS. The plate was incubated with anti-rabbit IgG peroxidase conjugate (2,500-fold diluted with PBS containing 3% BSA, 50 µl/well) for 1 hr and then washed with PBS 5 times. Freshly prepared substrate solution (0.003% H_2O_2, 0.42 m*M* TMB in 0.1 *M* sodium citrate buffer, pH 6.0) was transferred to the plate

(i.e., 50 µl/well) and incubated for ca. 10 min until color developed. The reaction was stopped by adding 50 µl of 2 *M* H_2SO_4 per well and OD_{450} determined. All procedures were carried out at room temperature.

CHAPTER III

RESULTS

A. Tissue Distribution and Identification of Permethrin CbE

1. Tissue Distribution of Permethrin CbE

In order to investigate the distribution of CbEs associated with permethrin resistance in CPB (60), the hydrolytic activities of 4 tissue fractions using αNB as substrate were measured (Fig. 1, panel A). Most of hydrolytic activity was found in the soluble (SOL) and hemolymph (HAE) fractions (i.e., 47-55% and 30-40% of total hydrolytic activity, respectively) rather than in the nucleolar-mitochondrial (NMT) or microsomal (MIC) fractions. The HAE and SOL fractions from the PE-R strain showed significantly elevated levels of αNB hydrolysis compared to the SS strain (2.3-fold and 1.5-fold, respectively; *t*-test, $n=3$, $P<0.05$). In contrast, the membrane-associated CbEs in the NMT and MIC fractions accounted for only 10-13% and 3-4% of total hydrolytic activity, respectively, although significantly higher hydrolytic activity were associated with the MIC fraction from the PE-R strain. These results suggest that the CbEs in HAE and SOL fractions are more likely associated with permethrin resistance in the PE-R strain than membrane-associated CbEs.

Distributions of the hydrolytic activities of these same 4 tissue fractions were likewise determined using [^{14}C]*trans*-permethrin as substrate (Fig. 1, panel B). The HAE and SOL fractions were found to contain most of the [^{14}C]*trans*-permethrin hydrolyzing activity (86% and 77% in the PE-R and SS strains, respectively) and the overall distribution pattern of permethrin hydrolysis was similar to that for αNB hydrolyzing activity. However, only the HAE fraction from the PE-R strain was assessed to contain significantly higher permethrin hydrolyzing activity when compared

to the SS strain (1.3-fold, *t*-test, $n=3$, $P<0.05$). This supports the contention that soluble CbEs in the hemolymph may be involved in permethrin resistance.

The overall level of permethrin hydrolysis was very low in all tissue fractions assessed (e.g., 5.6, 1.2, 0.3, and 3.6 pmole/hr/larva in the HAE, NMT, MIC, and SOL fractions of the PE-R strain, respectively) compared to αNB hydrolysis (e.g., 268.5, 63.5, 27.1, and 318.9 nmole/min/larva in the HAE, NMT, MIC, and SOL fractions of the PE-R strain, respectively). Nevertheless, a similar pattern in distribution was observed in the comparison of specific activities of permethrin hydrolysis among tissue fractions [i.e., high in the HAE and SOL fractions (3.6 and 2.9 pmole/hr/mg protein, respectively) *vs*. low in the NMT and MIC fractions (2.2 pmole/hr/mg protein, in both).

2. Identification of Permethrin CbE

In order to identify specific hemolymph CbEs that may be associated with permethrin resistance, native PAGE and IEF were employed to separate hemolymph proteins from the PE-R and SS strains (Fig. 2). Four CbE bands that appeared in both strains were identified by a αNB-dianisidine staining method. Among these, the band IV CbE from the PE-R strain (i.e., the fastest migrating band) possessed a greatly elevated level of hydrolytic activity toward αNB (i.e., 4.1 times increase as judged by scanning densitogram, Fig. 2, panel B) when compared to the corresponding band associated with the SS strain. The other three CbE bands were relatively faint and no significant differences in intensities between the two strains were observed. Although an extra CbE band (i.e., between band II and III CbEs, see Fig. 2, panel B) was observed in the PE-R hemolymph, this band was not particularly intense on a relative basis and was not consistently present in several separate electrophoretic separations. The band IV CbE, therefore, was responsible for most of the differences between the

strains as judged by αNB hydrolysis and, possibly, for their different levels of permethrin resistance.

To further clarify any differences in hemolymph CbE from the PE-R and SS strains that may be related with permethrin resistance, the hemolymphs from the PE-R and SS strains were isoelectricfocused (pH 3.0-10.0, Fig. 3). More than 20 multiple-charged CbEs were identified by αNB-dianisidine staining. Among these, only the several CbEs detected from the PE-R strain in the pH 4.6 region of the IEF gel possessed elevated αNB hydrolyzing activities in the PE-R hemolymph when compared to the SS hemolymph. Because the CbEs separated by IEF in the pH 4.6 range and the band IV CbE separated by native PAGE possess enhanced hydrolytic activities associated with the PE-R hemolymph, these proteins may be identical.

The band IV CbE was not well resolved by the native mini-PAGE method (see Fig. 2). Thus, band IV is not likely comprised of a single CbE but could be comprised of several CbEs with different levels of charge. Finally, the overall staining intensity and the difference in intensity between the strains were somewhat less when examined on IEF gels. This may be due to a temporary or partial inactivation of CbEs at their isoelectric points. Although the IEF gel was equilibrated in 40 m*M* Tris-HCl buffer (pH 6.6) for 10 min prior to αNB-dianisidine staining, this equilibration regime may not be sufficient to restore the optimum pH necessary for maximal hydrolytic activity.

To isolate CbEs in large quantity, aliquots from the SS and PE-R hemolymphs were chromatofocused and the hydrolytic activities of each fraction toward naphthyl substrates (i.e., αNA, αNB, and αNC) and [^{14}C]*trans*-permethrin were measured (Fig. 4). The CbEs associated with pH 4.5-4.8 fractions, particularly the pH 4.8 fraction, gave the largest differences in the hydrolysis of naphthyl substrates and permethrin when the PE-R and SS strains were compared. The pH 4.8 and pH 4.5 fractions from the PE-R strain had CbEs that resulted in 12-15 times and 5-6 times higher levels of α NB or αNC hydrolysis, respectively, compared to similar CbEs obtained from the SS

strain. Additionally, the hydrolysis rate of [^{14}C]*trans*-permethrin by the CbEs in the pH 4.2, 4.5, and 4.8 fractions from PE-R strain was measured to be ca. 1.7, 5.7, and 6.0 times higher than each corresponding fraction from the SS strain, respectively (Table 1). If the hydrolysis rate of permethrin is calculated on a per larva basis, the hydrolytic potential of the CbEs in the pH 4.2-4.8 fractions from a single larva was estimated to be ca. 18.9 and 4.1 pmole/hr/larva in the PE-R and SS strain, respectively. These findings suggest that p*I* 4.2-4.8 CbEs (i.e., CbEs associated with pH 4.2-4.8 fractions or CbEs whose p*I* values were determined to be p*I* 4.2-4.8), particularly p*I* 4.5-4.8 CbEs, are likely candidates responsible for permethrin resistance in the PE-R strain of CPB. Also, the distribution pattern of permethrin hydrolysis was better correlated with the hydrolysis of the more hydrophobic naphthyl substrate, αNC, than with either αNB or αNA (Note: αNA hydrolysis data not shown). This implies that more hydrophobic substrates, such as αNC, may be the more suitable substrate to predict the distribution of permethrin CbE activity associated with resistance.

To investigate whether the enhanced level of hydrolytic activity of p*I* 4.2-4.8 CbEs from the PE-R strain is due to the qualitative changes in the enzymes or due to the increased quantity of the CbEs, chromatofocused fractions containing p*I* 4.2-4.8 CbEs from each strain were separated by native PAGE. One section of the gel was stained with αNC-dianisidine for CbE hydrolysis activity determination and the other section stained with Coomassie brilliant blue for protein determination. Gel band intensities were analyzed by a scanning densitometer (Fig. 5). Two main CbE bands were observed in both activity- and protein-stained gels. A fast-migrating (band 1, R_f=0.67) and a slower-migrating (band 2, R_f=0.58) CbE from the PE-R strain showed 3.3 and 2.2 times higher levels of αNC hydrolysis, respectively, than the corresponding bands from the SS strain as judged by the densitogram (Fig. 5, panel A). This elevated level of activity of the band 1 and 2 CbEs from the PE-R strain correlated well with increased levels of the protein quantity as judged by the

densitogram (i.e., 4.9 and 1.8 times higher OD values for the band 1 and 2 CbEs from the PE-R strain, respectively, than the corresponding bands from the SS strain, Fig. 5, panel B), than the corresponding bands from the SS strain. Thus, increased levels of α NC hydrolysis were closely associated with increased amounts of CbE protein.

To confirm these results, each representative p*I* CbE (e.g., pH 4.2, 4.5, and 4.8 fractions) was individually collected from chromatofocusing columns and analyzed kinetically (Table 2). The V_{max} values for all three p*I* CbEs from the PE-R strain were higher (i.e., 5.1 to 17.6-times) than the corresponding p*I* CbEs from the SS strain. This difference between V_{max} values was more prominent in the less negatively charged CbE (i.e., p*I* 4.8 CbE). In contrast, the affinity constants (i.e., $1/K_m$) of all three p*I* CbEs from the PE-R strain were determined to be rather slightly lower than those from the SS strain (i.e., 0.4 to 0.6-times). As a result, the increased activities of the p*I* 4.2-4.8 CbEs (in particular, p*I* 4.5-4.8 CbEs) from the PE-R strain appears to be due to the elevated levels of enzyme rather than due to any increased catalytic efficiencies associated with an intramolecular alteration of the CbE. This finding agrees with the earlier result (Fig. 4) where the higher CbE activity found in the PE-R strain was mainly associated with the increased amount of the CbE rather than associated with any qualitative change in the enzyme, itself. Finally, the K_m values of p*I* 4.8, 4.5, and 4.2 CbE from the PE-R strain were 33.3, 42.4, and 56.6 μ*M* and 15.3, 15.4, and 31.5 μ*M* from the SS strain, respectively. These findings suggest that the affinity of CbE to α NC increases as the negative charges of the CbEs decrease.

3. Inhibition of Hemolymph CbEs by Permethrin

Since permethrin was determined to be a poor substrate for the CbE, the possibility that permethrin interacts with the enzyme as an inhibitor was assessed. When the PE-R and SS hemolymphs were diluted with the same dilution factor (i.e., 30-fold), a distinct difference in inhibition pattern of the CbEs between the strains was observed (Fig. 6).

The CbEs from the PE-R hemolymph showed a dose-dependent inhibition over the tested range of permethrin concentrations (i.e., 12.9-42.3% inhibition over a permethrin concentration range of 7.8-500 μ*M*). Although the range of permethrin concentrations used in the inhibition test (i.e., 7.8-500 μ*M*) was beyond the solubility limit of permethrin (i.e., 0.51 μ*M* in H_2O), permethrin was solubilized (or emulsified) in the reaction buffer in the presence of Triton X-100 (0.05% final conc.). Because the presence of Triton X-100 in the reaction buffer (0.05% final conc.) actually activates α NB hydrolysis (ca. 20%, data not shown), the resulting inhibition patterns must be due to permethrin itself rather than due to any possible artifact by the addition of Triton X-100.

The inhibition of the CbEs from the SS hemolymph was progressive up to 125 μ*M* permethrin (i.e., 9.5-27.4% inhibition over a permethrin concentration range of 7.8-125 μ*M*) but the rate of inhibition decreased at concentrations above 125 μ*M* (Fig. 6, panel A). This inhibition saturation phenomenon was observed only for CbEs from the SS hemolymph. One possible explanation for this phenomenon is as follows. At a given concentration of CbEs in the SS hemolymph, an equilibrium between αNB hydrolysis and permethrin inhibition is thought to be formed under the conditions of ca. 125 μ*M* of αNB and 125 μ*M* of permethrin so that no further inhibition can occur. Such an equilibrium between hydrolysis and inhibition was also determined to be dependent on the substrate concentration (i.e., as the αNB concentration was reduced to 63 μ*M*, the permethrin concentration required for saturation inhibition was also reduced to ca. 63 μ*M* in the SS hemolymph, data not shown). If the concentration of CbE is increased as in the case of the resistant PE-R hemolymph, more substrate will be hydrolyzed due to the increased amount of enzyme under otherwise identical conditions (i.e., αNB and permethrin concentrations). This shift in the equilibrium toward excess-inhibitor (i.e., permethrin) conditions by the depletion of substrate would result in higher levels of inhibition by permethrin. This relationship between the

amount of CbE and the level of inhibition saturation was clearly demonstrated by adjusting the amounts of CbE to the same level. If the final amounts of αNB hydrolyzing CbEs of the PE-R and SS hemolymphs were adjusted to give an optical density of either 0.26 OD_{600} (i.e., the activity level of 30-fold diluted SS hemolymph, Fig. 6, panel B) or 0.65 OD_{600} (i.e., the activity level of 30-fold diluted PE-R hemolymph, Fig. 6, panel C) by manipulating the dilution factor of hemolymphs, the inhibition patterns closely resembled each other. Because the PE-R hemolymph contains more αNB hydrolyzing CbE, it results in progressive inhibition at higher concentrations of permethrin without reaching inhibition saturation. Since the amount of αNB hydrolyzing CbEs in the SS hemolymph is less than that in the PE-R hemolymph, inhibition saturation occurs at low permethrin concentration (i.e., 125 μ*M* permethrin). However, it is still not clear why the inhibition pattern at permethrin concentrations above 125 μ*M* under the condition of low concentration of CbE (i.e., as in the case of the 30-fold diluted SS hemolymph or 75-fold diluted PE-R hemolymph) shows a decreasing inhibition.

The inhibition of CbE by permethrin was determined to be reversible from the fact that the inhibition was not time-dependent over increasing preincubation intervals (i.e., 0-50 min, data not shown). Considering the very low hydrolysis rate of permethrin, this implies that permethrin inhibition is likely to depend upon a strong affinity for the enzyme (i.e., competitive or non-competitive inhibition) rather than upon slow acylating-deacylating processes. The reversible inhibition also indicates that permethrin binds to sites (i.e., catalytic site, non-catalytic site, or both) on the CbEs with a similar level of affinity as αNB so that competition between permethrin and α NB can occur. Therefore, a sequestration of permethrin by the overproduced hemolymph CbEs through high affinity-binding is likely a major contributing factor of permethrin resistance in the PE-R strain of CPB in addition to the low level of permethrin hydrolysis.

B. Purification of Permethrin CbE

The CbEs associated with hemolymph were typically precipitated in a broad saturation range of ammonium sulfate (i.e., 40-90% saturation, data not shown) as judged by αNC hydrolysis. The broad precipitation range of this activity implied the presence of a heterogeneous group of CbEs with different solubilities. Since the majority of highly negative-charged CbEs (i.e., p*I*<4.0 CbEs) were not associated with resistance and precipitated at 80-90% saturation range because of their high water solubilities, only the fractions precipitated at 40-80% saturation were used for further purification. Although the resulting purification factor by the ammonium sulfate precipitation only reached 1.8-fold (i.e., specific αNC hydrolysis activity of ammonium sulfate-precipitated CbE sample/specific αNC hydrolysis activity of hemolymph = 87.5/47.3 = 1.8, Table 3), it was a prerequisite procedure for the following purification step (i.e., hydrophobic interaction chromatography) where protein samples should be equilibrated with high concentration of salting-out ions such as ammonium sulfate, etc.

Three distinct activity peaks (i.e., peak I, II, and III in the order of elution) were identified by αNC hydrolysis when ammonium sulfate-precipitated CbE sample was separated by methyl-hydrophobic interaction chromatography (methyl-HIC, Fig. 7, panel A). The peak I, II, and III fractions (i.e., fraction # 4-7, 10-18, and 19-26, respectively) accounted 27.8, 32.3, and 39.9% of total αNC hydrolysis activity, respectively. Since the hydrophobicity of the sample fraction is directly proportional to the order of elution in HIC, the CbEs associated with peak III (i.e., peak III CbE) was expected to be the most hydrophobic (i.e., hydrophobicity of peak III > peak II > peak I). The major constituents of peak III were determined to be the p*I* 4.2-4.8 CbEs by co-chromatographic behavior. A chromatofocused p*I* 4.2-4.8 CbE sample that was chromatographed under the above conditions was eluted in similar methyl HIC

fractions corresponding to peak III. The peak III CbE was determined also to contain the highest [^{14}C]*trans*-permethrin hydrolysis activity when selected fractions of peak I, II, and III (i.e., fraction # 4, 16, and 22, respectively) were compared (i.e., 6.7, 1.3, and 21.8 pmole permethrin/hr/ml for the fraction #4, 16, and 22, respectively).

The CbEs associated with peak III (i.e., p*I* 4.2-4.8 CbEs) was designated as permethrin CbE and routinely processed for large scale purifications. Since peak I was likely due to CbEs that were not adsorbed onto the HIC beads due to insufficient equilibration of sample with ammonium sulfate and therefore relatively impure, it was not processed further despite of its moderate level of permethrin hydrolysis (i.e., 6.7 pmole permethrin/hr/ml). The CbEs associated with peak II were identified later to contain primarily acidic CbEs (i.e., p*I* <4.0 CbEs), that were little associated with resistance, by a separate purification of peak II CbE through several steps described in following sections (data not shown). The purification factor for peak III CbE as judged by αNC hydrolysis activity was 1.6-fold (i.e., specific αNC hydrolysis activity of the CbE sample from HIC/specific αNC hydrolysis activity of ammonium sulfate-precipitated CbE sample = 138.4/87.5 = 1.6-fold, Table 3). This low level of purification was due mainly to the fact that only the peak III fractions (i.e., fraction # 19-26, accounted for only 39.9% of total αNC hydrolysis activity in the methyl-HIC fractions) were used for the calculation of purification factor.

When the peak III CbEs from the methyl-HIC were separated by DEAE-anionic exchange chromatography (DEAE-ion exchange), the major peak of CbE activity, as judged by αNC hydrolysis, was typically eluted over a 250-280 m*M* NaCl concentration range (i.e., fraction # 15-22, Fig. 7, panel B), which again indicated an overall negative-charged property of the peak III CbEs. Although a minor αNC hydrolysis activity peak was observed in the more basic fractions (i.e., fraction # 7, 8), it was not included in further purification because of its negligible αNC hydrolysis activity. The purification factor for the permethrin CbE through the DEAE-ion

exchange step was 5.6-fold (i.e., specific αNC hydrolysis activity of the CbE sample from DEAE-ion exchange/specific αNC hydrolysis activity of the CbE sample from HIC = 768.2/138.4 = 5.6, Table 3).

The CbE sample from DEAE-ion exchange (fraction # 15-22) was applied to a Sephacryl S-200-HR gel filtration column. A single peak of αNC hydrolysis activity (i.e., fraction # 17-24) was observed and its *Mr* was estimated as ca. 60 kDa (Fig. 7, panel C). A 2.2-fold purification factor (i.e., specific αNC hydrolysis activity of the CbE sample from gel filtration/specific αNC hydrolysis activity of the CbE sample from DEAE-ion exchange = 1680/768.2 = 2.2) was obtained from the gel filtration chromatography step (Table 3).

When the CbE sample from the gel filtration chromatography (i.e., fraction # 17-24) was further separated by chromatofocusing, the majority of CbE activity was eluted in the pH range of ca. 4.0-5.0 as expected (Fig. 7, panel D). Within this pH 4.0-5.0 range, 6-7 individual activity peaks as judged by αNC hydrolysis were identified. The presence of multiple peaks of activity correlated well with the sawtooth-like protein elution profile (i.e., fraction # 40-56, Fig. 7, panel D). These findings corroborate the presence of multiple-charged forms of permethrin CbE as previously demonstrated in the analytical IEF of hemolymph (see Fig. 3). The purification factor obtained from chromatofocusing was ca. 1.3-fold (i.e., specific αNC hydrolysis activity of the CbE sample from gel filtration/specific αNC hydrolysis activity of the CbE sample from chromatofocusing = 2390/2160 = 1.3, Table 3). This rather small increase in overall purity indicates that the CbE sample from the gel filtration step was relatively pure prior to chromatofocusing. Either individual p*I* fractions or a combined fraction containing the p*I* 4.2-4.8 CbEs was used for kinetic analyses and inhibition studies except when stated otherwise.

The chromatofocused p*I* 4.2-4.8 CbEs were determined to contain small amounts of two contaminating proteins, as judged by native-PAGE (data not shown), with no

hydrolytic activity toward naphthyl substrates. Prior to final characterizations, the pI 4.2-4.8 CbEs were further purified through preparative native-PAGE followed by electro-elution.

The overall purification factors were 51- and 77-fold as judged by αNC and [^{14}C]*trans*-permethrin hydrolysis, respectively (Table 3). The relatively low purification factor appears to be largely caused by the isolation of p*I* 4.2-4.8 CbEs from the entire CbE pool through multiple purification steps, particularly the methyl-HIC step. In this case, the peak III HIC fractions that accounted for 39.9% of total α NC hydrolysis activity were used for subsequent purification. Because of this loss, a reduction in the purification factor can be estimated as ca. 2.5-fold (i.e., 100/39.9=2.51). Additionally, even though αNC was determined to be the most suitable substrate among three naphthyl substrates tested for the prediction of permethrin hydrolysis activity (see Fig. 4), it can be still hydrolyzed by other non-specific esterases. Thus, when the calculation of purification factor is based on the hydrolysis activity of relatively less specific substrates, such as general naphthyl substrates, underestimation of the true purification factor is inevitable. With this in mind, the higher purification factor judged by permethrin hydrolysis (i.e., 77-fold) when compared to that by αNC hydrolysis (i.e., 47-fold) after the chromatofocusing step can be explained since permethrin is a more specific substrate for the permethrin CbE compared to other naphthyl substrates. Finally, the relatively low purification level is indicative of the relatively high abundance of the permethrin CbEs (i.e., protein content is inversely proportional to purification factor). Since 0.1 mg of permethrin CbE was purified from 185 mg of crude hemolymph proteins with an approximate 3% yield, the actual content of the permethrin CbE in the PE-R hemolymph would be 1.8% if the final preparation of the p*I* 4.2-4.8 CbE is 100% pure (i.e., 0.1/185/0.03× 100=1.8%).

C. Characterization of Permethrin CbE

1. Molecular Properties of Permethrin CbE

a. Native *Mr*(s) of permethrin CbE

A permethrin CbE sample from an additional chromatofocusing step (i.e., fraction # 20-40, p*I* 4.2-4.8 CbEs, see Fig. 10) was separated by Sephadex G-100 gel filtration chromatography to determine the native *Mr* more precisely. The *Mr*s of CbEs were estimated by measuring αNC hydrolysis activities in small fractions (i.e., 0.48 ml/fraction) in the presence of the specific inhibitors, PHMB and PMSF. Three CbEs with different *Mr*s (i.e., 59, 49, and 32 kDa CbEs) were identified in this manner (Fig. 8, panel A) although only a single 60 kDa CbE was found previously using gel filtration chromatography (see Fig. 7, panel C). Without the specific inhibitors, the three activity peaks could not be completely separated (see 'αNC only' line in Fig. 8, panel A). Three protein peaks were identified in the protein chromatogram (Fig. 8, panel B). The *Mr*s of these three protein peaks were determined to be 110, 53, and 1.1 kDa for the first, second and third peaks, respectively. The second protein peak appeared to be the CbE peak that was composed of three CbEs with slightly different *Mr*s (i.e., 59, 49, 32 kDa) although monitoring the protein profile by UV absorption could not resolve them. The first protein peak had no CbE activity and is likely an aggregation of protein since the CbE sample applied to the Sephadex G-100 gel filtration column had already undergone size-fractionation procedure through the Sephacryl S-200-HR gel filtration chromatography, one of the preceding purification steps. The third peak is likely to be degraded polypeptide because of its small *Mr*. In the second protein peak, the 59 and 49 kDa CbEs were the predominant forms of CbE compared to the 32 kDa CbE as judged by both αNC hydrolysis activity (Fig. 8, panel A) and protein content (Fig. 8, panel B).

To confirm the native *Mr*s of the permethrin CbE, fractions containing the 59, 49, 32 kDa CbEs (i.e., fraction # 30-43, Ve = ca. 14-21 ml, see Fig. 8, panel A) from the Sephadex G-100 gel filtration chromatography were concentrated and separated again by Bio-Sil SEC 250 size exclusion HPLC (SE-HPLC) in the presence of PHMB and PMSF. Similar results were obtained in which a 57 kDa and 50 kDa CbE were identified (Fig. 9, panel A). In the absence of the specific inhibitors, the CbE peaks eluted as a single peak. The smaller 32 kDa CbE was not identified by SE-HPLC. This result could be due to the conversion to another larger form through aggregation, to degradation to smaller peptides, or to substantial loss through sample preparation procedures including the concentration step. Three protein peaks (i.e., 104, 45, and 2.2 kDa) were detected spectrophotometrically at OD_{280} and were similar to the results obtained by the gel filtration (Fig 9, panel B). The second protein peak was determined to be the CbE peak containing the 57 and 50 kDa CbEs by matching the *Mr*s of the protein and αNC hydrolysis activity peaks although the protein profile was not completely resolved into two separate peaks (Fig. 9, panel B). The large amount of the first peak with a *Mr* ca. 104 kDa supports a possible aggregation of the CbE proteins because the majority of the large *Mr* proteins (i.e., >110 kDa protein in the Sephadex G-100 gel filtration chromatography) was substantially removed through the previous gel filtration step. Since no αNC hydrolysis activity was detected from the 104 kDa protein peak, the aggregation appears to cause inactivation of the CbE. The mechanism of the aggregation is not clear but sudden changes in the surrounding environment of the protein (e.g., salt concentration, pH, pressure, etc.) are the possible causes. The third peak was thought to be degraded polypeptides because of its small size (e.g., 2.2 kDa).

In summary, the p*I* 4.2-4.8 CbEs exist as at least three separate molecular forms (i.e., 57-59, 49-50, and 32 kDa CbE) under native conditions but the 57-59 and 49-50 kDa forms of CbE were predominant as demonstrated by the gel filtration

chromatography and SE-HPLC. Although the identities and natures of the different molecular forms are not completely understood, they are likely to be closely related each other because they co-purify through several purification steps.

b. Denatured *Mr*(s) of permethrin CbE

The purified p*I* 4.2-4.8 CbE sample from the preparative PAGE was analyzed by SDS-PAGE to determine the denatured *Mr*s of the CbEs. A representative protein banding pattern on SDS-polyacrylamide gel and the scanning densitogram of the gel are shown in Fig. 10, panel A and B, respectively. Three major protein bands (i.e., designated as band 1, 2, and 3; ca. 31, 46-48, and 59 kDa proteins, respectively) and trace amounts of minor protein bands (i.e., 39, 43, 44, 67, 73, 77, and 114 kDa proteins) were identified. The proteins associated with major bands 1, 2, and 3 accounted for ca. 46, 33, and 16% of the total amount of proteins as judged by scanning densitogram, respectively (Fig. 10, panel B). The denatured *Mr*s of the three major proteins matched well with the native *Mr*s of the permethrin CbE.

A slightly different banding pattern, however, was sometimes observed as shown in Fig. 10, panel C and D. In this case, the 31 kDa protein disappeared or was greatly reduced and a 25 kDa protein appeared in its stead. In addition, the 46 and 48 kDa proteins were not separated, resulting in the appearance of only one 48 kDa protein band. The 59 kDa protein was resolved into three closely adjacent bands (i.e., 57, 59, and 60 kDa proteins). The minor protein bands identified in this case were 39, 42, and 79 kDa proteins. The major band 1, 2, and 3 proteins in this case accounted for ca. 65, 22, and 6% of total amount of proteins as judged by scanning densitogram, respectively (Fig. 10, panel D). The minor proteins were thought to be contaminating proteins because the amount is relatively small (i.e., ca. 5 and 7% of the total amounts of protein) and because their *Mr*s are not correlated with the native *Mr*s of the permethrin CbE.

Because one of the above two banding patterns were always observed in different preparations of permethrin CbE, the protein bands in similar size range (i.e., 31 *vs*. 25 kDa protein, 46-48 *vs*. 48 kDa protein, and 59 *vs*. 57-60 kDa protein) appear to be related. How these different banding patterns are generated is not clear. It is likely that the different banding patterns are associated with differences in the hemolymph samples, themselves, such as unique fragmentation mechanisms rather than with purification procedures, which were the same for the purification of different batch of hemolymph samples.

Regardless of the banding pattern, however, no differences in separation patterns were evident in the presence or absence of reducing agent, β-mercaptoethanol (see lanes '-β' and '+β' in Fig. 10, panel A and C)). This finding indicates that none of the proteins identified by the SDS-PAGE (i.e., band 1, 2, and 3 proteins) are covalently associated polymeric proteins. The *Mr*s of the three major band proteins identified by SDS-PAGE matched well with the *Mr*s of three native molecular forms of CbE identified previously (i.e., 32, 49-50, and 57-59 kDa CbE). Therefore, the three major protein bands (i.e., band 1, 2, and 3 proteins) are likely to be the denatured forms of the permethrin CbE.

As a way of confirmation, renaturation of the proteins separated by SDS-PAGE was attempted. The purified CbE was denatured by incubating with SDS/β-mercaptoethanol with or without boiling, separated by SDS-PAGE, and renatured. After renaturation, the polyacrylamide gel was stained with αNB-dianisidine for the determination of CbE activity associated with each protein band (Fig. 11). No CbE activity could be restored when the CbEs were boiled prior to SDS-PAGE (Fig. 11, panel B). Without boiling in the denaturation step, however, the 48 kDa protein retained detectable level of αNB hydrolysis activity while the 59 and 31 kDa proteins remained inactive (Fig. 11, lane 1 and 2). These findings substantiate that the 48 kDa protein (i.e., band 2 protein) is a true CbE. Because the 59 and 31 kDa proteins (i.e.,

band 3 and 1 proteins, respectively) lacked αNB hydrolysis activity, it is still unresolved whether they are permanently inactivated CbEs or not.

To verify that the 57-60 and 25-31 kDa proteins are the denatured permethrin CbE, a [^{3}H]DFP-labeling experiment was conducted. Since permethrin CbE was determined to be strongly inhibited by DFP (see Table 5 in Inhibition of p*I* 4.8 and 4.5 CbEs by Selective Inhibitors), it was labeled with [^{3}H]DFP, separated by SDS-PAGE, and the radioactivity in gel slices determined. As illustrated in Fig. 12, high levels of radioactivity were detected in 5 zones of the gel (i.e., 30, 38, 46, 57, and 73 kDa zones). The 30 kDa zone (gel slice # 20-27) was determined to possess the highest radioactivity (i.e., 8280 cpm), followed by the 73 kDa zone (i.e., gel slice # 5-8, 6800 cpm), the 57 kDa zone (gel slice # 10-13, 5300 cpm), the 46 kDa zone (gel slice # 15-17, 1860 cpm), and the 38 kDa zone (i.e., gel slice # 18-19, 1520 cpm). This finding confirms that all the band 1, 2, and 3 proteins (i.e., 30, 46 and 57 kDa proteins, in this case) are true esterases and most likely the denatured forms of the permethrin CbEs. The proteins associated with the 73 and 38 kDa zones, in spite of being labeled with [^{3}H]DFP, are not likely related directly with the permethrin CbE. The amount of these proteins are relatively small (see minor band proteins identified by the SDS-PAGE in Fig. 10) and their sizes do not match with any native CbE on the basis of *Mr*. Thus, the 73 and 38 kDa proteins are likely associated with some other group of esterases, such as cholinesterases.

c. Multiple charged forms of permethrin CbE

Each major protein identified by the SDS-PAGE was further determined to be composed of ca. 3-6 proteins with very similar *Mr*s but different p*I* values through 2-DGE (urea-denatured IEF *vs*. SDS-PAGE) followed by silver staining (Fig. 13).

The band 1 protein (i.e., 25-31 kDa protein in the SDS-PAGE) was resolved into two groups of protein based on their clearly distinguishable p*I* values. The first p*I* 4.3-

4.7 protein group was composed of ca. 4 proteins with very similar *Mr*s (i.e., 31 kDa) but with uniformly different p*I* values (i.e., equal spacing of proteins in the first dimensional IEF). The second p*I* 4.1-4.2 protein group was composed of two proteins with very similar *Mr*s (i.e., 30-33 kDa range) but with different p*I* values. Based on the median p*I* values, the first p*I* 4.3-4.7/31 kDa protein group appears to be associated with the p*I* 4.5 form of the permethrin CbE while the second p*I* 4.1-4.2/30-33 kDa protein group appears to be the p*I* 4.2 form of the permethrin CbE.

The band 2 protein (i.e., 46-48 kDa protein in the SDS-PAGE) was resolved into 6-7 charged forms located in the pH 4.4-4.9 region. Thus, the p*I* 4.4-4.9/46 kDa protein group appears to be associated with the p*I* 4.8 form of the permethrin CbE on the basis of the median p*I* value.

The band 3 protein (i.e., 57-60 kDa protein in the SDS-PAGE) was resolved into two groups based on p*I* values. The first group, which was barely detected, was found in the pH 4.6-5.0 region while second group found in the pH 5.1-5.4 region. Both protein groups were composed of ca. proteins with very similar *Mr*s (i.e., 57 and 58 kDa for the first and second groups, respectively). The first p*I* 4.6-5.0/57 kDa protein group can be matched to the p*I* 4.8 form of the permethrin CbE based on its p*I* value. However, the amount of this protein group is too small to be the p*I* 4.8 form of the permethrin CbE, itself. The second p*I* 5.1-5.4 protein group may be a contaminating protein derived from the adjacent high pH fractions from the chromatofocusing step of the purification process.

In summary, the complete categorization of the denatured permethrin CbE based on its p*I* value was difficult because of overlapping p*I* values. By using the median p*I* value of each p*I* protein group, however, the molecular compositions of the denatured p*I* 4.8, 4.5, and 4.2 CbEs can be classified. The p*I* 4.8 CbE appears to be composed of 6-7 charged proteins with similar *Mr*s of ca. 46 kDa (or 46-48 kDa, if estimated from the SDS-PAGE). The p*I* 4.5 CbE appears to be composed of 4 charged proteins

with similar *Mr*s of ca. 31 kDa. The p*I* 4.2 CbE appears to be composed of 2 charged proteins with similar *Mr*s of ca. 30-33 kDa. The identity of the p*I* 4.6-5.0/57 kDa protein group is not clear although it can be classified by its median p*I* value as the denatured protein associated with the p*I* 4.8 CbE.

d. Quaternary structural association of permethrin CbE

The relative proportions of the band 1, 2, and 3 proteins (i.e., 25-31, 46-48, and 57-60 kDa proteins, respectively) were 46-65, 22-33, and 6-16% of the total proteins identified under denaturing conditions (Fig. 10). The most predominant form of denatured protein was the 25-31 kDa protein (i.e., band 1 protein), followed by the 46-48 kDa protein (i.e., band 2 protein), and the 57-60 kDa protein (i.e., band 3 protein). Under native conditions, however, the 49-50 and 57-59 kDa CbEs were quantitatively the most predominant forms with the smaller form (i.e., 32 kDa CbE) less prominent as determined by gel filtration and SE-HPLC (Fig. 8 and 9). Thus, the amount of the 25-31 kDa CbE appears to be increased while the amount of 57-59 kDa CbE is decreased under denaturing conditions whereas under native conditions the reverse is found. The amount of the 49-50 kDa CbE was present at similar levels under both native and denaturing conditions.

These findings suggest that majority of the 57-59 kDa CbE that is predominant under native conditions (i.e., native 57-59 kDa CbE) may be converted into the 25-31 kDa protein under denaturing conditions. One possible mechanism that explain this result is that the native 57-59 kDa protein is a noncovalent dimeric protein composed of two 25-31 kDa subunits. In this case, the native 32 kDa CbE is likely a dissociated subunit that was generated from the noncovalent dimeric 57-59 kDa CbE by changes in environmental conditions such as pH, ionic strength, etc. (61, 62). This hypothesis dictates, however, that the band 3 protein (i.e., 57-60 kDa protein), which consistently present in the denaturing conditions (i.e., SDS-PAGE and 2-DGE), should be a

separate monomeric CbE that is not directly related with the dimeric 57-59 kDa CbE. Another possibility, of course, is that the 25-30 kDa protein is cleaved from the native 57-59 kDa CbE by an unknown mechanism.

The band 2 protein (i.e., 46-48 kDa proteins) identified by the SDS-PAGE was determined to be the denatured form of the native 49-50 kDa CbE by the renaturation and [^{3}H]DFP- labeling experiments (see Fig. 11 and 12). It appears to be a monomeric protein with similar *Mr* under both native and denaturing conditions (i.e., 49-50 kDa under native condition *vs*. 46-48 kDa under denaturing condition). The small discrepancy in the *Mr*s between the native and denatured CbEs (i.e., 1-4 kDa difference) can be attributed to *Mr* estimation error.

The 57-59 kDa CbE was more sensitive to inhibition by PMSF whereas the 49-50 and 32 kDa CbEs were more sensitive to inhibition by PHMB (Fig. 8, panel A, Fig. 9. panel A). The p*I* 4.8 and p*I* 4.5 CbEs were determined to be selectively inhibited by PHMB and PMSF, respectively (Fig. 14), when the representative p*I* CbEs (i.e., fractions from the re-chromatofocusing of the purified permethrin CbE) were examined. The p*I* 4.2 CbE was selectively inhibited by PMSF even though the overall level of CbE hydrolysis activity associated with the p*I* 4.2 peak was too low to judge accurately (Fig. 14). Thus, the selectivity of PHMB and PMSF inhibition of the p*I* 4.8 and 4.2-4.5 CbEs were similar to the 49-50 kDa and 57-59 kDa CbEs, respectively.

In summary, the p*I* 4.8 CbE appears to be a monomeric protein and to be composed of ca. 6-7 charged forms whose *Mr*s are ca. 49-50 kDa. The p*I* 4.5 CbE appears to be dimeric protein composed of ca. 4 charged forms whose *Mr*s are 57-59 kDa under native conditions but 25-31 kDa under denaturing conditions. The p*I* 4.2 CbE is likely a dimeric protein rather than a monomeric protein from the fact that its inhibition specificity (i.e., PMSF-specific inhibition, see Fig. 14) did not coincide with that of the 32 kDa CbE identified by gel filtration (i.e., PHMB-specific inhibition, see Fig. 8, panel A). It also appears to be composed of ca. 2 charged forms whose *Mr*s are 57-59

kDa under native conditions but 30-33 kDa under denaturing conditions. This finding agrees well with the separation patterns produced during 2-DGE where the denatured 46, 31, and 30-33 kDa proteins were detected in the pH 4.4-4.9, 4.3-4.7, and 4.1-4.2 regions of the gel, respectively.

2. Naphthyl Substrate Specificities of the p*I* 4.8, 4.5, and 4.2 CbEs

The kinetic constants (i.e., K_m and V_{max}) for the p*I* 4.8, 4.5, and 4.2 CbEs were determined using three naphthyl substrates, αNA, αNB, and αNC (Fig. 15, see Appendix A for chemical structure). With all three substrates, a consistent tendency was established that results in decreased K_m values as the negative charge associated with the three p*I* forms of the CbE decreased (Fig. 15, panel A). The K_m values using αNA were 191, 83, and 45 μ*M* for the pI 4.2, 4.5, and 4.8 CbEs, respectively. The K_m values using αNB were 105, 75, and 36 μ*M* for the p*I* 4.2, 4.5, and 4.8 CbEs, respectively. The K_m values using αNC were 51, 33, and 14 μ*M* for the p*I* 4.2, 4.5, and 4.8 CbEs, respectively. This consistent tendency implies that reduction of negative charge associated with the CbE may result in an increase in affinity to the three naphthyl substrates tested, regardless of the substrate, itself.

When the K_m values for each substrate were compared across each p*I* CbE form, a consistent tendency of decreasing K_m values was observed as the hydrophobicity of substrate increased, regardless of the charge state of the CbE (Fig. 15, panel A). The K_m values of the p*I* 4.8 CbE using αNA, αNB, and αNC were 45, 36, and 14 μ*M*, respectively. The K_m values of the p*I* 4.5 CbE using αNA, αNB, and αNC were 83, 75, and 33 μ*M*, respectively. The K_m values of p*I* 4.2 CbE using αNA, αNB, and α NC were 191, 105, and 51 μ*M*, respectively. This result indicates that the catalytic sites for all three p*I* CbEs are hydrophobic so that they exhibit higher affinities toward the more hydrophobic substrates.

When V_{max} values for each substrate are compared across each of the three forms of the p*I* CbEs, a consistent tendency of increasing V_{max} values was observed as the negative charge of the p*I* CbEs decreased, regardless of the naphthyl substrate used (Fig. 15, panel B). The V_{max} values using αNA were 0.8, 1.1, and 2.5 μmole/min/mg protein for the p*I* 4.2, 4.5, and 4.8 CbEs, respectively. The V_{max} values using αNB were 0.6, 1.3, and 1.9 μmole/min/mg protein for the p*I* 4.2, 4.5, and 4.8 CbEs, respectively. The V_{max} values using αNC were 0.3, 0.5, and 1.1 μmole/min/mg protein for the p*I* 4.2, 4.5, and 4.8 CbEs, respectively. This consistent tendency suggests that the less negatively charged CbE (i.e., p*I* 4.8 CbE) is more efficient in the hydrolysis of these naphthyl substrates.

When the V_{max} values for each substrate were compared within each p*I* CbE form, the V_{max} values decreased as the carbon number of the substrate increased, regardless of the level of negative charge of the CbE (Fig. 15, panel B). The V_{max} values of the p*I* 4.8 CbE using αNA, αNB, and αNC were 2.5, 1.9, and 1.1 μmole/min/mg protein, respectively. The V_{max} values of the p*I* 4.5 CbE using αNA, αNB, and αNC were 1.1, 1.3, and 0.5 μmole/min/mg protein, respectively. The V_{max} values of p*I* 4.2 CbE using αNA, αNB, and αNC were 0.75, 0.58, and 0.25 μmole/min/mg protein, respectively. These results indicate that the hydrolytic efficiency of the CbEs is reduced as relatively more hydrophobic substrate, such as αNC, are used in spite of their relatively higher affinity to the more hydrophobic substrate. This trend was also maintained in the hydrolysis of α-naphthyl caprylate (i.e., C8 acyl naphthyl ester) where the V_{max} and K_m values of the combined p*I* 4.2-4.8 CbEs were ca. 0.13 μ mole/min/mg protein and 13 μ*M*, respectively (data not shown).

The [^{14}C]*trans*-permethrin hydrolytic activities of the p*I* 4.8, 4.5, and 4.2 CbEs were determined in a similar manner (Table 4). As seen in the hydrolysis of naphthyl substrates, the relatively less negative charged CbE possessed higher [^{14}C]*trans*-permethrin hydrolytic activity. The [^{14}C]*trans*-permethrin hydrolysis rates by the p*I*

4.8, 4.5, and 4.2 CbEs were 70, 66, and 18 pmole/hr/mg protein. This result agrees well with the previous findings that showed the same trend in the hydrolysis of permethrin by the charged forms of the permethrin CbEs prepared from the direct chromatofocusing of hemolymph (see Table 1). Nevertheless, the hydrolysis rates of permethrin were extremely low compared to those of the naphthyl substrates. The permethrin hydrolysis rates by the permethrin CbEs were ca. 0.5-1 $\times 10^6$ times lower when compared to the V_{max} values obtained with αNC.

In summary, the low rate of permethrin hydrolysis and the high affinity toward hydrophobic substrates implies a major sequestration role for the permethrin CbE in CPB resistance to permethrin. The less negative charged CbEs (e.g., p*I* 4.8 and 4.5 CbEs) are, nevertheless, more active in the hydrolysis of permethrin and the naphthyl substrates, which indicates that they are major CbEs associated with permethrin resistance in the PE-R strain of CPB. It is not clear, however, whether the differences in the kinetic constants for the naphthyl substrates and in the rates of permethrin hydrolysis among the p*I* 4.8, 4.5, and 4.2 CbEs are due to different catalytic sites or due to other factors modifying the hydrolysis activity of these enzymes.

3. Inhibition of p*I* 4.8 and 4.5 CbEs by Selective Inhibitors

The inhibition of the p*I* 4.8 and 4.5 CbEs by several inhibitors is presented in Table 5. DEF, a potent CbE inhibitor, was not particularly effective in the inhibition of the p*I* 4.8 and 4.5 CbEs when compared to the level of inhibition achieved on typical pyrethroid-hydrolyzing CbEs from other species of arthropod (34, 63). The calculated I_{50} values for DEF were 1068 μ*M* and 710 μ*M* for the p*I* 4.8 and 4.5 CbEs, respectively. There was no significant difference in the level of inhibition of the two CbEs by DEF. Thus, the p*I* 4.8 and 4.5 CbEs are different from the classical groups of CbE in terms of DEF sensitivity. In contrast, DFP was a very potent inhibitor for both p*I* 4.8 and 4.5 CbEs (i.e., I_{50} values were 0.4 μ*M* and 0.27 μ*M* for the p*I* 4.8 and

4.5 CbEs, respectively, Table 5). This finding establishes both CbEs as typical B-type esterases based on the definition of Aldridge (64).

Addition of PMSF, another serine-hydroxyl group esterase inhibitor, resulted in differential inhibition between the p*I* 4.8 and 4.5 CbEs (Table 5, see Appendix B for the chemical structure of PMSF). The p*I* 4.5 CbE was three times more sensitive to PMSF inhibition than the p*I* 4.8 CbE as judged by I_{50} values (i.e., 232 μ*M* and 80 μ*M* for the p*I* 4.8 and 4.5 CbEs, respectively). The differential inhibition of the p*I* 4.8 and 4.5 CbEs by PMSF suggests that structure and/or conformation associated with the serine hydroxyl moiety of the catalytic sites of the p*I* 4.8 and 4.5 CbEs are not identical.

The p*I* 4.8 and 4.5 CbEs were also inhibited by parathion (Table 5). However, no significant difference between the levels of inhibition of the two CbEs were apparent. The potency of parathion (I_{50} value 71.8-73.1 μ*M*) is 180-270 times lower than that of DFP but it is 1.1-3.3 and 10-15 times more potent than PMSF and DEF, respectively, as judged by I_{50} values. This moderate level of inhibition is likely caused by parathion itself not by its oxon analogue because the parathion standard used in this inhibition study was highly pure (i.e., 99.9%) and the test stock solution was freshly prepared prior to use. If this is true, the nature of the inhibition by parathion is more likely due to hydrophobic affinity binding of parathion to the enzyme rather than to phosphorylation of enzyme because thio-phosphates are generally poor phosphorylating agents. Eserine was the least potent inhibitor among the serine-hydroxyl group esterase inhibitors tested (Table 5). The I_{50} values for the p*I* 4.8 and 4.5 CbEs were in the range of 2-3 mM. Because eserine is a potent cholinesterase inhibitor, the permethrin CbE is likely to be quite distinct from cholinesterases. Since the positively charged quaternary ammonium ion of eserine is one of the most essential factors in its toxicodynamic mechanism, the lack of substantial inhibition by eserine implies that the p*I* 4.8 and 4.5 CbEs do not have an anionic binding site that is available for interaction

with positively charged inhibitors, including eserine. This result corroborates the previous finding that the charged forms of CbE, particularly less negatively charged forms of CbE (e.g., p*I* 4.8 CbE), possesses a hydrophobic substrate binding site, which is not likely compatible with positively charged substrates.

The p*I* 4.8 CbE was determined to be 3-17 times more sensitive to inhibition by PHMB, a cysteine group arylesterase inhibitor, than the p*I* 4.5 CbE when the percent inhibition at each concentration of PHMB was compared (Table 5, see Appendix B for the chemical structure of PHMB). This agreed well with the specific inhibition patterns observed in previous experiments (see Fig. 14). Although a dose-dependent inhibition was observed at concentrations of PHMB below 1-5 μ*M,* no further inhibition was observed above this concentrations as illustrated in Fig. 16, panel A. Neither the p*I* 4.8 nor 4.5 CbE was completely inhibited even at concentrations of PHMB as high as 1 m*M* (Fig. 16, panel A). PHMB was more potent than all the other serine-hydroxyl group esterase inhibitors tested except DFP (i.e., 21-66% inhibition by PHMB *vs.* 0%, 0-9%, 5-9%, and 100% inhibitions by PMSF, DEF, parathion, and DFP, respectively, data not shown) when the inhibition level at the same low concentration of inhibitors was compared (e.g., 5 μ*M*).

The time-progressive inhibition by 5 μ*M* PHMB is presented in Fig. 16, panel B. The intercept value on the vertical axis (i.e., ca. 21% inhibition at 0 min preincubation time) indicates a rapid equilibrium process that is usually a feature typical of reversible inhibition. Conversely, the straight inhibition line (i.e., first order rate of inhibition) that is proportional to the preincubation time is indicative of irreversible inhibition. These findings suggest that PHMB inhibits the p*I* 4.5 and 4.8 CbEs both in a reversible manner through high affinity binding and in an irreversible manner, most probably, through covalent modification of free sulfhydryl groups. The lack of complete inhibition by PHMB implies that it functions as an allosteric inhibitor that binds to non-catalytic site(s) and downregulates the CbE activity. Additionally, the PHMB-binding

site(s) on the CbE appear to be hydrophobic and to contain free sulfhydryl moiety(ies) for the efficient interaction and modification with relatively low concentrations of PHMB that is also hydrophobic. The lower sensitivity but similar pattern of inhibition of the pI 4.5 CbE by PHMB compared to the p*I* 4.8 CbE suggest that the PHMB-binding site of the p*I* 4.5 CbE is less hydrophobic and that its overall greater negative charge may be responsible for the lowered affinity for PHMB.

In contrast to the inhibition by PHMB, the addition of $HgCl_2$, another sulfhydryl group inhibitor, resulted in a distinctly different inhibition profile on the p*I* 4.8 and 4.5 CbEs (Table 5). The inhibition potency of $HgCl_2$ was lower than PHMB (i.e., 0-4% inhibition by 50 μ*M* $HgCl_2$ *vs*. 21-66% inhibition by 5 μ*M* PHMB) but complete inhibition was obtained by 1 m*M* $HgCl_2$. The potency and efficacy differences between PHMB and $HgCl_2$ inhibitions imply that $HgCl_2$ is more likely inhibitory by nonspecific modifications of sulfhydryl groups rather than by specific interaction between the CbE and inhibitor as in the case of PHMB inhibition. This nonspecific interaction may be a reason for the lack of significant differences in the inhibition of the p*I* 4.8 and 4.5 CbEs by $HgCl_2$ (Table 5). These results further suggests that hydrophobicity or stereospecificity is an essential factor in determining inhibitory potency of hydrophobic compound such as PHMB.

NaCN (i.e., 100 μ*M)* did not inhibit a combined p*I* 4.2-4.8 CbE preparation indicating that transition metals are not involved in catalysis or enzyme stability (Table 5). The lack of inhibition by high concentration of EDTA (i.e., 890 μ*M*) supports our contention that the p*I* 4.2-4.8 CbEs are not metalloenzymes (Table 5). Also, E-64, a cysteine group protease inhibitor, and pepstatin, an aspartic acid protease inhibitor, were not inhibitory to the p*I* 4.2-4.8 CbEs at concentrations previously reported to be effective (i.e., 20 μ*M* E-64 and 10 μ*M* pepstatin, see Ref. 65)(Table 5). These findings suggest that the p*I* 4.2-4.8 CbEs are not likely to be cysteine- or aspartic acid-type protease and implies additionally that neither cysteine nor acidic amino acid residues,

such as aspartic acid and glutamic acid, are likely associated with the catalytic sites of the p*I* 4.2-4.8 CbEs.

4. PCMB-Agarose Affinity Chromatography of Permethrin CbE

At least three CbE activity peaks (i.e., peak I, II, and III; peak fraction # 10, 13, and 21, respectively) as judged by αNC hydrolysis were identified from the washing fractions (i.e., fractions not bound to PCMB-agarose) although the peak III possessed negligible amount of activity (i.e., 0.04-0.06 OD_{600})(Fig. 17). The CbEs associated with the three eluted peaks were more inhibited by PMSF (87.6, 93.7, and 97.5% inhibitions for the peak I, II, and III, respectively) than PHMB (7.8, 15.6, 10.0% inhibitions for the peak I, II, and III, respectively) indicating that their binding potentials for PCMB (or PHMB) were poor. The proteins associated with these three peaks appear to be the p*I* 4.5-4.2 CbEs based on the inhibition specificities (i.e., more sensitive to PMSF- than PHMB-inhibition). The earliest eluted peak (i.e., peak I) appears to have the least binding capacity for PCMB (or PHMB) followed by peak II and III, which are also slightly more inhibited by PHMB.

The total combined hydrolytic activity of the three peaks accounted ca. 41% of the initial activity of the CbE sample applied to the PCMB-column indicating that considerable amounts of CbEs are immobilized by PCMB. However, no CbE activity was observed in the fractions eluted either with the elution buffer A (i.e., 0-1.0 *M* NaCl) or with the elution buffer B (i.e., 50 m*M* DTE) (Fig. 17). This result is suggestive of a strong interaction between PCMB and the remaining CbEs. The lack of CbE activity in the fractions eluted with the elution buffer B was later determined to be due, in part, to the inactivation of the CbEs by high concentration (i.e., 50 m*M*) of DTE. Nevertheless, when a small aliquot (i.e., 20 μl) of bead was taken from the column after elution with the elution buffer A and assessed for αNC hydrolysis activity, it showed detectable activity (i.e., 0.091 OD_{600}). The retention of hydrolytic

activity of the PCMB-bound CbE implies that the active site of the retained CbE is physically separated from the PCMB-binding site. This finding agrees well with the previous results that showed an allosteric inhibition property of PHMB (see Fig. 16). Although the PCMB-bound CbE could not be eluted as an active enzyme from the column, it appeared to be mainly the p*I* 4.8 CbE.

5. Characterization of the Hydrophobic Nature of the p*I* 4.8 and 4.5 CbEs

To determine any possible relationship between the charged states of the p*I* 4.8 and 4.5 CbEs and their surface hydrophobicity, purified p*I* 4.8 and 4.5 CbEs (i.e., pH 4.9-4.6 and pH 4.6-4.2 fractions from chromatofocusing, respectively) were separated by methyl HIC (Fig. 18). Three CbE peaks (i.e., peak I, II, and III CbEs in an increasing order of hydrophobicity) were commonly identified from the HIC of both the p*I* 4.8 CbE (i.e., 4.8 HIC) and the p*I* 4.5 CbE (i.e., 4.5 HIC) as judged by αNB and αNC hydrolysis. The presence of multiple CbEs with different hydrophobicities were indicated by the unique separation pattern. The peak II CbE was the most predominant form of CbE from the 4.8 HIC (Fig. 18, panel A) while the peak III CbE was the most predominant form from the 4.5 HIC (Fig. 18, panel B) in terms of hydrolytic activity. The peak II CbE was more specific in its hydrolytic activities toward αNC, a property associated with the p*I* 4.8 CbE (see αNC and αNB hydrolysis line in Fig. 18). The peak III CbE was more specific in its hydrolytic activity toward αNB, a property associated with the p*I* 4.5 CbE. The peak II CbE was more selectively inhibited by PHMB than PMSF (i.e., 61.0-76.1% inhibition by PHMB *vs.* 0-1.7 % inhibition by PMSF) whereas the peak III CbE was more selectively inhibited by PMSF than by PHMB (i.e., 41.8-56.0 % inhibition by PMSF *vs.* 0-13.1 % inhibition by PHMB). These results on substrate and inhibition specificities indicate that peak II CbE and peak III CbE are the major representative forms of CbE present in the p*I* 4.8 and 4.5 CbE samples, respectively. Using HIC, the p*I* 4.8 CbE, less

negatively charged form of CbE, was actually found to be less hydrophobic in surface hydrophobicity than the p*I* 4.5 CbE (see relative elution order of peaks I, II, and III, Fig.). This finding suggests that the negative-charge states of CbE do not equate to the overall surface hydrophobicity of CbE. Although surface hydrophobicity of the p*I* 4.8 CbE is less than that of the p*I* 4.5 CbE, the substrate binding site of the p*I* 4.8 CbE is more hydrophobic than that of the p*I* 4.5 CbE (see Fig.). This discrepancy between the hydrophobicity of substrate binding site and the overall surface hydrophobicity of the CbE suggests that the hydrophobic substrate-binding site may be separate from the domain determining overall surface hydrophobicity of CbE or that the hydrophobic substrate-binding site may be in a hydrophobic pocket concealed from the enzyme surface.

The peak I CbE was less hydrophobic than the peak II CbE but was similar to peak II CbE in that it was more specifically inhibited by PHMB (i.e., 60.8-70.0% inhibition by PHMB *vs.* 0-9.8% inhibition by PMSF). One possibility is that under high salt conditions, peak I CbE is formed by the aggregation of a portion of the peak II CbEs through an attraction between hydrophobic domains that results in a physical masking of hydrophobic domains and consequently reduction of hydrophobicity. If this is true, the PHMB-binding site would have been located in a separate region from the domain determining the surface hydrophobicity since the peak I CbE still selectively inhibited by PHMB.

A peak IV CbE was found only in the 4.8 HIC (Fig. 18, panel A). It possessed more specific hydrolysis activity toward αNC than αNB but was only slightly inhibited by either PHMB or PMSF (i.e., 1.0-10% and 0-5.6% inhibitions by PHMB and PMSF, respectively). The substantial reduction of PHMB-specific inhibition allows the speculation that the hydrophobic PHMB-binding site(s) can be reduced by the aggregation of the CbE through the attraction between the PHMB-binding sites in high salt conditions. If the domain determining the surface hydrophobicity is separate from

the PHMB-binding hydrophobic region as suggested in the aggregation of peak II CbE, it is likely to be more exposed to the outside of the aggregated protein and be readily available for interaction with HIC binding moieties. This scenario would render a relatively more hydrophobic property to the aggregated protein as evidenced in the late-elution HIC profile of the peak IV CbE.

6. Effects of pH and Temperature on Permethrin CbE

Optimum pH for αNC hydrolysis activity of the p*I* 4.8 and 4.5 CbE were determined to be approximately pH 7 for both CbEs (Fig. 19, panel A). Because CPB hemolymph is pH 7.4, the permethrin CbE would be most active in its endogenous milieu. The hydrolytic reaction of the p*I* 4.5 CbE showed a typical bell-shaped pH profile implicating the involvement of at least two ionizable groups in catalysis. The p*I* 4.8 CbE had an elevated level of hydrolytic activity at higher pH (i.e., pH 7-10) when compared with the p*I* 4.5 CbE. At lower pH (i.e., pH 3-7), they closely resembled each other. The similarities of the pH-activity profiles at low pH observed for both CbEs indicates that certain common ionizable group(s) with p*K* values of ca. 6, such as the imidazole ring in histidine, may exist in the catalytic sites of both enzymes. It is not still clear, however, whether the retention of hydrolytic activity at the high pH range found in the p*I* 4.8 CbE is due to specific differences in certain ionizable group with p*K* value of ca. 8-9 (e.g., ionizable sulfhydryl group of cysteine) or due to selective difference in other non-ionizable amino acid residue between the two CbEs. Since the substrate binding site of the p*I* 4.8 CbE is thought to be more hydrophobic than that of the p*I* 4.5 CbE (see Fig. 15), a hydrophobic amino acid having an ionizable group with high pK values, such as tyrosine (i.e., pK_R=10.1) or lysine (i.e., pK_R=10.8), is more likely to function in the catalytic site of the p*I* 4.8 CbE rather than in the catalytic site of the p*I* 4.5 CbE.

The effects of temperature on αNC hydrolysis by the p*I* 4.8 and 4.5 CbEs are presented in Fig. 19, panel B). Both p*I* 4.8 and 4.5 CbEs showed the highest activity at ca. 50°C. However, the p*I* 4.5 CbE lost ca. 50% of activity at 60°C whereas the p*I* 4.8 CbE activity was relatively unaffected at 60°C. This finding indicates that the p*I* 4.8 CbE is conformationally more stable than the p*I* 4.5 at high temperature.

7. Glycoprotein Nature of Permethrin CbE

To determine if the permethrin CbE is a glycoprotein, purified permethrin CbE (i.e., p*I* 4.2-4.8 CbEs) was separated by ConA-sepharose affinity chromatography. As illustrated in Fig. 20, no CbE activity as judged by αNC hydrolysis was found in the eluted fractions even after extensive washing of the column with binding buffer. This indicates that the permethrin CbE binds tightly to ConA and thus has *N*-glycosylated glycans containing α-D-mannopyranosyl, α-D-glucopyranosyl and/or sterically-related residues available for binding (66, 67). Bound CbE was eluted from the ConA-column by applying binding buffer amended with high concentration of mannopyranoside (i.e., 0.5 *M*). The CbE, however, was not eluted as a single sharp peak but rather eluted as several contiguous peaks (Fig. 20). This finding is suggestive of the possibility that the p*I* 4.2-4.8 CbEs are composed of several forms that differ in their *N*-glycosylation levels.

For comparative purposes, the pI < 4.0 CbE, which is not related to permethrin resistance in CPB, was also separated by ConA-Sepharose affinity chromatography under the same conditions. This highly negative-charged CbE was not eluted until more than 10 column-volumes of elution buffer (i.e., 53 ml) was applied. This indicates that the level of *N*-glycosylation of the p*I* < 4.0 CbE is higher than that associated with the p*I* 4.2-4.8 CbEs.

To determine whether the glycosylation levels are directly related with the negative charge level, the permethrin CbE was *N*-deglycosylated using F/*N*-glycosidase F. The

N-deglycosylated and control CbE (i.e., incubated in deglycosylation buffer without F/*N*-glycosidase F) were analyzed by IEF. As judged by the separation patterns of CbE bands on the IEF gel, neither a shift in the position of the CbE bands nor a change in the number of CbE bands was observed (Fig. 21, panel A). When the control CbE was analyzed by SDS-PAGE, 4 protein bands were identified (i.e., 46.2, 58.5, 95.3, and 104 kDa proteins in control sample)(Fig. 21, panel B). The 30 kDa protein, which is one of the major protein bands routinely identified by SDS-PAGE (i.e., band I protein, Fig. 10), disappeared and 104 and 95 kDa band proteins appeared. Although the identities of the 104 and 95 kDa proteins are not known, they appear to be generated by the aggregation of the 30 kDa protein during the long period of incubation (i.e., 20 hrs) with deglycosylation buffer (50 m*M* potassium phosphate, 20 m*M* EDTA, pH 7.5) and/or by aggregation during electrophoresis. Aggregation of the 30 kDa protein to multimeric forms was demonstrated in a 2-DGE format (i.e., 1st dimensional SDS-PAGE vs. 2nd dimensional SDS-PAGE, Fig. 22). The appearance of 60, 90, 120 kDa proteins formed in the second dimensional gel from only the 30 kDa protein region in the first dimensional gel corroborates that the large multimeric forms are due to 30 kDa aggregates. The *Mr*s of all proteins from the deglycosylated sample were measured to be smaller than those of corresponding proteins from the control sample (i.e., 1.9, 2.4, 3.7, and 3.5 kDa reduction in *Mr* for the 46.2, 58.5, 95.3, and 104 kDa proteins, respectively). This result indicates that the size of *N*-glycan moieties of permethrin CbE is 1.9-3.7 kDa under the assumption that the 95-104 kDa protein is aggregated form of the 30 kDa protein.

In summary, the charge heterogeneity of the permethrin CbE is not associated with the degree of *N*-glycosylation but is likely associated with the amino acid structure of polypeptide itself and/or possibly with *O*-glycan moieties.

8. Inhibition of Permethrin CbE by Insecticides and Eserine

Inhibition experiments were performed on the p*I* 4.8 and 4.5 CbEs, to determine whether the permethrin CbE can interact with several groups of insecticides and eserine that are not considered to be strong irreversible B-type esterase inhibitors (see Appendix C for the chemical structure of insecticides and eserine) and whether different charged forms of CbE interact with such compounds differentially. As illustrated in Fig. 23, the p*I* 4.8 and 4.5 CbEs were inhibited in a dose-dependent manner by permethrin, cypermethrin, DDT, abamectin, and azinphos-methyl but not by eserine over a concentration range of 5-80 μ*M*. No significant differences in the level of inhibition between the p*I* 4.8 and 4.5 CbEs were found (*t*-test, $n=4$, $P>0.05$). The highest level of inhibition was observed in the presence of cypermethrin (i.e., 15.6-31.8%) followed by DDT (i.e., 11.7-28.4%), permethrin (i.e., 12.5-22.0%), abamectin (i.e., 3.6-22.8%), and azinphos-methyl (i.e., 8.9-12.7%). Only slight inhibition (i.e., 3.4-4.2%) was observed in the presence of a 320 μ*M* concentration of eserine. The inhibition by DDT and abamectin is likely to be due to a high-affinity binding to a non-catalytic hydrophobic site of the CbEs as initially suggested in the PHMB inhibition experiments (see Table 5 and Fig. 16). Because neither of the two compounds have an ester moiety, they are not expected to interact with the esteratic catalytic site of the CbE.

The levels of inhibition by the insecticides and eserine appear to increase proportionally with the hydrophobicity of the compounds as judged by their water solubilities (i.e., cypermethrin, 0.005-0.01 ppm; DDT, 0.001-0.002 ppm; permethrin, 0.2 ppm; abamectin, 0.01 ppm; azinphos-methyl, 33 ppm; and eserine sulfate, 20%). The positively charged quaternary ammonium ion moiety of eserine adversely influences the hydrophobicity of eserine and apparently its inhibitory potency. These findings corroborate that the p*I* 4.8 and 4.5 CbEs can interact with a variety of hydrophobic compounds through non-specific hydrophobic site(s). The lack of

significant differences in the levels of inhibition by specific insecticidal compounds between the p*I* 4.8 and 4.5 CbEs implies that the different levels of negative charge associated with these two forms of CbE are not particularly important in their interaction with these insecticides. However, the hydrophobicities of the insecticidal compounds seem to be important with the more hydrophobic compounds being the best inhibitors of the p*I* 4.8 and 4.5 CbEs.

To characterize the inhibition of the permethrin CbE by permethrin and DDT in detail, inhibition kinetics of these two insecticides against the permethrin CbE (i.e., p*I* 4.5-4.8 CbEs) were analyzed (Fig. 24 and 25). As demonstrated by a Lineweaver-Burk double reciprocal plot, addition of permethrin resulted in an increase in the K_s value (i.e., substrate dissociation constant, see 1/[S]-axis intercepts in Fig. 24, panel A) and a decrease in the V_{max} value (see 1/υ-axis intercepts in Fig. 24, panel A) for αNC. These results are consistent with a mixed-type noncompetitive inhibition (i.e., mixed kinetics of competitive and noncompetitive inhibition) of the CbE and support the contention that permethrin can bind to a non-catalytic site as well as a catalytic site of the permethrin CbE. The K_s constant for αNC calculated from the initial double reciprocal plot was 35 μ*M* (see 1/[S]-axis intercept of control regression line in Fig. 24, panel A). The K_i (i.e., inhibitor dissociation constant from enzyme-inhibitor, EI, complex) and αK_i (i.e., inhibitor dissociation constant from the enzyme-substrate-inhibitor, ESI, complex) values for permethrin were calculated as 137 and 274 μ*M*, respectively (see [I]-axis intercepts in Fig. 24, panel B and C, respectively). From these results, the relative affinity of permethrin to free CbE (E) and to CbE-substrate (ES) complex can be calculated to be 0.26 and 0.13, respectively, of that determined for αNC. The data point from 80 μ*M* permethrin concentration was not included in linear regression of the replots since it deviated greatly from the data points from the lower concentration (0-40 μ*M*) possibly due to the limited solubility of permethrin in the reaction buffer (see square symbol in Fig. 24, panel B and C).

Inhibition kinetic constants were likewise determined for DDT. As established from the double reciprocal plot (Fig. 25, panel A), DDT resulted in a reduction in the V_{max} without changing of K_s value, indicating a typical noncompetitive inhibition process. This finding demonstrates that DDT binds only to the non-catalytic site and is consistent with the chemical structure of DDT in that it does not contain any ester moiety necessary for binding to the catalytic site. The nature of the noncompetitive inhibition by DDT is likely associated with the high affinity of DDT to the hydrophobic non-catalytic site(s) on the permethrin CbE. The K_s constant determined from the double reciprocal plot (see 1/[S]-axis intercept of control regression line in Fig. 25, panel A) and the K_i constant for DDT determined from the replot (see [I]-axis intercept in Fig. 25, panel B) were 75 and 190 μM, respectively. From these values, the affinity of DDT to the permethrin CbE was estimated as approximately 2.5 times less than that of the αNC substrate. The data point from 80 μM DDT concentration was not included in linear regression of the replots since it deviated greatly from the data points from the lower concentration (0-20 μM) possibly due to limited solubility of high concentration of DDT in the reaction buffer as discussed previously for permethrin (see square symbol in Fig. 25, panel B).

In summary, the inhibition kinetics of permethrin and DDT are consistent with the existence of hydrophobic non-catalytic site(s) to which hydrophobic compounds can bind nonspecifically in addition to the hydrophobic catalytic site to which only hydrophobic ester compounds can bind. Because the permethrin CbE is capable of only an extremely low rate of permethrin hydrolysis (i.e., see Table 4), the hydrophobic interaction between the CbE and permethrin is likely to play a major role in the sequestration of permethrin even though the affinities of permethrin and DDT are not quite as high as that for the αNC substrate (i.e., 3.8 and 2.5 times lower affinity for permethrin and DDT as judged by K_i and K_s constants, respectively). Thus, the sequestration of permethrin by the permethrin CbE is more likely governed by a rapid

equilibrium process between the CbE and permethrin at both the catalytic and non-catalytic sites rather than by a slow acylation-deacylation process at the catalytic site. Also, noncompetitive inhibition of the permethrin CbE by DDT implies that DDT can be similarly sequestered by the non-catalytic hydrophobic site of the permethrin CbE. The interaction of cypermethrin with the permethrin CbE must be similar to that of permethrin because of its close structural relationship to permethrin. The interaction of abamectin with the permethrin CbE is likely occurred by nonspecific binding of abamectin to non-catalytic site of the CbE, as demonstrated in DDT, since abamectin is also a non-ester compound. Finally, the nonspecific sequestration of DDT by the permethrin CbE may be a factor in the cross-resistance of the PE-R strain to DDT in addition to the possible target site insensitivity mechanism associated with the nervous system (60). The previously reported cross-resistance of the PE-R strain to other pyrethroids, such as cyflumethrin and fenvalerate, can be explained in a similar manner (7).

D. Development of Immunoassay for the Detection of Permethrin CbE

1. Purification of Denatured 30, 48, and, 60 kDa Immunogens

Denatured CbE protein immunogens were purified by chromatofocusing of hemolymph followed by preparative SDS-PAGE and electro-elution. The purified denatured proteins (i.e., 30-31, 46-48, and 57-60 kDa proteins) were used as immunogens (i.e., designated as 30, 48, and 60 kDa immunogens, respectively) for the generations of polyclonal antibodies. The purification scheme resulted in a high degree of purity for each immunogen as judged by SDS-PAGE (Fig. 26).

2. Titration of Antibody and Evaluation of Cross-Reactivity of Antibodies to Immunogens by Antibody Capture Immunoassay

After 3 booster injections of the 30 kDa immunogen and 7 booster injections of the 48 and 60 kDa immunogens, antisera were collected and their titers analyzed by an antibody capture immunoassay (59)(Fig. 27). The antiserum raised against the 30 kDa immunogen (i.e., 30 kDa antiserum) possessed the highest titer. The 30 kDa antiserum produced significantly higher signal level compared to control serum (i.e., the serum collected before immunization) up to the level of 10^6-fold dilution (ca. 0.40 OD_{450} difference in the signal level between the 10^6-fold diluted 30 kDa antiserum and control serum, Fig. 27, panel A). The antisera raised against 48 kDa immunogen (i.e., 48 kDa antiserum) and 60 kDa immunogen (i.e., 60 kDa antiserum) possessed relatively lower titers so that distinguishable signals from that of control serum were only observed by the sera diluted less than 10^4-fold (i.e., 0.47 and 0.51 OD_{450} differences using a 10^4-fold diluted 48 and 60 kDa antisera, respectively, Fig. 27, panel B and C). The relative titer of the 30 kDa antiserum was determined therefore to be ca. 100 times higher than that of the 48 and 60 kDa antisera. This finding was unexpected in that the 30 kDa antiserum was collected after only 3 separate booster injections but contained higher titer than the 48 and 60 kDa antisera collected after 7 separate booster injections. This result suggests that the 30 kDa immunogen is more immunogenic than the 48 and 60 kDa immunogens.

The 30 kDa antiserum also showed strong cross-reactivities to the 48 and 60 kDa immunogens. In the detection of the 48 kDa immunogen (Fig. 27, panel B), the signal level produced in the presence of a 10^5-fold diluted 30 kDa antiserum (i.e., 0.40 OD_{450}) was similar to that produced in the presence of a 10^4-fold diluted 48 kDa antiserum (i.e., 0.47 OD_{450}). In the detection of the 60 kDa immunogen (Fig. 27, panel C), a signal level of 0.5 OD_{450} was obtained in the presence of a ca. 5×10^4-fold diluted 30 kDa antiserum whereas a similar signal level (i.e., 0.51 OD_{450}) was obtained

in the presence of a 10^4-fold diluted 60 kDa antiserum. Thus, the 30 kDa antiserum was determined to possess ca. 5 and 10 times higher sensitivities in the detection of the 60 and 48 kDa immunogens, respectively, than the 48 and 60 kDa antisera, themselves.

The 48 kDa antiserum, likewise, revealed cross-reactivities to the 30 and 60 kDa immunogens. In the detection of the 30 and 60 kDa immunogens, the 48 kDa antiserum was at least 10 times more sensitive when compared to control sera but was ca. 2-100 times less sensitive when compared to the signal level obtained in the presence of their own antisera (Fig. 27, panel A and C), as judged by comparing the serum dilution factors that produced the same levels of signal (i.e., 0.75 OD_{450} levels in the detection of the 30 kDa immunogen; 0.5 OD_{450} levels in the detection of the 60 kDa immunogen).

As expected, the 60 kDa antiserum also showed cross-reactivities to the 30 and 48 kDa immunogens. The 60 kDa antiserum detected the 30 and 48 kDa immunogens at ca. 100 times higher sensitivity than control sera (Fig. 27, panel A and B). However, the detection sensitivity of the 30 kDa immunogen by the 60 kDa antiserum was ca. 100 times lower than the 30 kDa antiserum itself in the detection of the 30 kDa immunogen, and was similar in its level of signal production as the 48 kDa antiserum itself in the detection of 48 kDa immunogen.

In summary, the cross-reactivities of the antisera to the three immunogens indicate that all of them must share similar or identical epitopic domains. In particular, the 30 kDa immunogen appears to have a considerable degree of structural homology with the 48 and 60 kDa immunogens since the 30 kDa antiserum has stronger reactivity to the 48 and 60 kDa protein immunogens than the 48 and 60 kDa antisera, themselves. This implies that epitope of the 30 kDa immunogens may encompass those of the 48 and 60 kDa immunogens. These findings also indicate that the denatured 57-60 kDa protein, which was thought to be a separate monomeric CbE from the dimeric 57-59 kDa CbE (i.e., p*I* 4.5 CbE), shares in fact structural similarities with both the p*I* 4.8 CbE (i.e.,

46-48 kDa protein under denaturing conditions, 48 kDa immunogen) and the p*I* 4.5 CbE (i.e., 25-31 kDa protein under denaturing conditions, 30 kDa immunogen) in terms of protein structure.

Because the 30 kDa antiserum had the highest titer of antibody and possessed the highest reactivity even to the 48 and 60 kDa immunogens, the IgG from the 30 kDa antiserum (i.e., 30 IgG) was purified and further used in the development of an immunoassay for the detection of the permethrin CbE in CPB.

3. Antigen Capture Immunoassay

An antigen capture assay was performed by incubating serially-diluted CPB hemolymph with the 30, 48, and 60 IgG (i.e., immunoglobulins purified from the 30, 48, 60 kDa antisera, respectively) previously immobilized onto a 96-well plate. CbE activity was measured in the presence of αNB or αNC. Using this format, no measurable level of CbE hydrolysis activity was detected by any of the combinations of IgG and hemolymph concentrations (data not shown). This result suggests that the antibodies generated by the denatured permethrin CbE proteins (i.e., 30, 48, and 60 kDa immunogens) can not recognize the native forms of the permethrin CbE found in the hemolymph.

4. Antibody Capture Immunoassay for the Detection of Permethrin CbE

Since the antigen capture immunoassay using native hemolymph was not successful, an antibody capture immunoassay using denatured hemolymph was attempted. In order to determine the optimum conditions for the antibody capture immunoassay, various combinations of hemolymph dilution (i.e., denatured hemolymphs from the SS and PE-R strains, 10^1 to 10^5-fold dilution, 5.5 ng-55 μg total protein/well) and primary antibody dilution (i.e., 1°AB, 30 IgG, 50 to 250-fold dilution, 100 ng-2.5 μg 1° AB/well) were tested. Hemolymph diluted more than 10^4-fold did not produce a

sufficient level of signal for quantitative detection (i.e., $OD_{450} < 0.01$, Fig. 28) regardless of 1°AB concentration. This finding indicates that sufficient antigen (i.e., denatured 30 , 48, or 60 kDa CbE proteins) was not immobilized onto the internal surface of each well when the highly diluted hemolymph samples (i.e., $>10^4$-fold) were used. Hemolymph diluted 10^3-fold produced detectable levels of signal (i.e., $OD_{450} > 0.01$) only in the combination with less diluted 1°AB (i.e., 50 to 250-fold dilution). Hemolymph diluted 10^1 to 10^2-fold produced sufficient levels of signal (i.e., $OD_{450} > 0.02$) in all the combinations tested.

In all cases, the hemolymph from the PE-R strain produced 1.1-5.3 times higher signal levels than that from the SS strain as judged by OD_{450} (Fig. 28). This indicates that the hemolymph from the PE-R strain contains more permethrin CbE than that from the SS strain and corroborates our original biochemical determination of this phenomena. The specificity of the immunoassay, as judged by the signal ratio between the SS and PE-R strains, however, was reduced as the amount of 1°AB was increased. This inverted relationship indicates that high concentrations of 1°AB that apparently exceed the saturation point of 1°AB can result in a high degree of non-specific binding of antibody. The saturation point of the 1°AB was expected to be not higher than 100 ng/well since maximum protein (i.e., antigen) binding capacity of a well is ca. 100 ng/well (59). This non-specific interaction was most prominent in the combination of high concentration of 1°AB (e.g., 50-fold dilution) and high concentration of hemolymph (e.g., 10-fold dilution), which resulted in only a 1.1-fold signal difference between the SS and PE-R strains. In considering several factors including signal specificity, signal intensity, and convenience of hemolymph dilution, the combination of 100-fold dilution of hemolymph (i.e., 5.5 μg denatured total protein/well) and 250-fold dilution of 1°AB (i.e., 500 ng/well) was determined to be the optimum condition for the detection of CbE proteins in CPB hemolymph.

To test the sensitivity of the antibody capture immunoassay for the detection of the permethrin CbE from individual CPB, hemolymph samples from individual larva of 4 different CPB strains were comparatively analyzed using the CbE hydrolysis activity assay and the antibody capture immunoassay. The CbE hydrolysis activity of the hemolymph of individual larvae were determined by using αNC as a substrate and the results presented in Fig. 29, panel A. The levels of the permethrin CbE in the hemolymph of individual larvae were determined by the antibody capture immunoassay and the results presented in Fig. 29, panel B. In the CbE hydrolysis activity assay, the resistant PE-R strain showed the highest αNC CbE activity (0.434 ± 0.131 OD_{600}) and followed by the Maryland-Resistant (Mar-R, 0.372 ± 0.206 OD_{600}), the susceptible SS (0.320 ± 0.127 OD_{600}), and Maine-Susceptible (Mai-S, 0.304 ± 0.126 OD_{600}) strains (Fig. 29, panel A). The CbE hydrolysis activity was statistically elevated in the PE-R strain when compared with the SS and Mai-S strain (*t*-test, $n=90\text{-}91$, $P<0.05$). The PE-R, Mar-R, and Mai-S strains had 1.36, 1.16, and 0.95 times higher levels of the α NC CbE activity when compared with the SS strain based on mean values. Since the Mar-R strain has a similar level of permethrin resistance compared with the PE-R strain and the Mai-S strain has similar level of permethrin-susceptibility compared with the SS strain (unpublished observations, R. Alford, G. Dively, and S. H. Lee), the levels of αNC CbE activity correlate to a considerable degree with the levels of permethrin resistance. The Mar-R strain had a relatively high degree of variation in α NC CbE activity among individuals when compared with other strains as judged by standard deviation of αNC hydrolysis (i.e., 0.206 *vs*. 0.126-0.131 S.D., respectively). Due to this high variation among individuals, the elevated level of αNC CbE activity of the Mar-R strain could not be determined to be significantly different either from that of the PE-R and SS strains, respectively (*t*-test, $n=85\text{-}88$, $P=0.094\text{-}0.156$). However, the mean value of CbE hydrolysis activity and bioassay data confirm that the strain is in fact permethrin-resistant.

In the antibody capture immunoassay, the PE-R strain showed the highest level of the permethrin CbE (i.e., 0.348 ± 0.062 OD_{450}) followed by the Mar-R (0.325 ± 0.082 OD_{450}), Mai-S (0.238 ± 0.067 OD_{450}), and SS (0.217 ± 0.069 OD_{450}) strains (Fig. 29, panel B). Both the PE-R and Mar-R strains were determined to have significantly higher levels of the permethrin CbE than the SS or Mai-S strains (*t*-test, n=83-91, $P<0.05$). The PE-R, Mar-R, and Mai-S strains had 1.6, 1.5, and 1.1 times higher levels of the permethrin CbE when compared with the level of the permethrin CbE in the SS strain based on mean values. In terms of inter-strain comparisons, therefore, the average levels of the permethrin CbE, determined by the antibody capture assay, were better correlated with the levels of permethrin resistance than the αNC CbE activity determinations. This result indicates that the antibody capture immunoassay is more accurate and specific in evaluating the mean levels of the permethrin CbE in CPB populations than the CbE hydrolysis activity assay.

In the pair-wise comparison between the level of the permethrin CbE and the αNC CbE activity in each individual within a strain, both factors were positively correlated but very low correlation coefficients were obtained (i.e., r^2=0.0648, 0.0966, 0.0084, and 0.1721 in the SS, PE-R, Mai-S, and Mar-R strains, respectively, see also the regression lines in Fig. 29). On the other hand, overall variance in the levels of the permethrin CbE among individuals was relatively low when compared with the variance in the levels of αNC CbE activity within each strain [i.e., 0.062-0.082 S.D. (or 0.078-0.104 S.D., if corrected on the basis of the difference in the mean OD values between the antibody capture immunoassay and CbE activity assay) for permethrin CbE levels determined by immunoassay *vs*. 0.126-0.206 S.D. for αNC CbE activity]. The poor correlation between the level of the permethrin CbE and the αNC CbE activity in each individual within a strain is likely derived from overall experimental error associated with the procedures of the immunoassay. Also, the low level of variance among individuals obtained from the antibody capture immunoassay is likely due to the

same experimental error associated with the procedures of the immunoassay. Consequently, the differences in the level of permethrin CbE among individuals may not be assessed precisely by the antibody capture immunoassay as presently formatted.

The poor correlation coefficient and relatively low variance in the intra-strain comparisons (i.e., comparisons of permethrin CbE levels and CbE activity within a specific strain) are more likely artifacts caused by the procedures of antibody capture immunoassay rather than a true reflection of actual differences. Because the antibody capture immunoassay requires excessive handling of samples (e.g., two separate dilution of hemolymph, denaturation, immobilization of denatured hemolymph, blocking, 1°AB binding, secondary antibody binding, and, detection) compared to the CbE hydrolysis activity assay that requires only two handling steps (i.e., dilution of hemolymph, and detection), the true difference in the level of permethrin CbE among individuals may be obscured by handling errors even though differences between the mean signal levels among the strains can still be statistically detected.

In summary, the antibody capture immunoassay could detect mean differences in the level of the permethrin CbE among the strains more specifically than the CbE hydrolysis activity assay although it could not detect the differences among individuals as specifically as the enzyme assay. If pooled hemolymph from several individuals (e.g., 10-20 equal aliquots of individual hemolymphs per sample) rather than hemolymph from single individuals is used for the antibody capture immunoassay, the detection of differences in the levels of permethrin CbE in CPB population is likely to be improved.

Table 1. Comparison of [^{14}C]*trans*-permethrin hydrolysis activities of the p*I* 4.2, 4.5, and 4.8 CbEs from the PE-R and SS strains of CPB.

	Strain	p*I* 4.8 CbE[a]	p*I* 4.5 CbE	p*I* 4.2 CbE
Permethrin hydrolysis	PE-R	6.6 ± 0.9[b]	5.1 ± 0.9	2.0 ± 0.3
(pmole/hr/ml CabE)	SS	1.1 ± 0.3	0.9 ± 0.5	1.2 ± 1.2
Hydrolysis ratio (PE-R/SS)		6.0	5.7	1.7

[a] Each p*I* CbE sample was taken from the fraction of chromatofocusing with corresponding pH.
[b] Values represent the mean ± S.D. (n=3).

Table 2. Comparison of kinetic constants of the p*I* 4.2, 4.5 and 4.8 CbEs from the PE-R and SS strains of CPB when αNC was used as the substrate.

Constant	Strain	p*I* 4.8 CbE[a]	p*I* 4.5 CbE	p*I* 4.2 CbE
K_m (μ*M*)	PE-R	33.3 ± 1.9[b]	42.4 ± 3.2	56.6 ± 2.7
	SS	15.3 ± 1.9	15.4 ± 2.7	31.5 ± 5.7
V_{max}	PE-R	146 ± 21	117 ± 22	63.0 ± 8.0
(nmole/min/ml CbE)	SS	8.3 ± 4.2	16.9 ± 9.0	12.4 ± 6.0
$1/K_m$ ratio (PE-R/SS)		0.5	0.4	0.6
V_{max} ratio (PE-R/SS)		17.6	6.9	5.1

[a] Each p*I* CbE sample was taken from the fraction of chromatofocusing with corresponding pH.

[b] Values represent the mean ± S.D. (n=6).

Table 5. Inhibition of the p*I* 4.8 and 4.5 CbEs by several inhibitors.

Inhibitors	Concentration (μ*M*)	I_{50} (μ*M*, 95% CL) or % Inhibition ± S.D.		
CbEs		p*I* 4.8 CbE	p*I* 4.5 CbE	p*I* 4.2-4.8
Serine-hydroxyl inhibitors				
DEF		1068 (531-2973)	710 (374-1769)	
DFP		0.40 (0.08-1.66)	0.27 (0.06-1.17)	
PMSF		232 (119-503)[a]	79.5 (41.0-158)	
Parathion		71.8 (54.4-95.0)	73.1 (55.3-96.8)	
Eserine		2680 (2160-3370)	2970 (2390-3750)	
Cysteine-sulfhydryl inhibitors				
PHMB	50	64.6 ± 2.3 %[b]	21.5 ± 3.4 %	
	5	65.6 ± 1.2 %[b]	21.4 ± 1.6 %	
	0.2	27.5 ± 4.7 %[b]	1.8 ± 0.5 %	
$HgCl_2$	1000	100 %	100 %	
	50	4.4 ± 3.0 %	0 %	
Transition metal inhibitor				
NaCN	100			0 %[c]
Proteinase inhibitors				
EDTA	890			0 %[c]
E-64	20			0 %[c]
Pepstatin	10			0 %[c]

[a] Significantly different from the p*I* 4.5 CbE by maximum log-likelihood test (χ^2=30.6, *df*=2, *P*<0.001).
[b] Significantly different from the p*I* 4.5 CbE by t-test (*n*=4, *P*<0.05)
[c] The p*I* 4.2-4.8 CbE sample was used for inhibition studies.

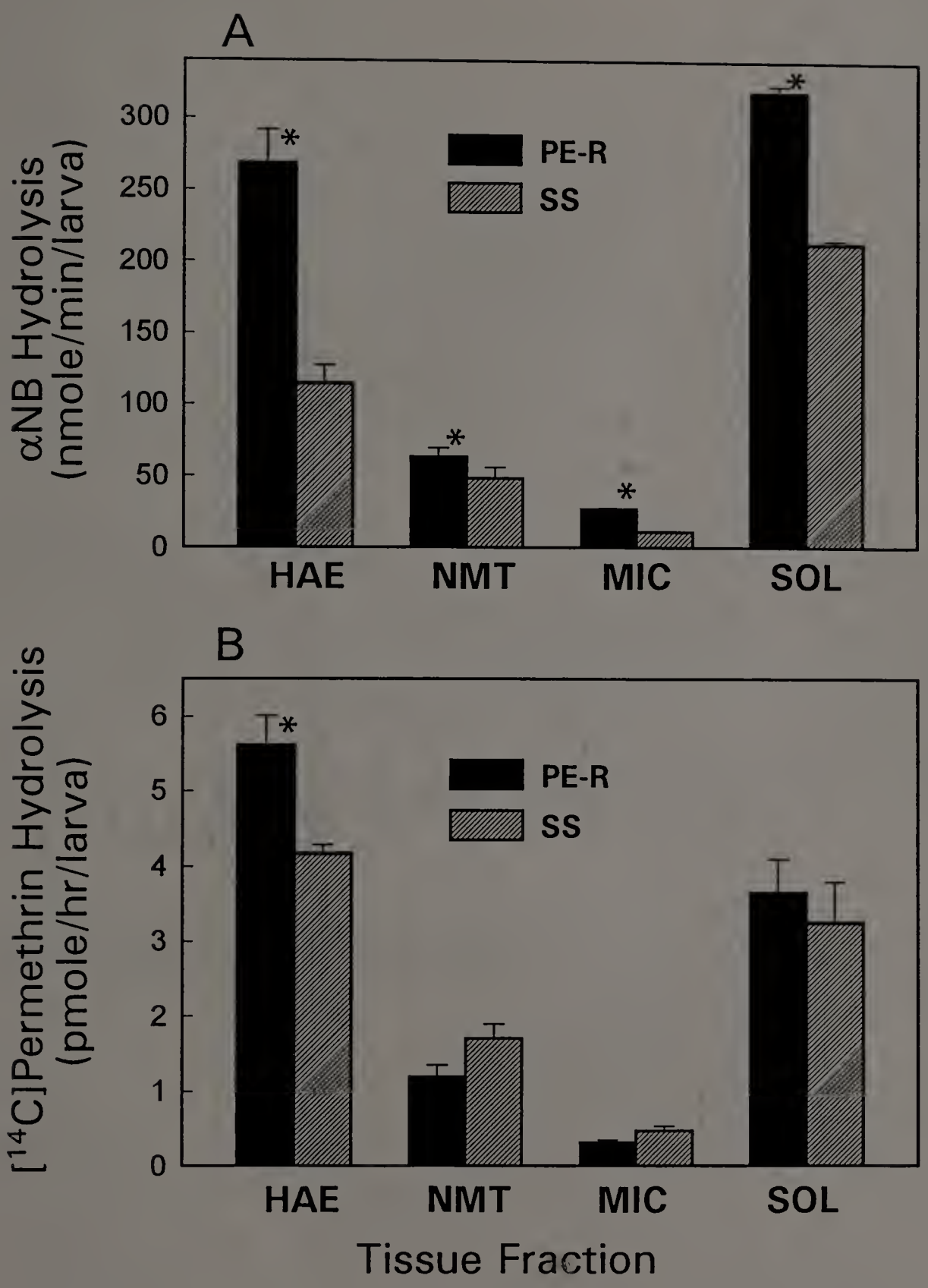

Fig. 1. Tissue distribution of αNB hydrolysis and [^{14}C]*trans*-permethrin hydrolysis activities. (A) Distribution of αNB hydrolysis; (B) Distribution of [^{14}C]*trans*-permethrin hydrolysis. HAE, hemolymph fraction; NMT, nucleolar-mitrochondrial fraction; MIC, microsomal fraction; SOL, soluble fraction. Asterisk denotes significantly higher activity than the SS strain (*t*-test, n=3-6, $P<0.05$).

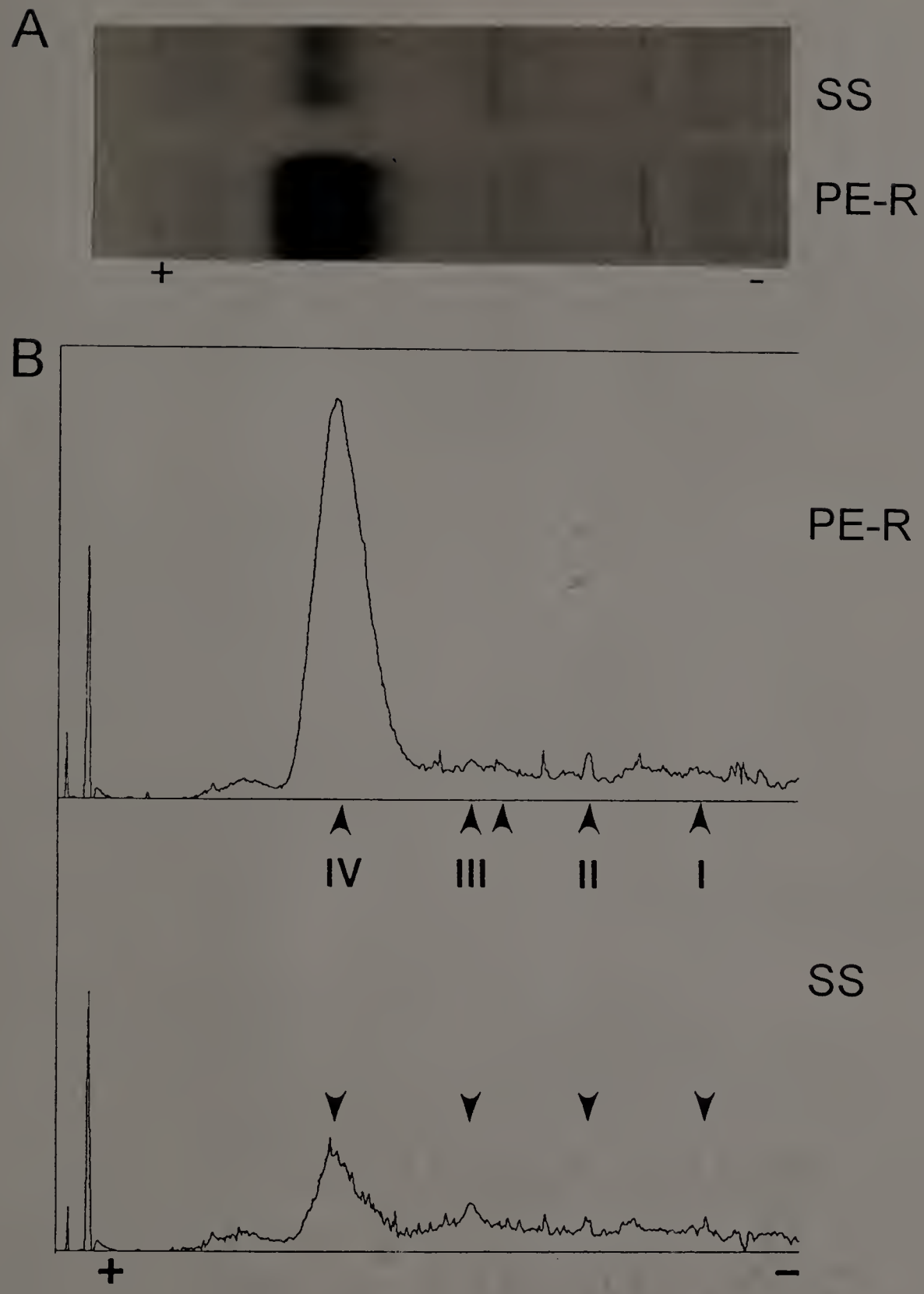

Fig. 2. Native PAGE of hemolymphs from the PE-R and SS strains of CPB. Aliquots of the PE-R and SS hemolymph, each containing 100 μg of total protein, were separated by native PAGE. (A) Native polyacrylamide gel stained with αNB-dianisidine; (B) Scanning densitogram of native polyacrylamide gel. Protein bands were marked as I, II, III, and IV. The *y*-axis is a relative scale of optical density. The *x*-axis is a gel distance running top (right-hand side) to bottom (left-hand side).

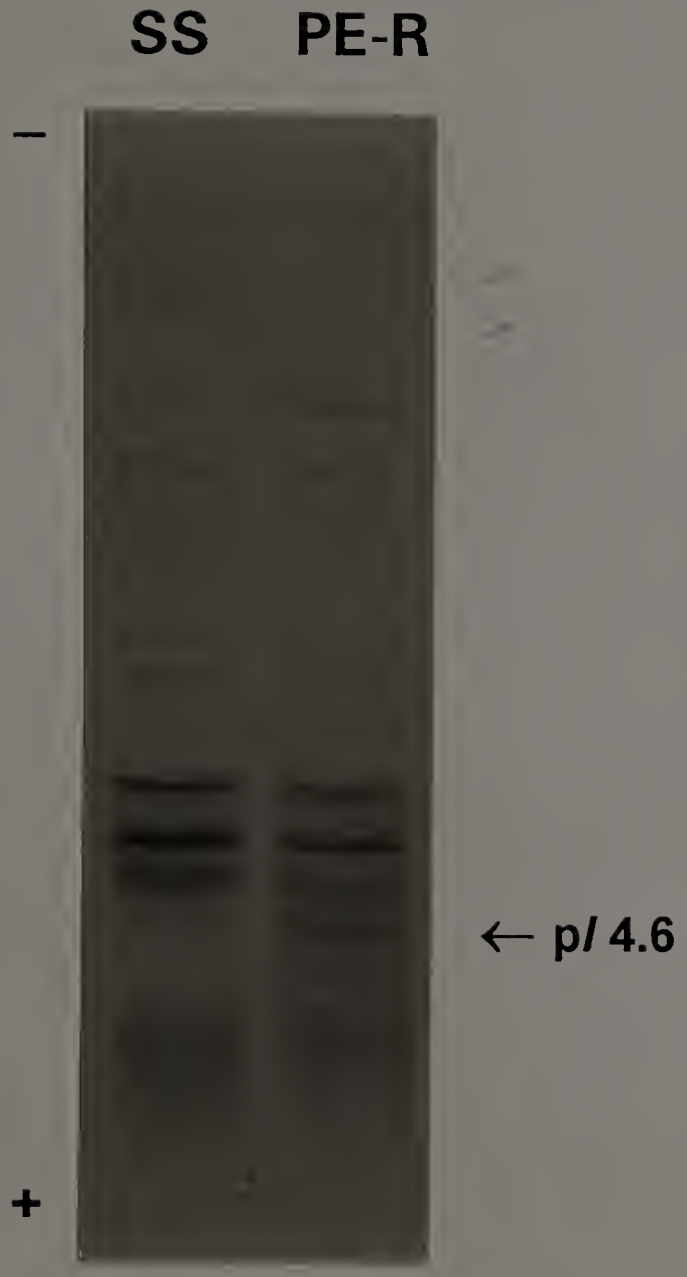

Fig. 3. Isoelectricfocusing (pH 3-10) of hemolymphs from the PE-R and SS strains of CPB. Aliquots of the PE-R and SS hemolymph, each containing 100 μg of total protein, were isoelectricfocused and the gel was stained with αNB-dianisidine.

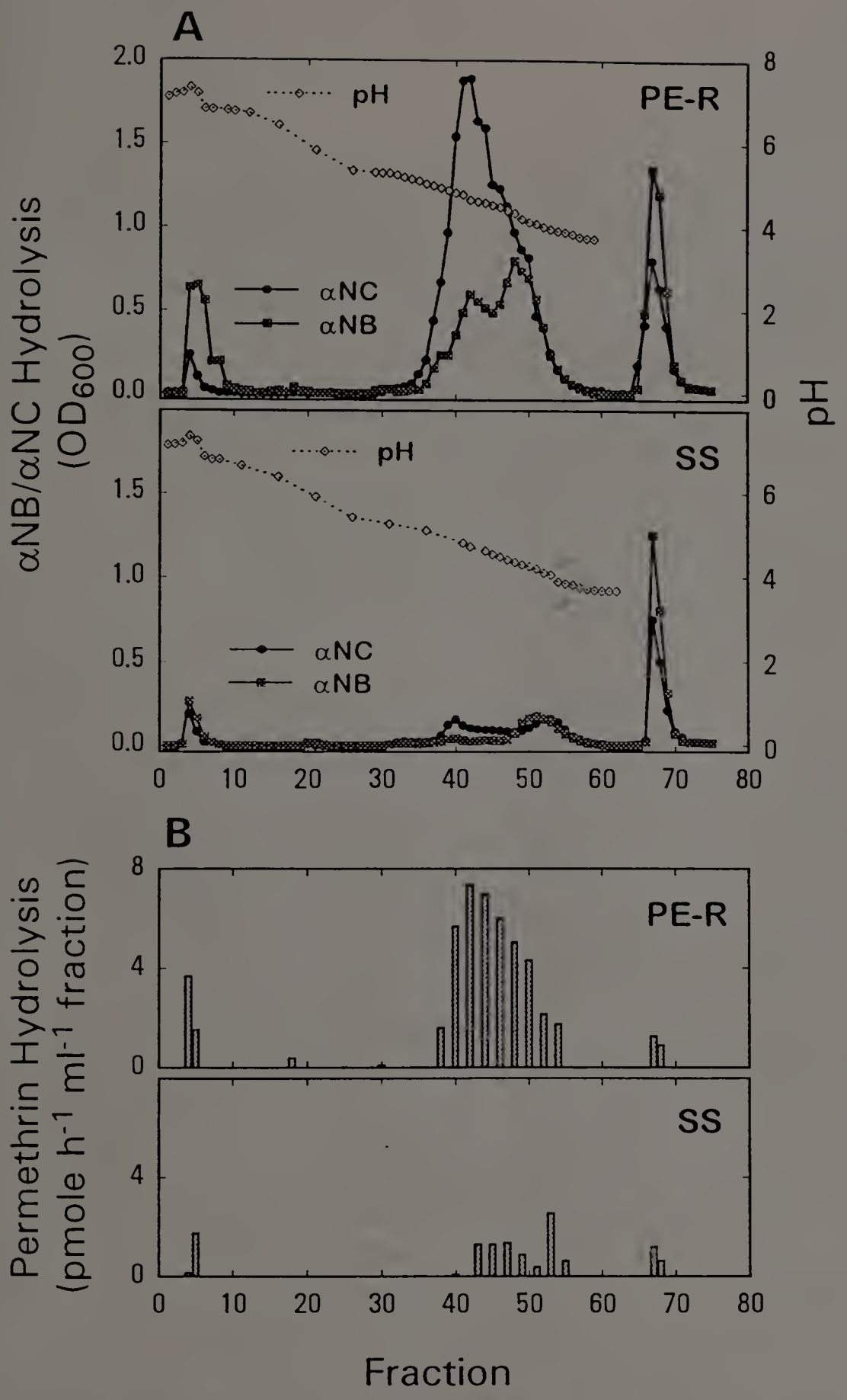

Fig. 4. The activity and distribution of αNB/αNC hydrolysis and [^{14}C]*trans*-permethrin hydrolysis activities when hemolymphs from the PE-R and SS strains of CPB were chromatofocused. Aliquots of the PE-R and SS hemolymphs, each containing 21 mg of total protein were separated by chromatofocusing (pH 4-7). After elution with Polybuffer74, the column was washed with 25 m*M* *l*-histidine buffer containing 1 *M* NaCl (pH 4.0) from fraction # 63. (A) αNB/αNC hydrolysis; (B) [^{14}C]*trans*-permethrin hydrolysis.

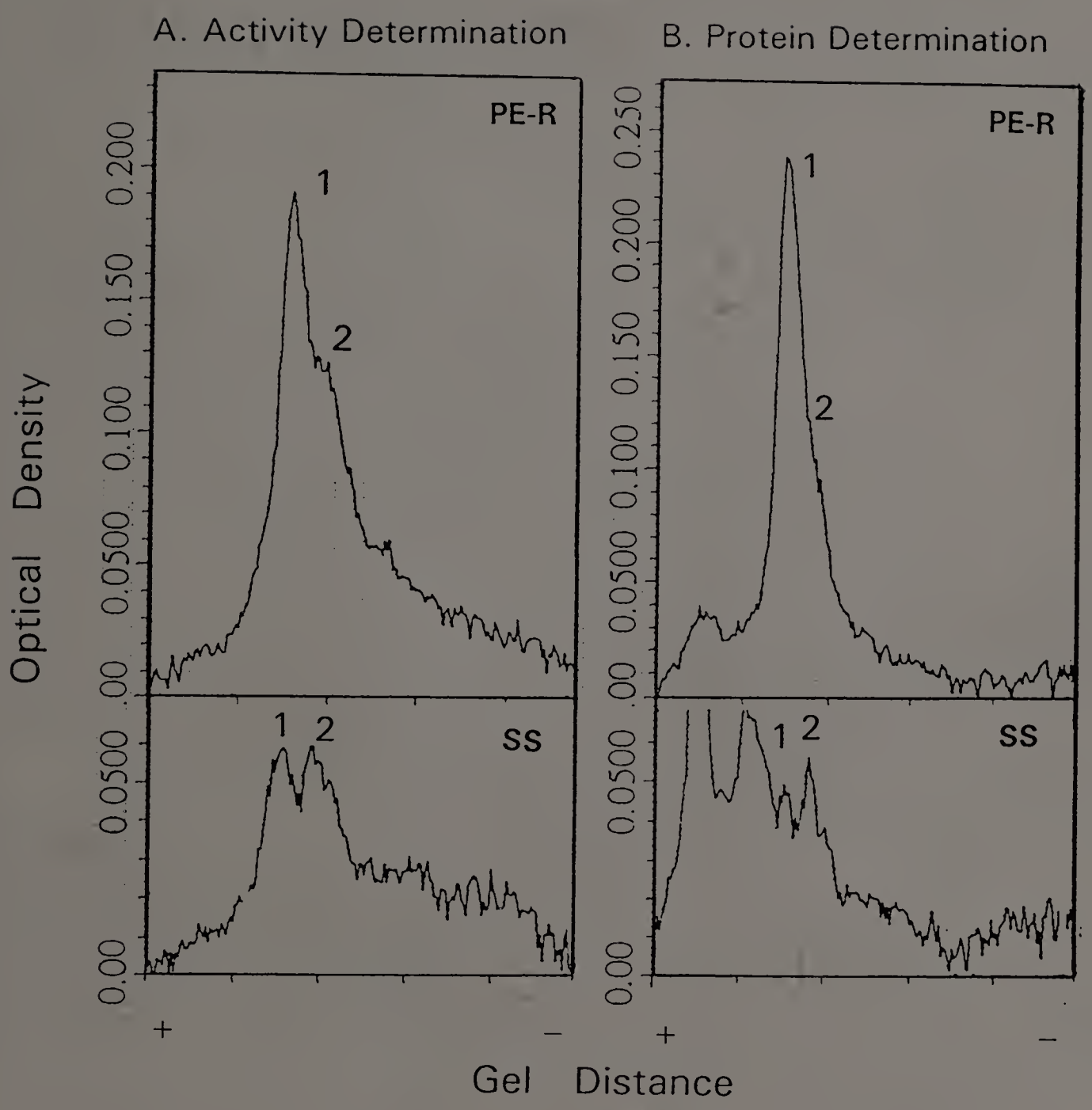

Fig. 5. Densitometric comparison of the αNB hydrolysis activity (A) and protein quantity (B) of the p*I* 3.9-4.8 CbEs from the PE-R and SS hemolymphs after electrophoresis on native PAGE.

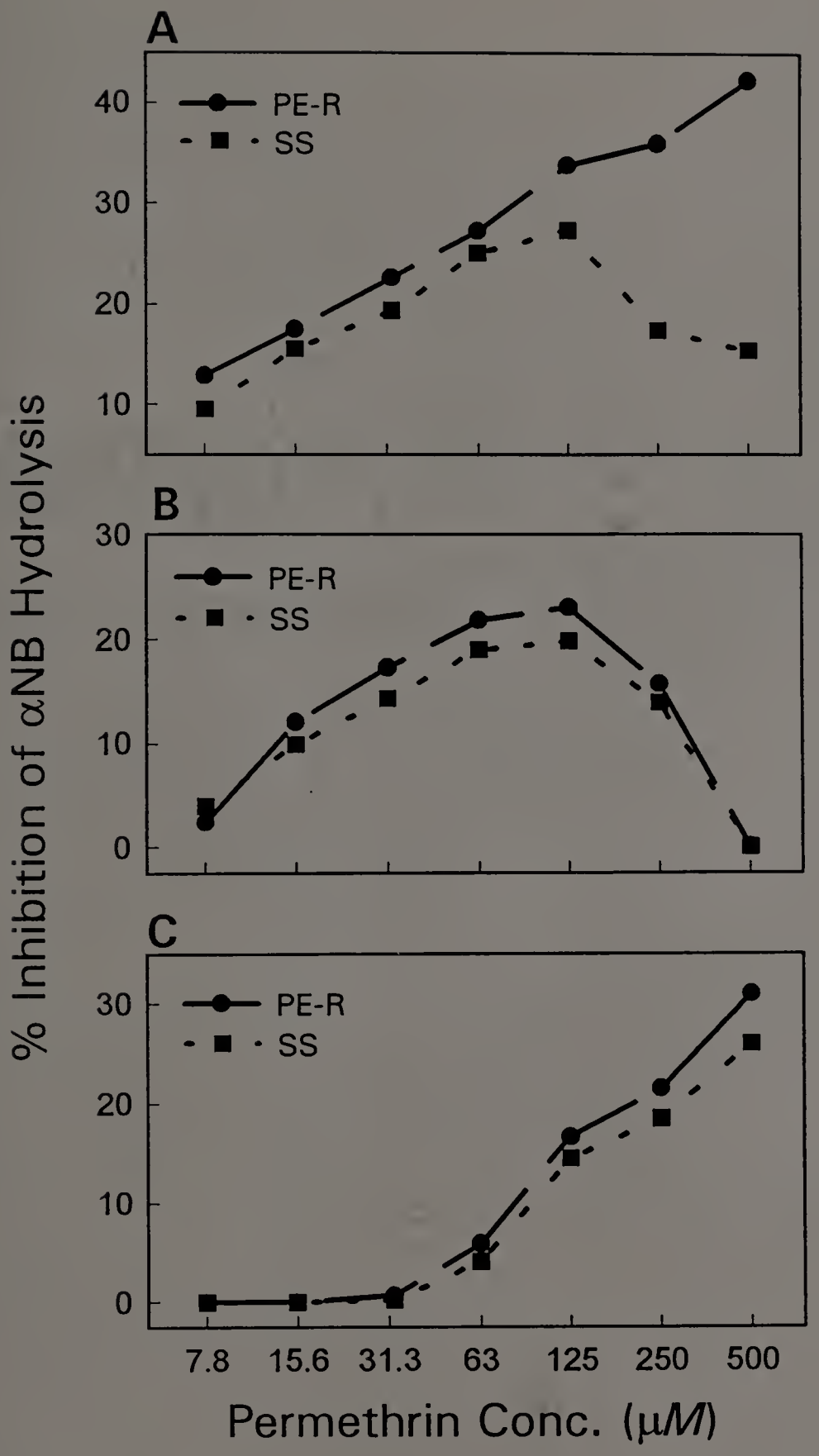

Fig. 6. Inhibition of hemolymph CbEs from the SS and PE-R strains of CPB by permethrin. (A) 30-fold diluted SS and PE-R hemolymphs; (B) 75-fold diluted PE-R hemolymph *vs*. 30-fold diluted SS hemolymph; (C) 33-fold diluted PE-R hemolymph *vs*. 13-fold diluted SS hemolymph.

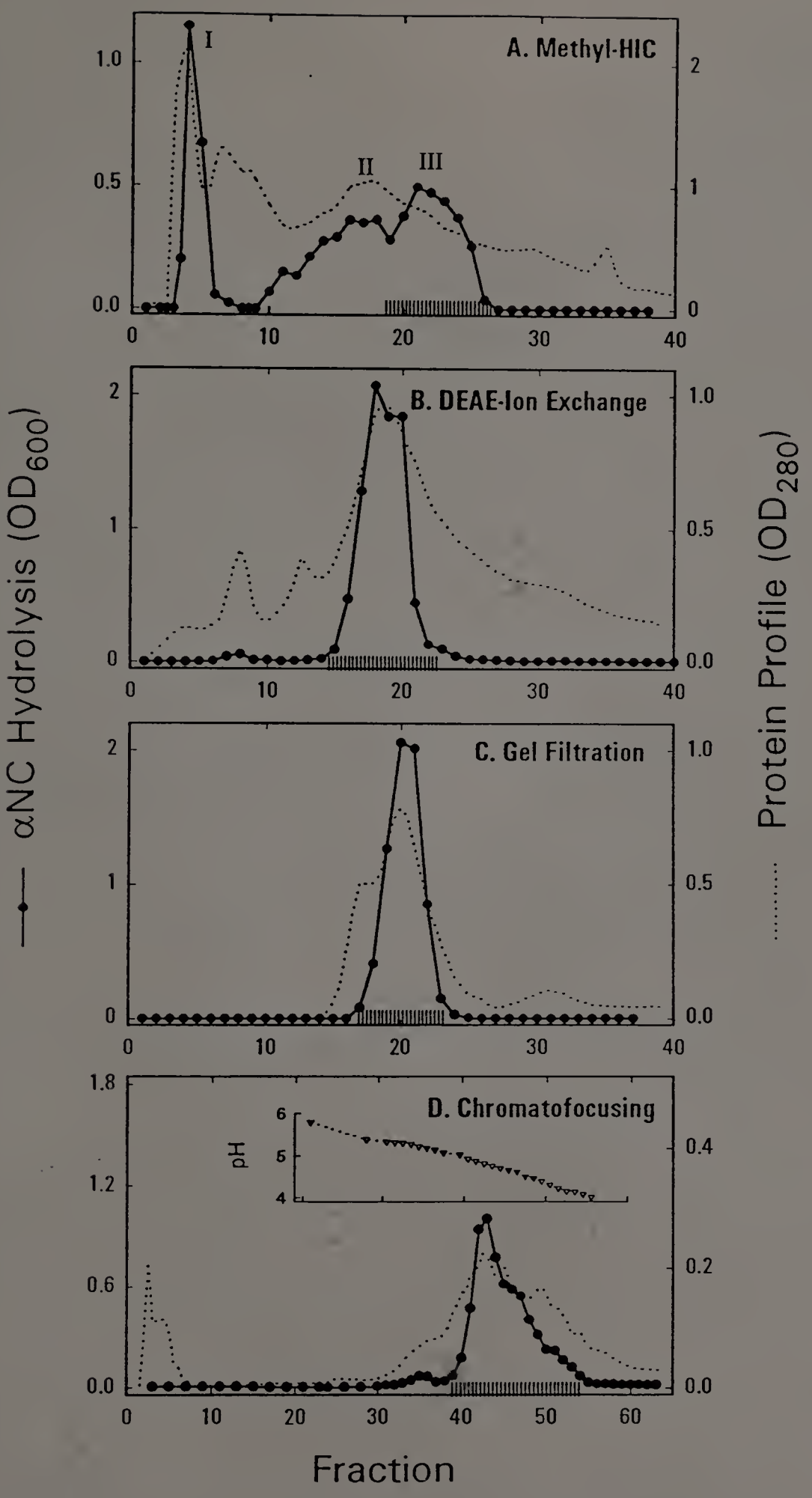

Fig. 7. Chromatographic purification of permethrin CbEs from hemolymph of the PE-R strain of CPB. The fractions marked with 'IIIIII' were collected and processed in the next purification step.

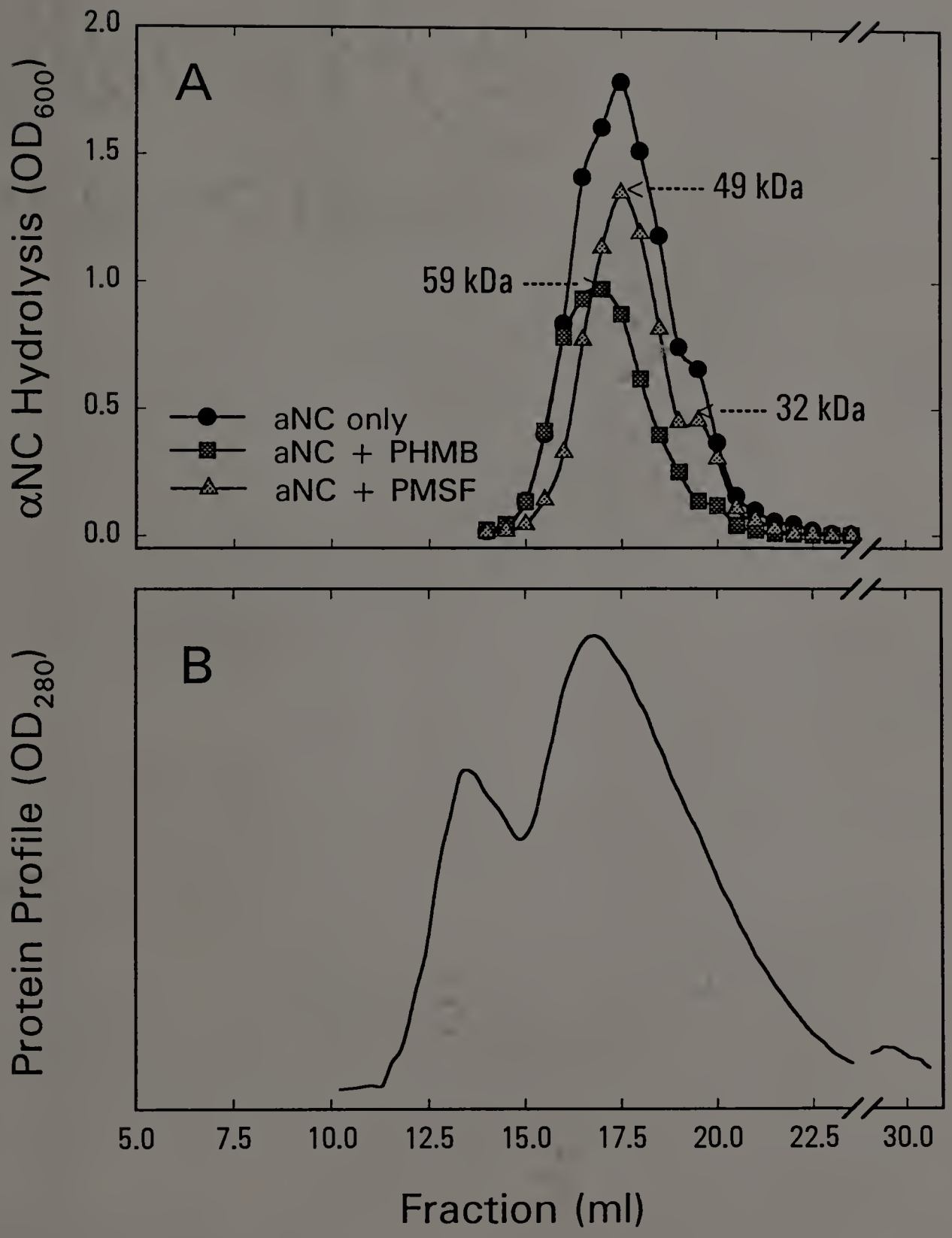

Fig. 8. Estimation of native molecular mass of the permethrin CbE by Sephadex G-100 gel filtration chromatography. (A) αNC hydrolysis activity profile in the presence or absence of PHMB and PMSF; (B) protein chromatogram.

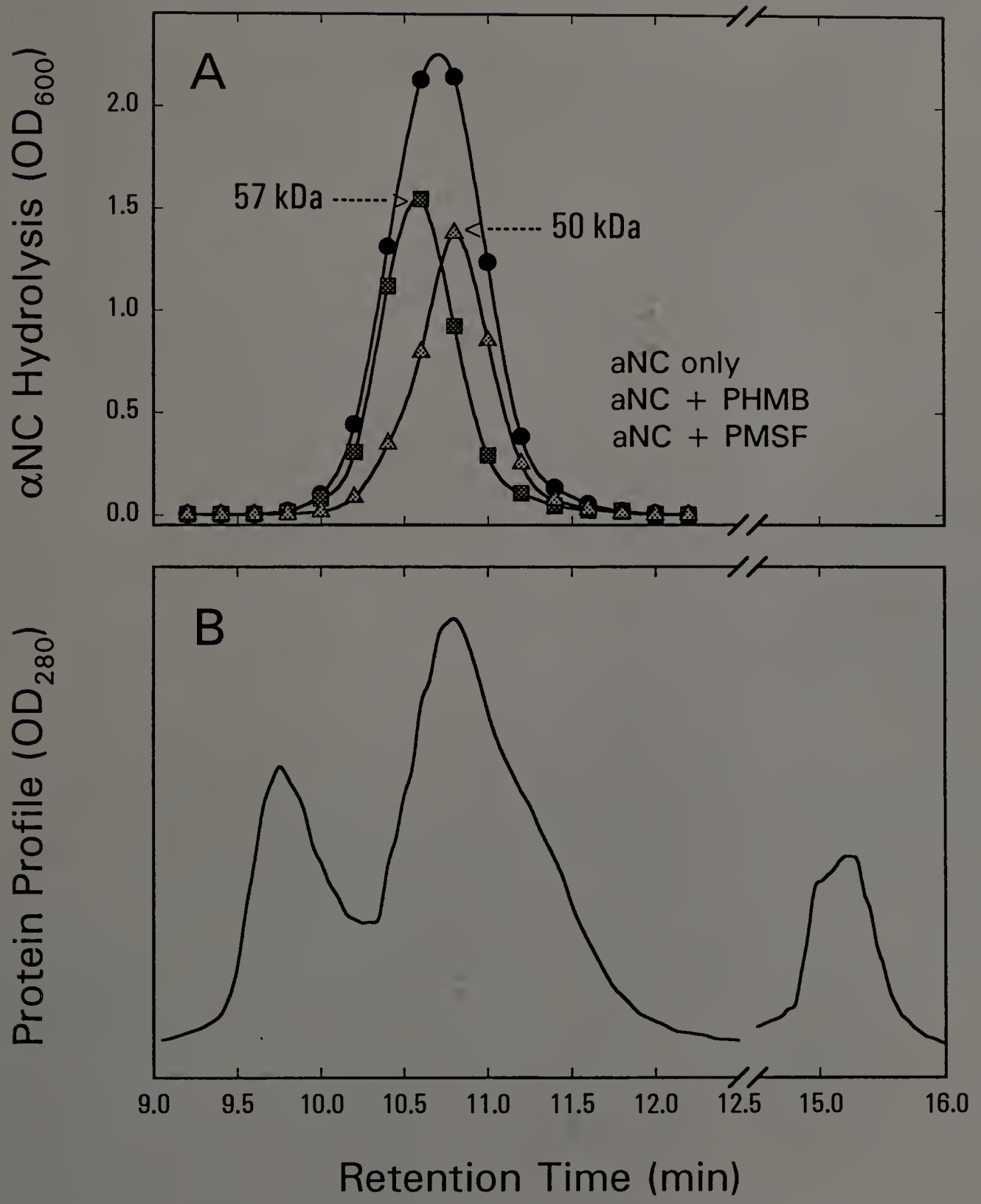

Fig. 9. Estimation of native molecular mass of permethrin CbE by size exclusion-HPLC. (A) αNC hydrolysis activity profile in the presence or absence of PHMB and PMSF; (B) protein chromatogram.

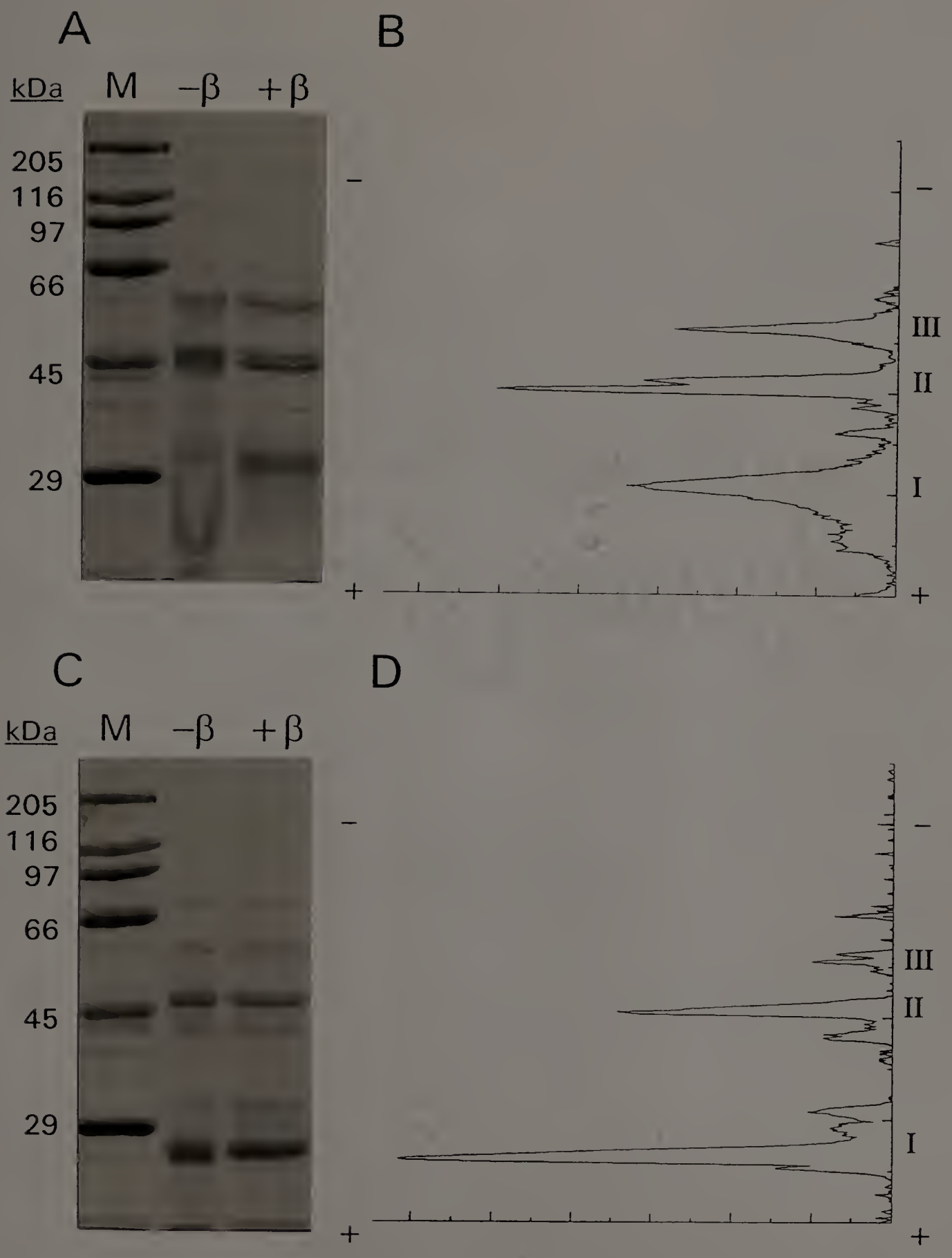

Fig. 10. SDS-PAGE of the purified permethrin CbE. (A, C) Two representative banding patterns; (B, D) Corresponding scanning densitograms. The horizontal axis is optical density (arbitrary unit) and vertical axis is gel distance (70 mm, running top to bottom). The '-β' and '+β' represent the absence and presence of β-mercaptoethanol, respectively. The major band proteins were designated as I, II, and III on the right side of the densitograms.

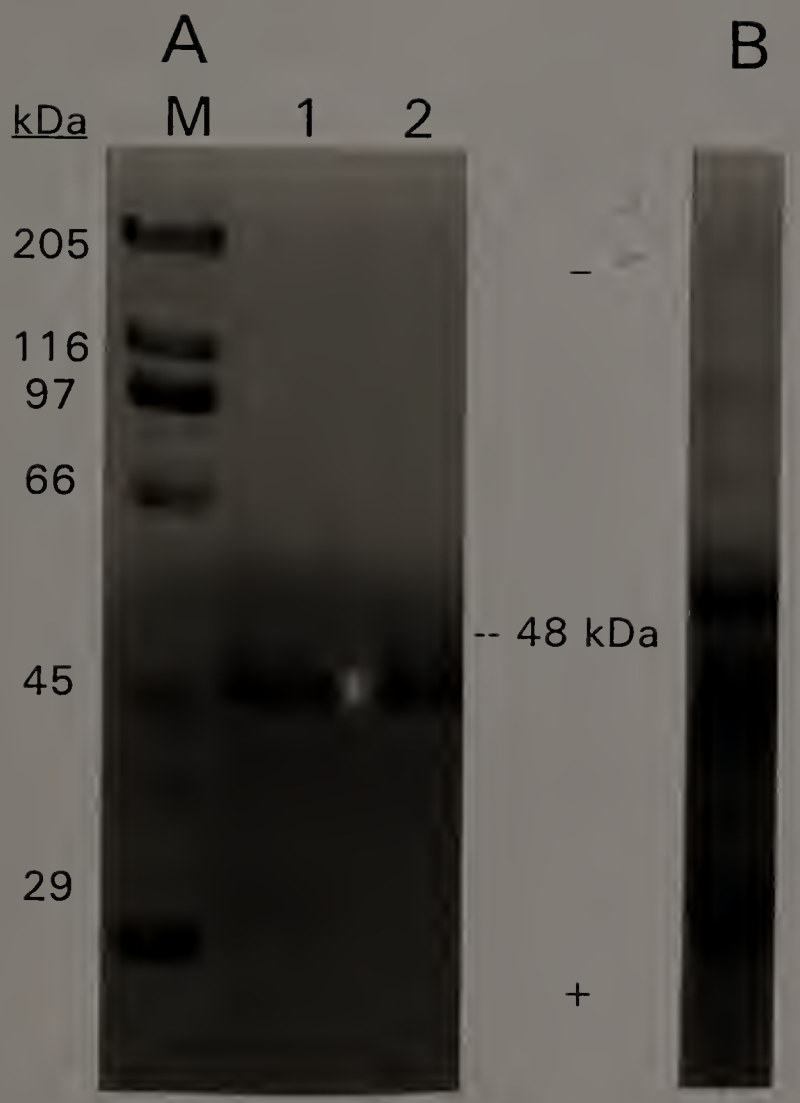

Fig. 11. Attempted renaturation of the permethrin CbE proteins separated by SDS-PAGE. Purified permethrin was denatured by incubating with SDS-sample buffer for 1 hr (A, lane 1), 30 hrs (A, lane 2) or by boiling for 5 min in SDS-sample buffer (B) and separated by SDS-PAGE. The proteins in the gel were renatured, stained with αNB-dianisidine, and further stained with Coomassie brilliant blue. Only the 48 kDa protein restored αNB hydrolysis activity. The molecular mass of marker proteins (M) are shown on the left side of the gel.

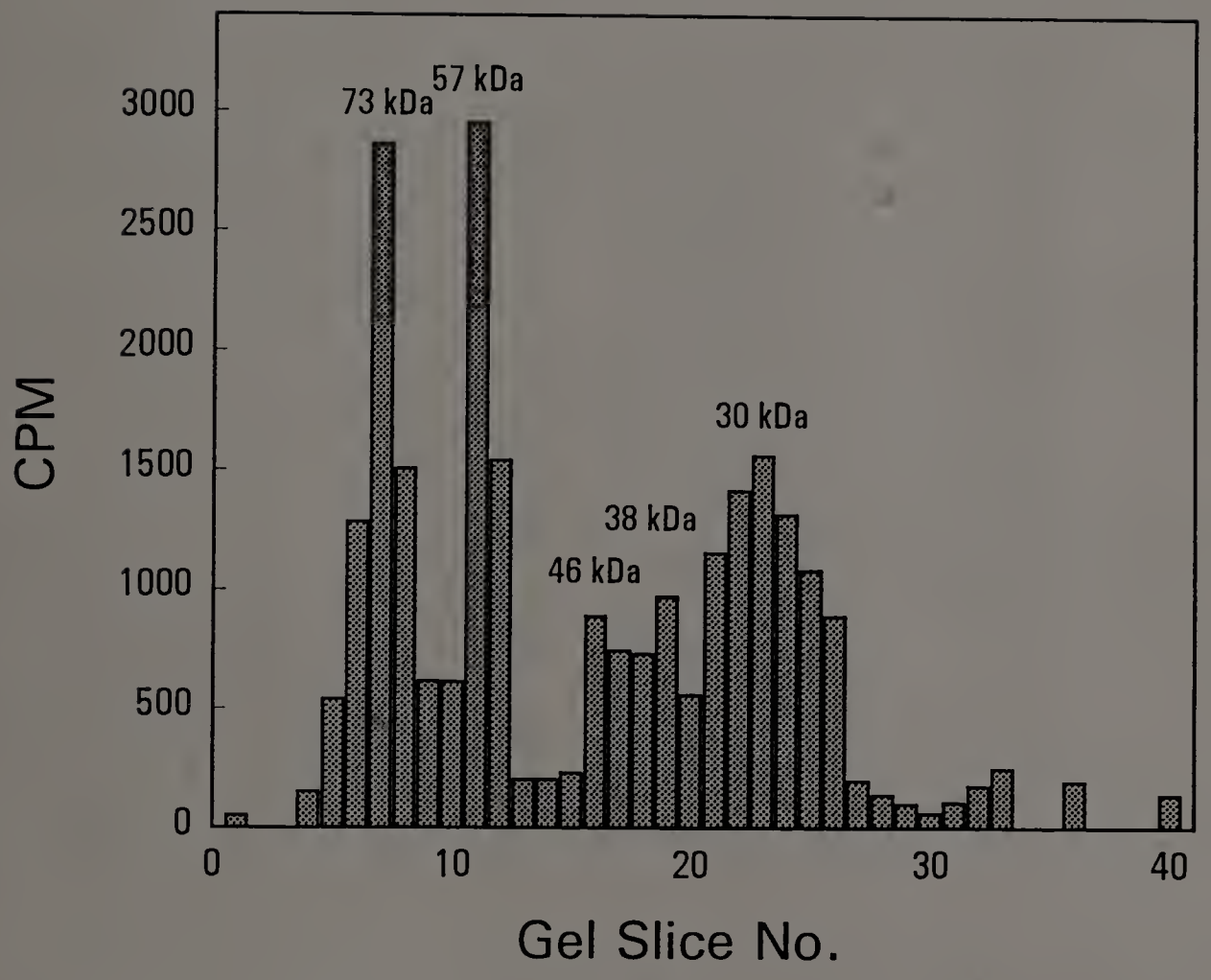

Fig. 12. Identification of the permethrin CbE proteins by [^{3}H]DFP-labeling. The [^{3}H]DFP-labeled permethrin CbE sample was separated by SDS-PAGE and the radioactivities associated with the gel slices were determined using a liquid scintillation counter.

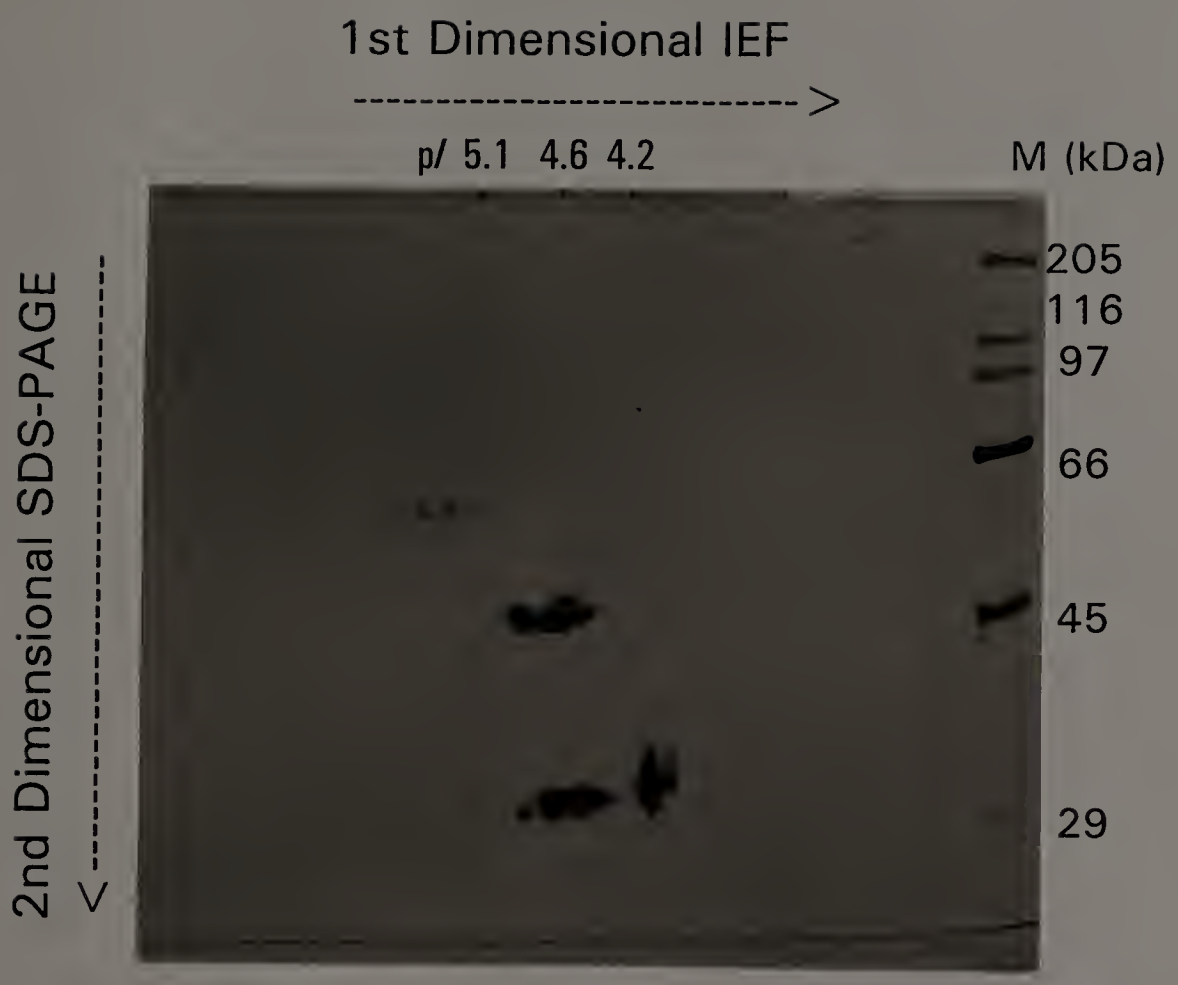

Fig. 13. Two-dimensional gel electrophoresis of the purified permethrin CbE (denatured IEF *vs*. SDS-PAGE). The p*I* values determined by pI marker proteins are shown on the top of the gel. The molecular mass of marker proteins are shown on the right side of the gel.

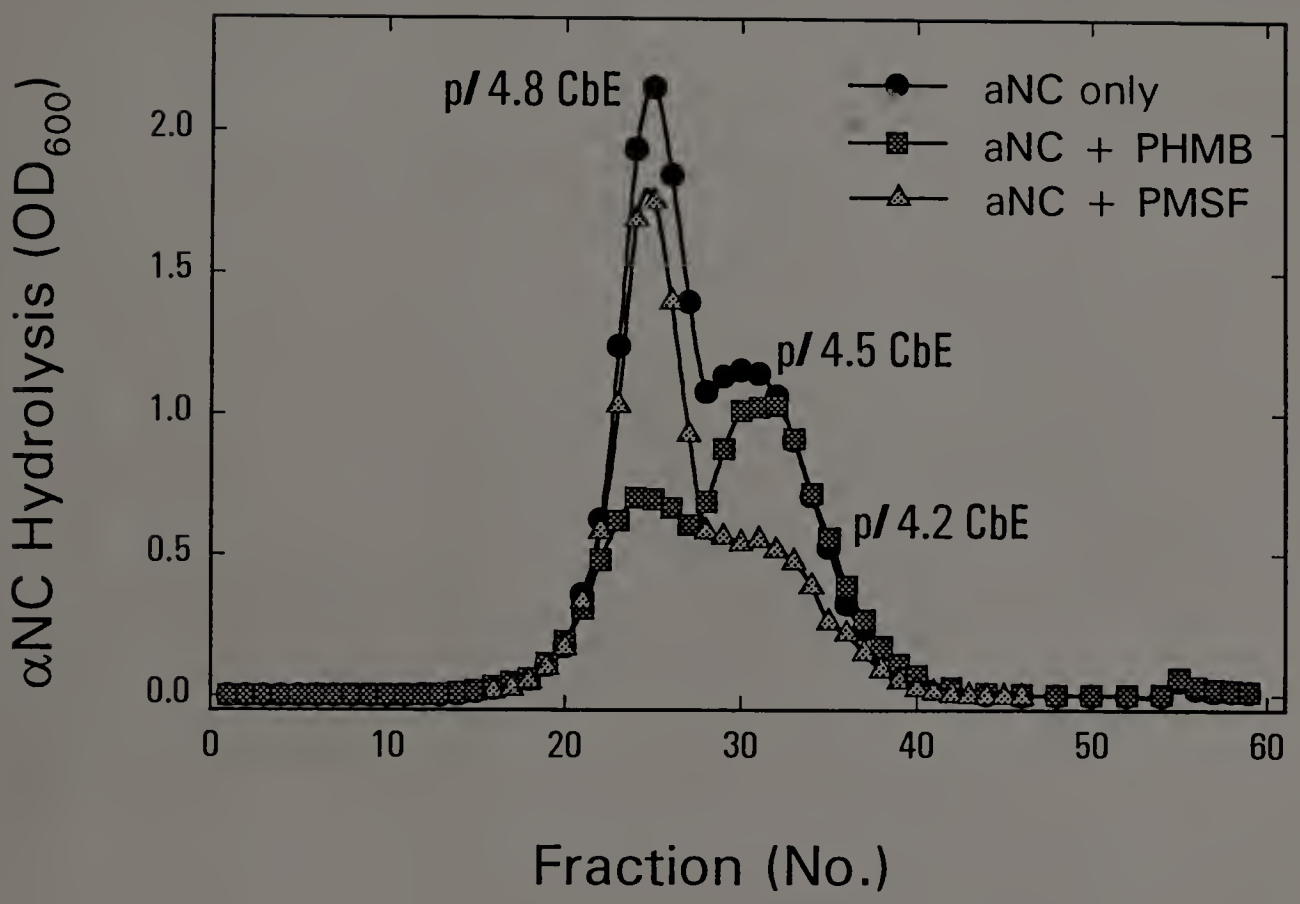

Fig. 14. Identification of the PHMB-sensitive and PMSF-sensitive CbEs following re-chromatofocusing of the purified permethrin CbE. The purified p*I* 4.2-4.8 CbE were re-chromatofocused using a narrow pH gradient (pH 4-5) and the αNC hydrolysis activity for each fraction was determined in the presence or absence of PHMB and PMSF.

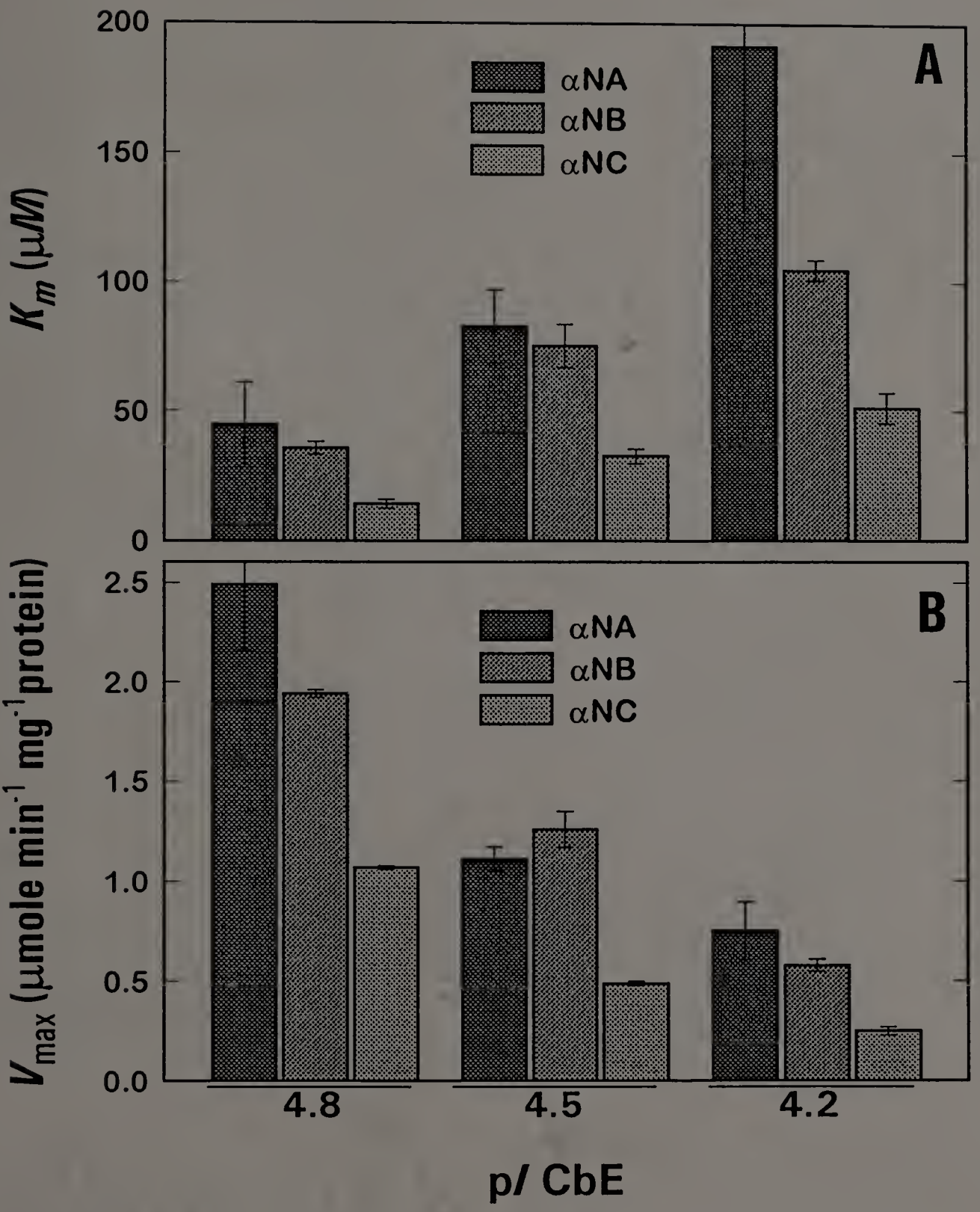

Fig. 15. Kinetic analysis of the p*I* 4.2, 4.5, and 4.8 CbEs from the PE-R strain of CPB using three naphthyl substrates, αNA, αNB, and αNC. (A) Comparisons of K_m values; (B) Comparisons of V_{max} values.

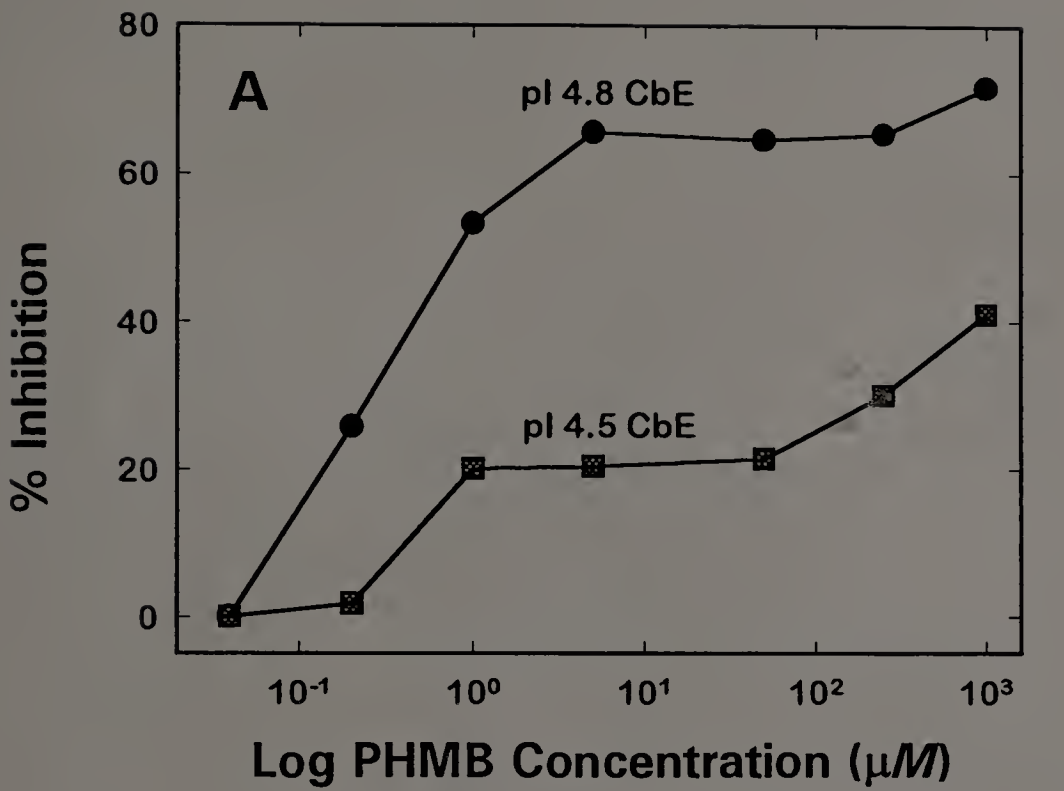

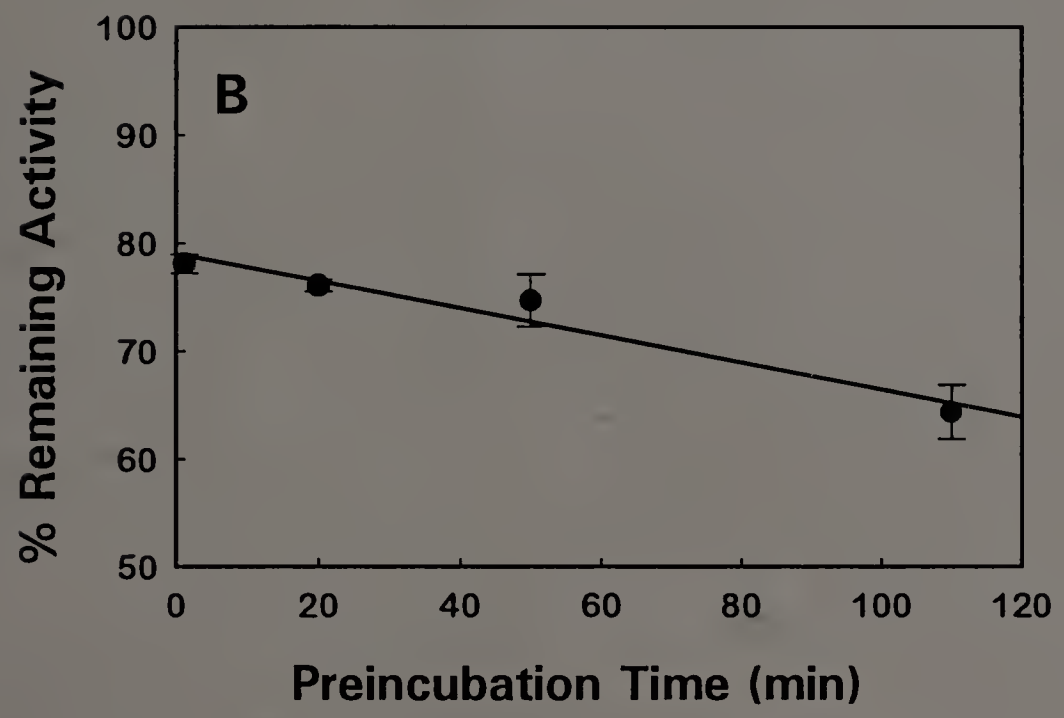

Fig. 16. Inhibition of the p*I* 4.5 and 4.8 CbEs by PHMB. (A) Dose-dependent inhibition; (B) Time-progressive inhibition of combined p*I* 4.5-4.8 CbEs by 5 μ*M* PHMB.

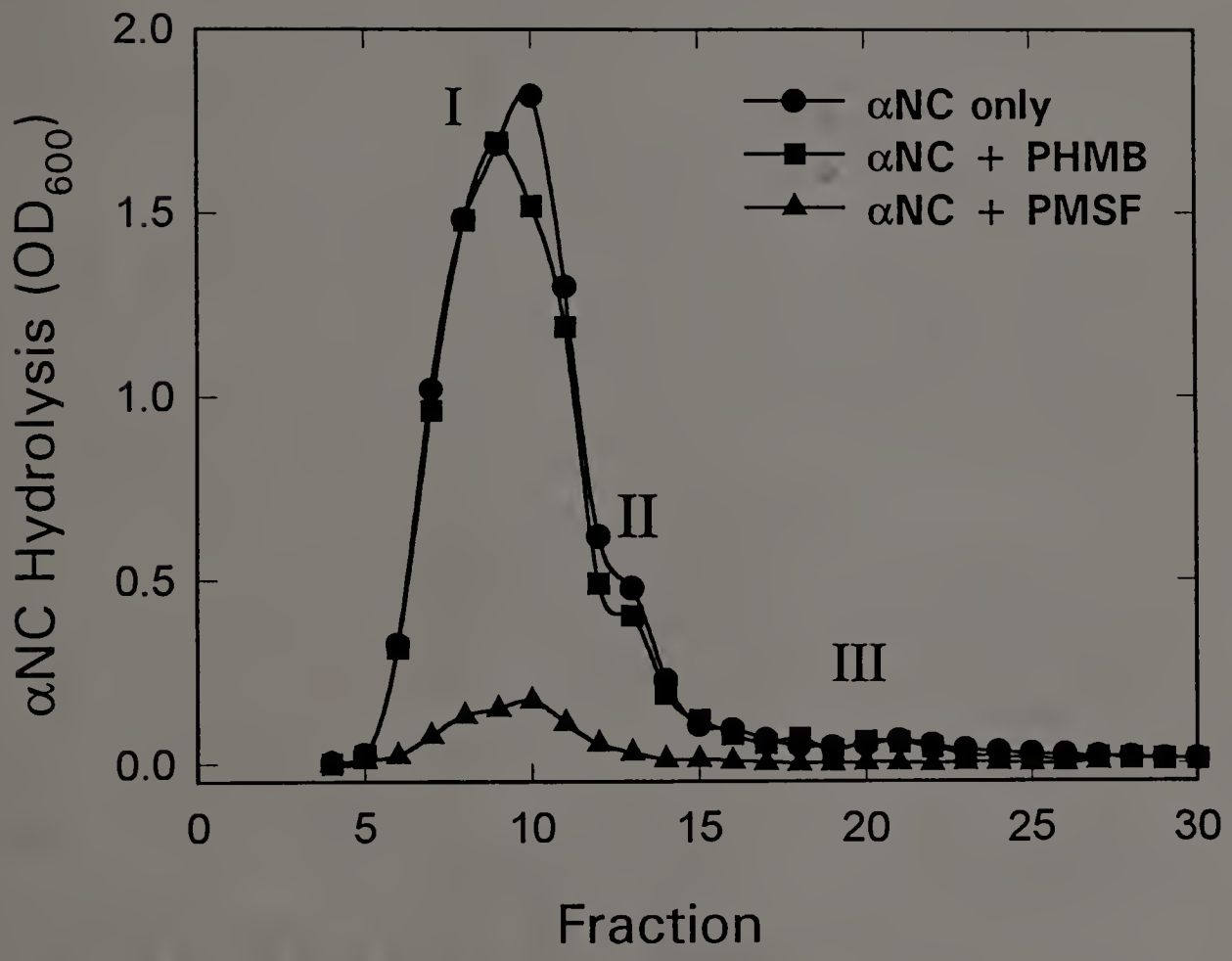

Fig. 17. Separation of PHMB-sensitive and PMSF-sensitive CbEs by PCMB-agarose affinity chromatography. Three αNC hydrolysis activity peaks were designated as I, II, and III. Note: elution fractions, in which no αNC hydrolysis activity was detected, were not shown.

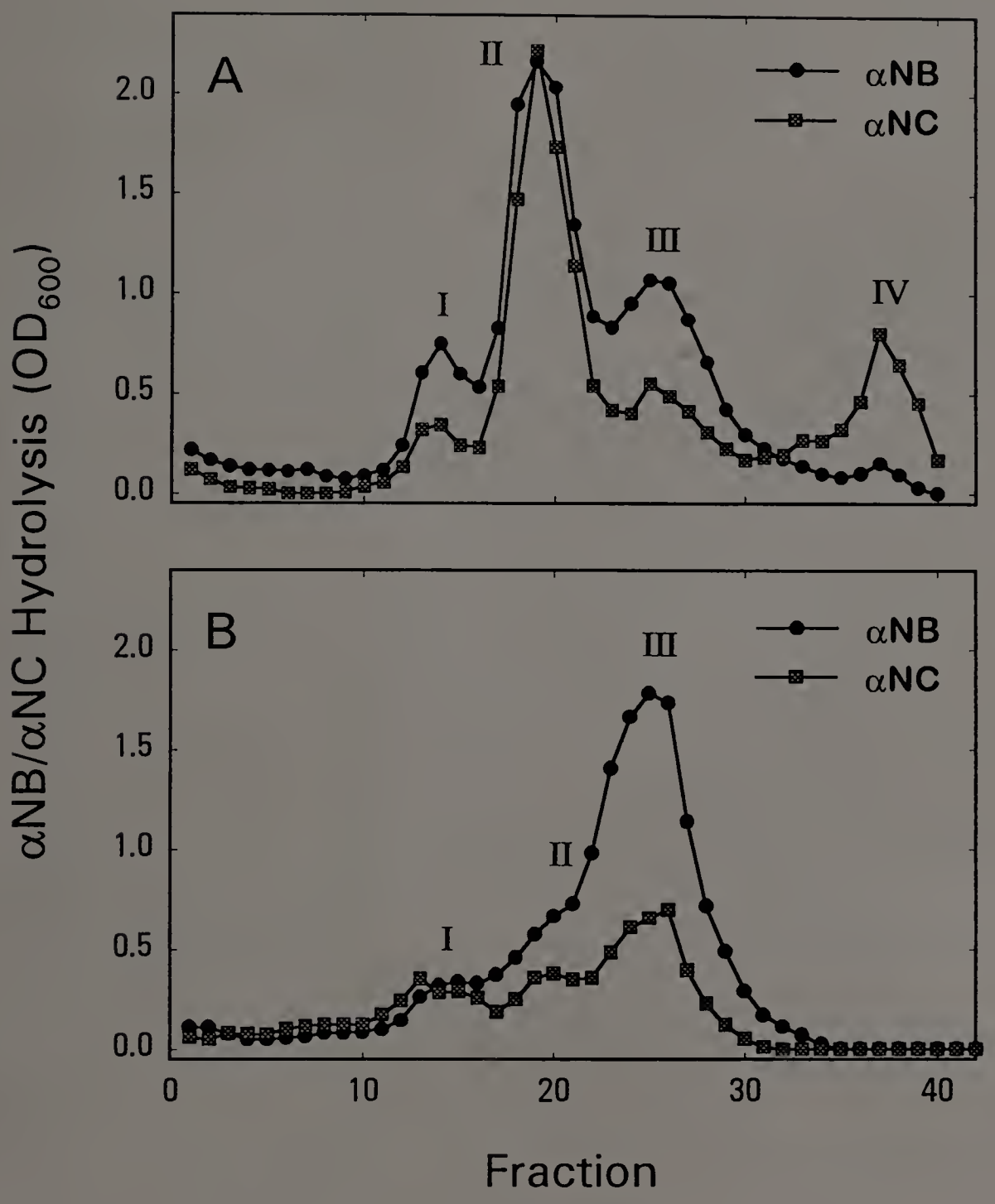

Fig. 18. Determination of surface hydrophobicities of the p*I* 4.8 (A) and 4.5 CbEs (B) by methyl-hydrophobic interaction chromatography (methyl-HIC). The p*I* 4.5 and 4.8 CbE samples from re-chromatofocusing were separated individually by methyl-HIC and hydrolysis activities using αNB and αNC as substrates were determined.

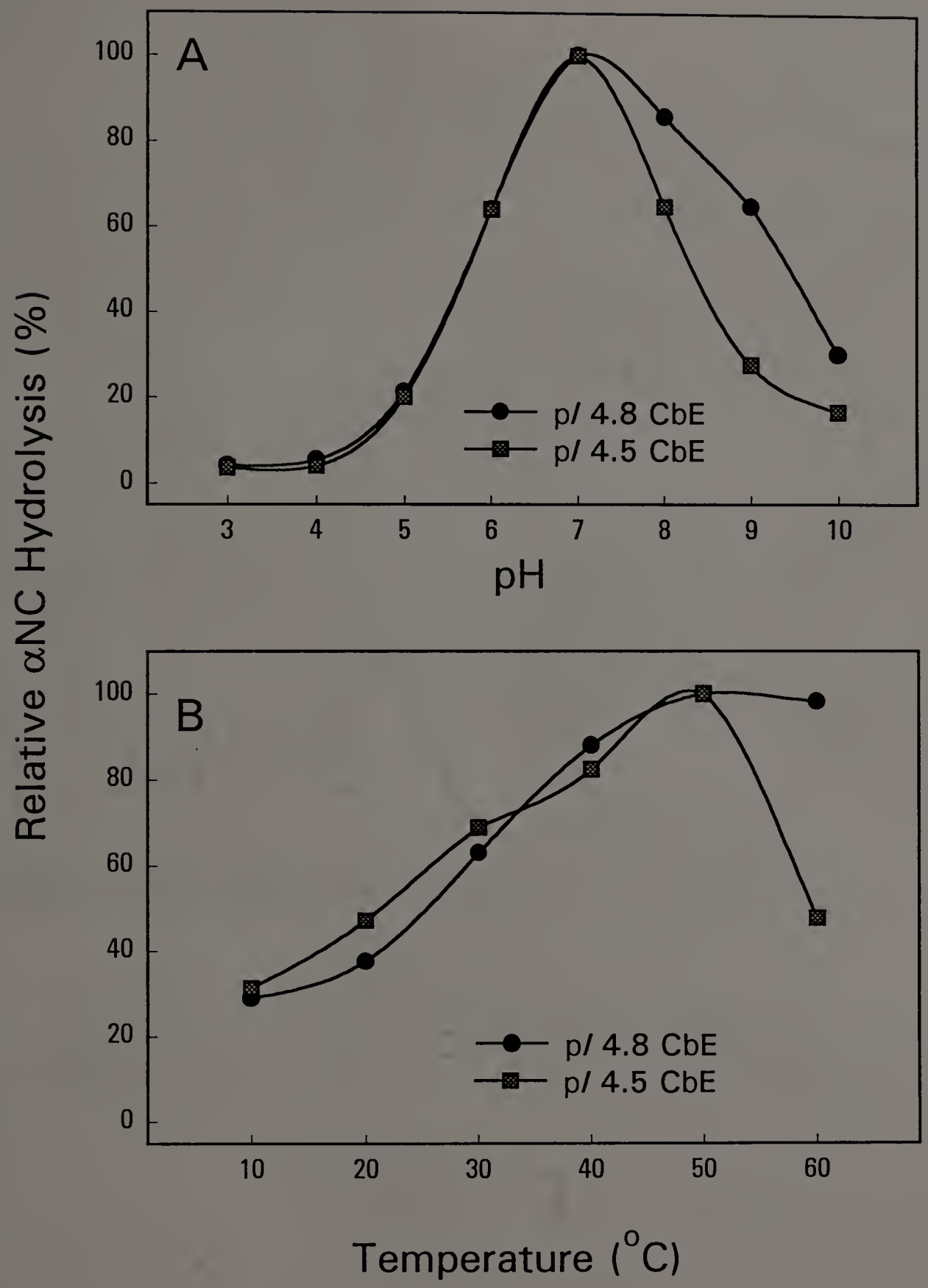

Fig. 19. Effects of pH (A) and temperature (B) on αNC hydrolysis by the p*I* 4.5 and 4.8 CbEs.

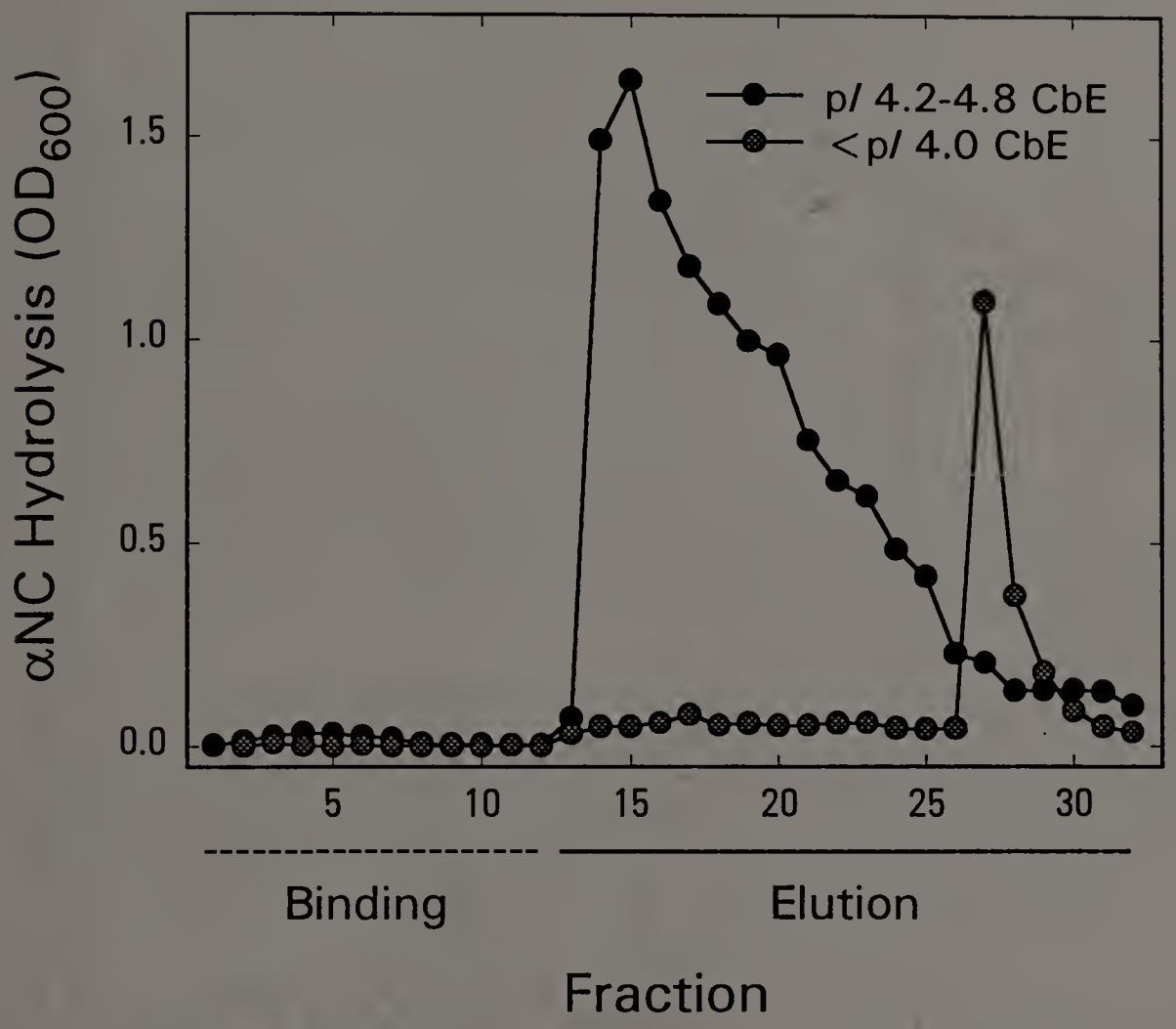

Fig. 20. Concanavalin A-Sepharose affinity chromatography of the p*I* 4.2-4.8 CbEs.

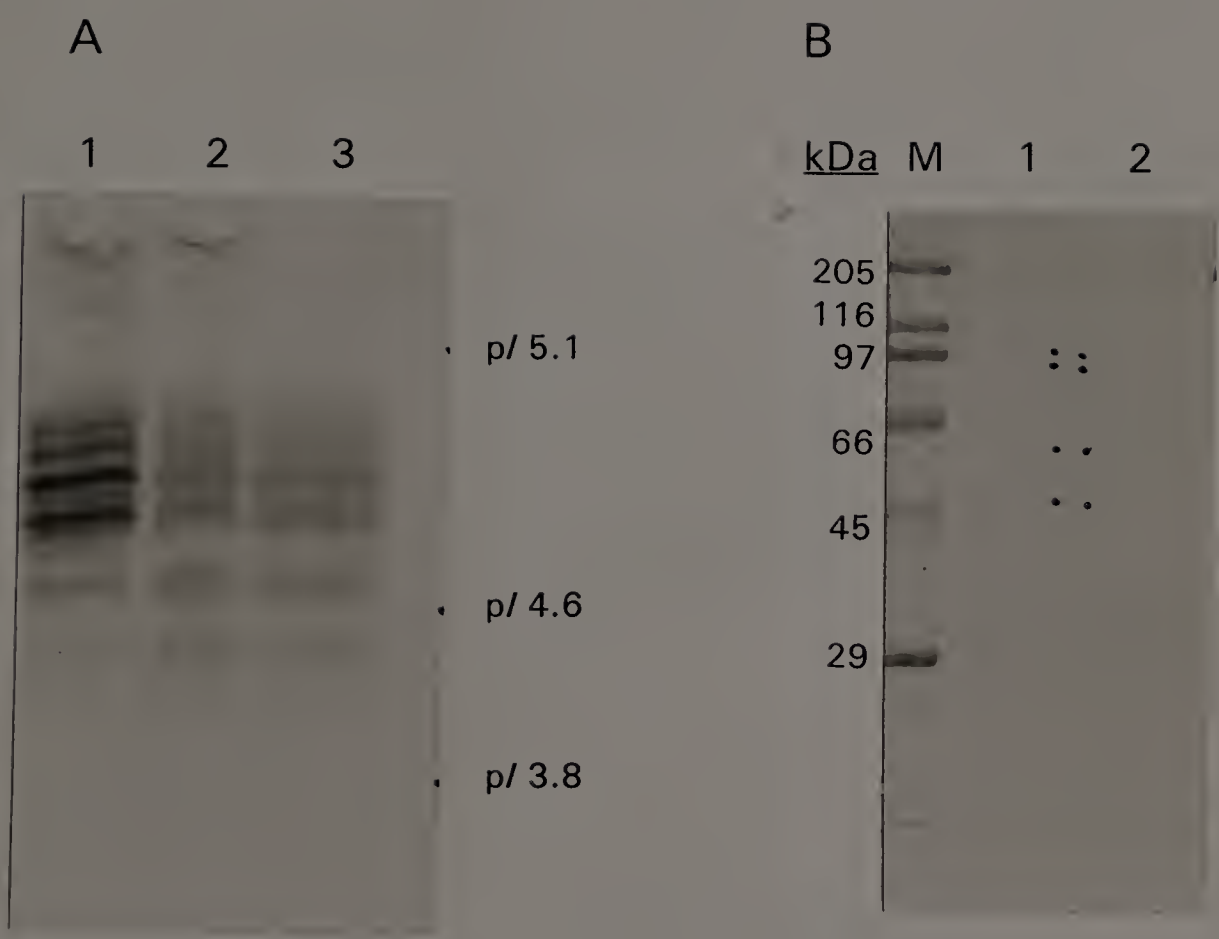

Fig. 21. Analysis of the deglycosylated p*I* 4.2-4.8 CbEs by isoelectricfocusing (A) and SDS-PAGE (B). The isoelectricfocusing gel was stained with αNB/αNC-dianisidine. Lanes 1, 2, and 3 are untreated, control (i.e., incubated without *N*-glycosidase F), and deglycosylated (i.e., + 20 U *N*-glycosidase F) p*I* 4.2-4.8 CbEs, respectively. The SDS-polyacrylamide gel was stained with Coomassie blue. Lanes 1 and 2 are control and deglycosylated p*I* 4.2-4.8 CbEs, respectively.

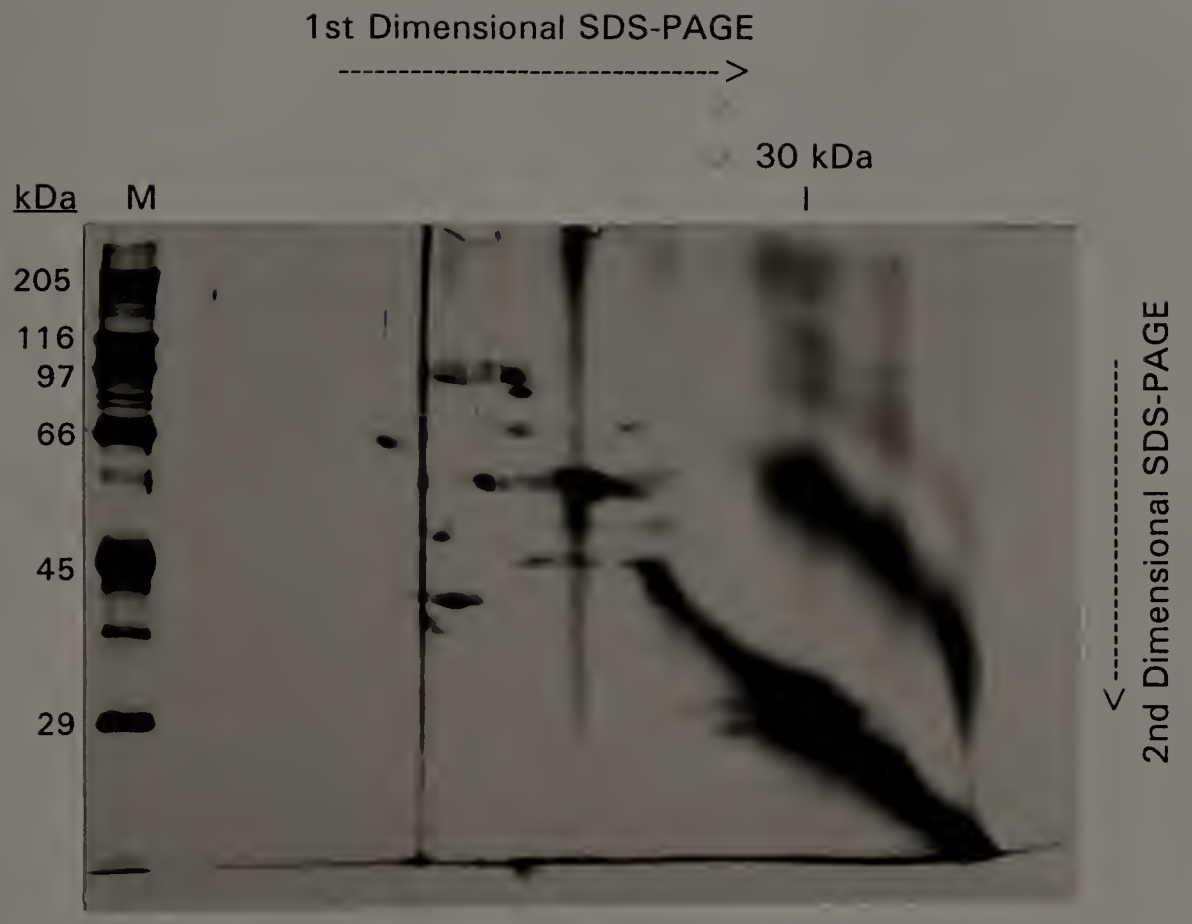

Fig. 22. Two-dimensional gel electrophoresis of the denatured p*I* 4.2-4.8 CbEs (1st dimension SDS-PAGE vs. 2nd dimension SDS-PAGE). The gel was silver-stained. M, molecular weight marker proteins. The molecular mass of marker proteins are shown on the left side of the gel.

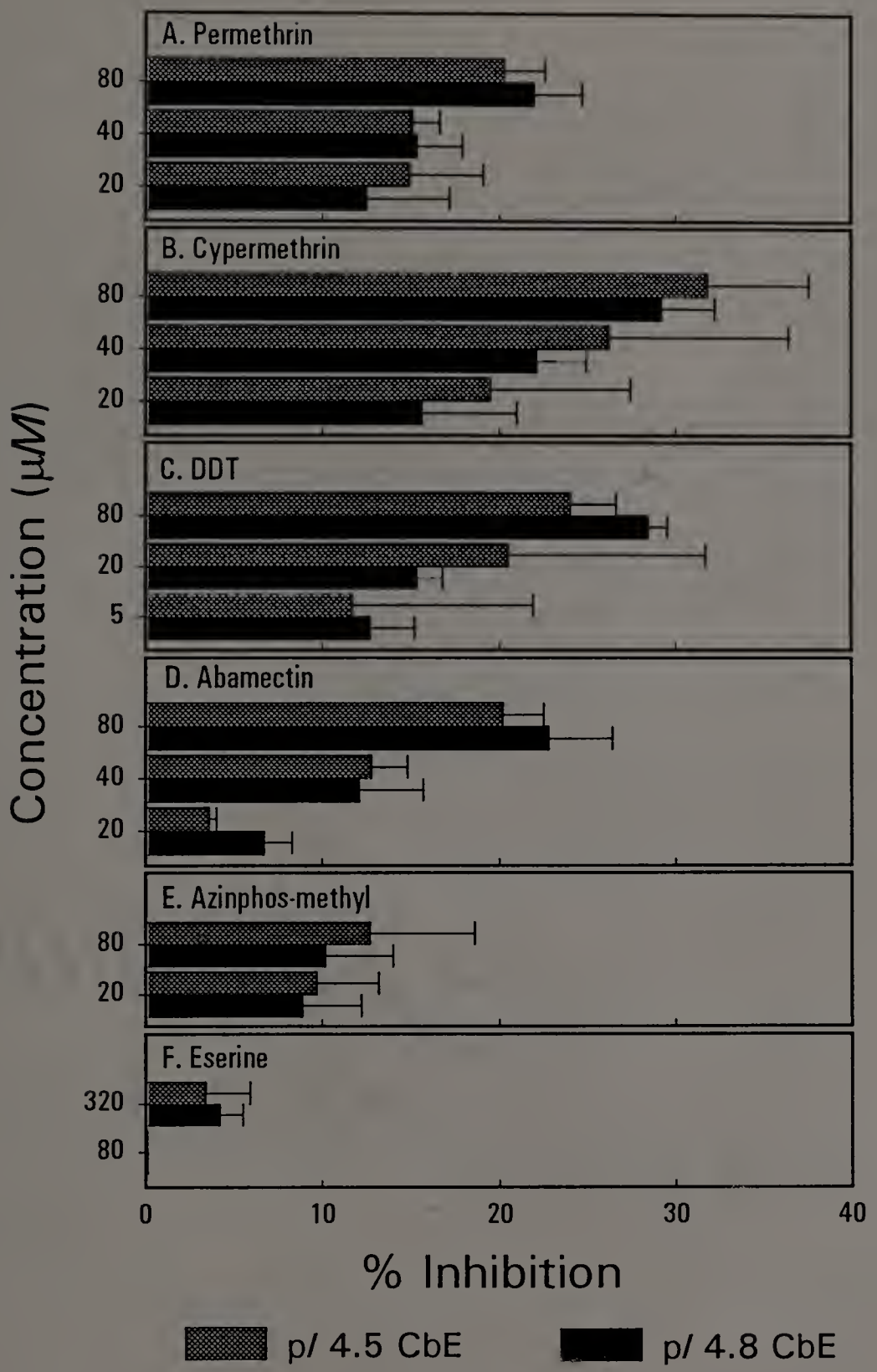

Fig. 23. Inhibition of the p*I* 4.5 and 4.8 CbEs by several insecticides and eserine.

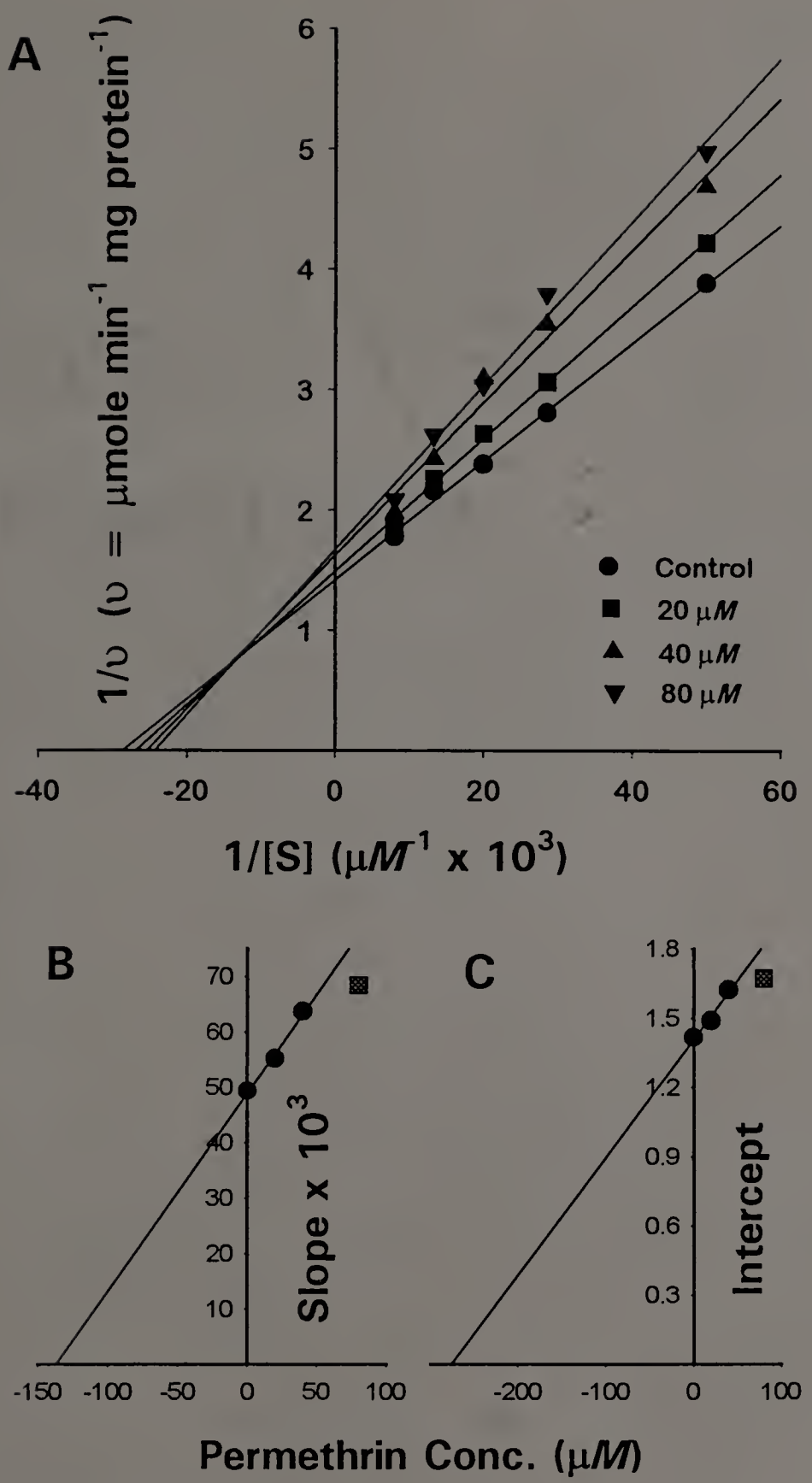

Fig. 24. Kinetic analysis for the inhibition of the p*I* 4.5-4.8 CbEs by permethrin. (A) Lineweaver-Burk plot of 1/υ *vs*. 1/[S] in the presence of various concentrations of permethrin (0-80 μM); (B) replot of slope *vs*. permethrin concentration; (C) replot of intercept *vs*. permethrin concentration.

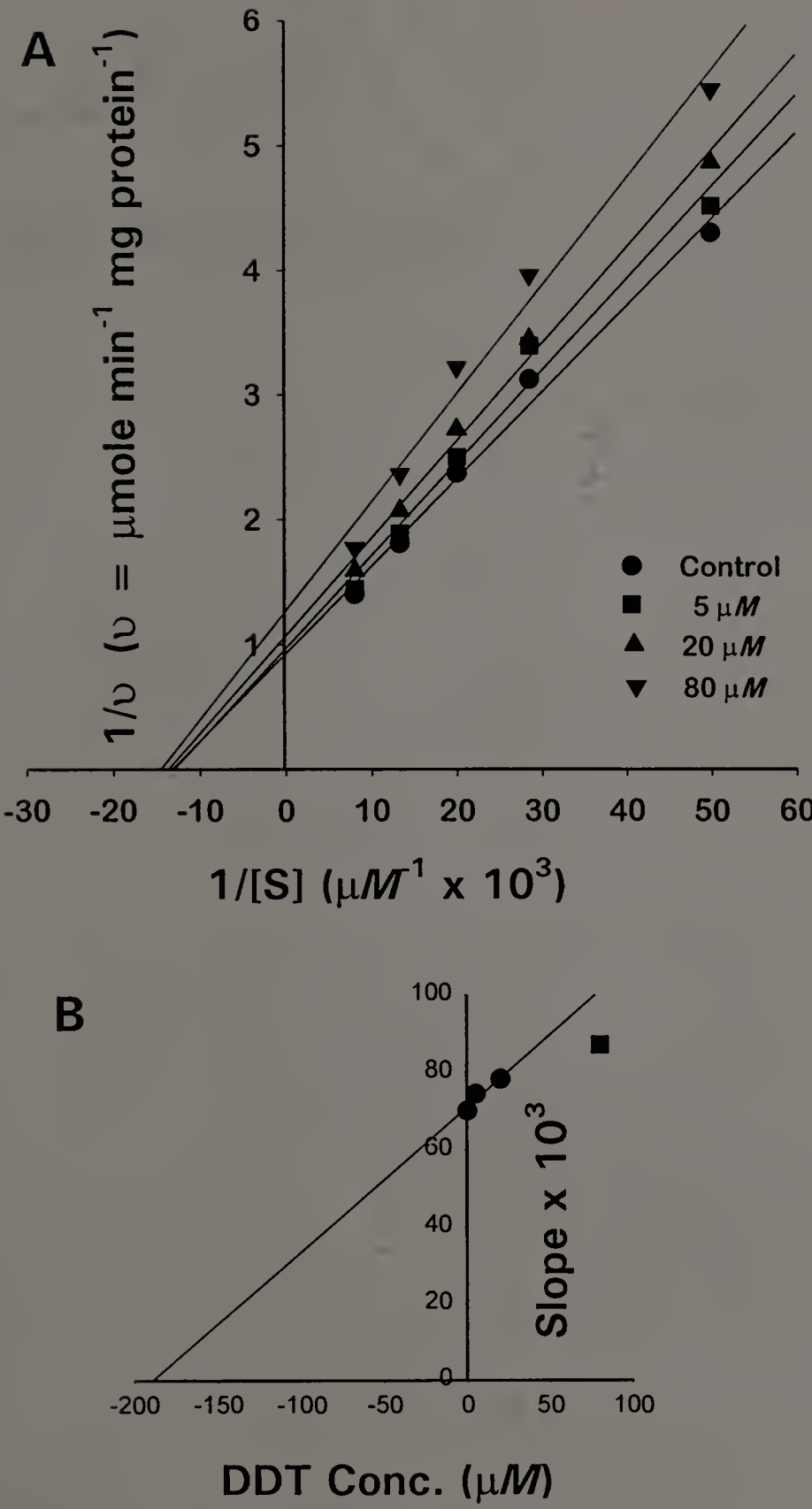

Fig. 25. Kinetic analysis for the inhibition of the p*I* 4.5-4.8 CbEs by DDT. (A) Lineweaver-Burk plot of 1/υ *vs*. 1/[S] in the presence of various concentrations of DDT (0-80 μM); (B) replot of slope *vs*. DDT concentration.

Fig. 26. SDS-PAGE of the purified 30, 48, and 60 kDa CbE protein immunogens.

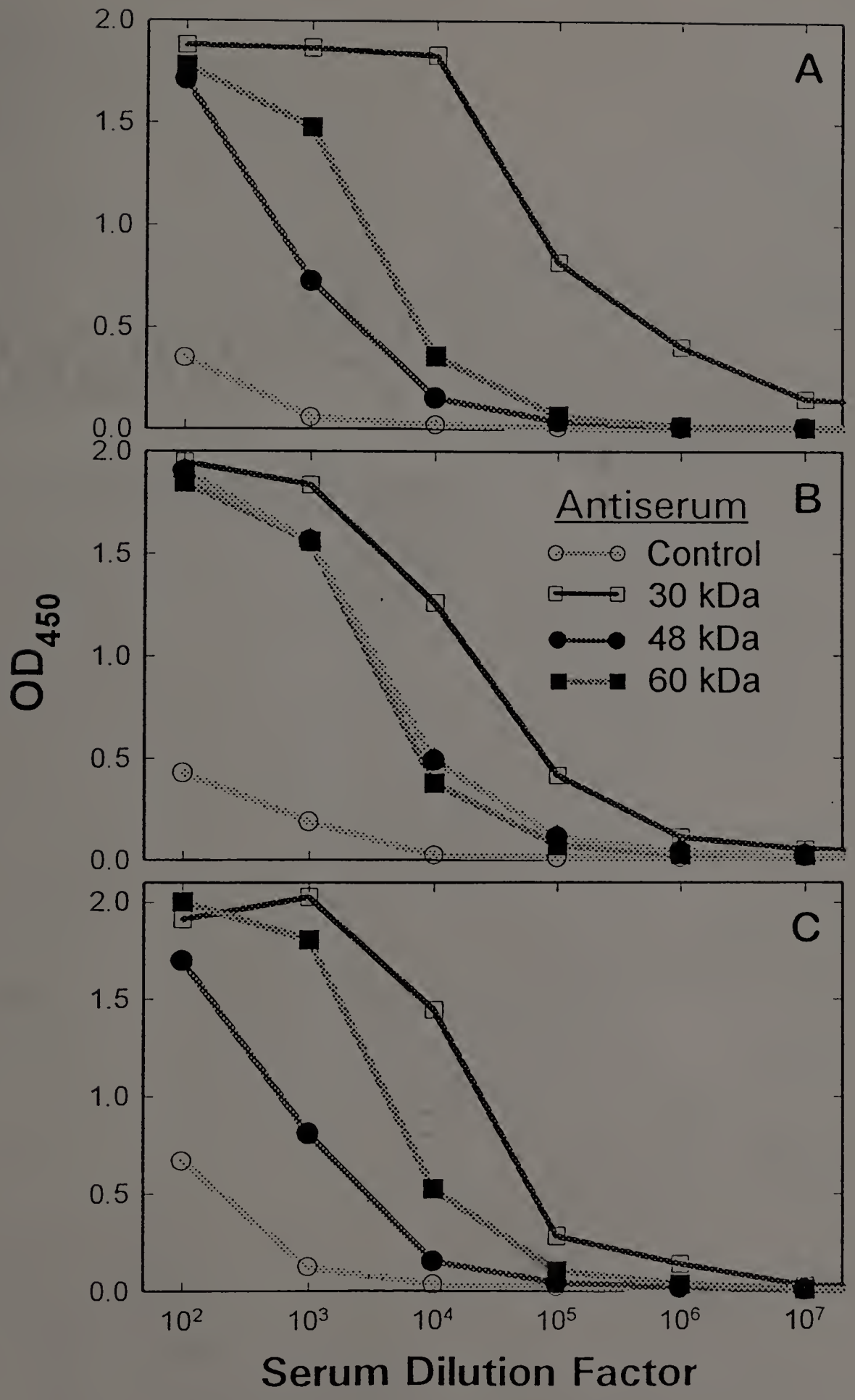

Fig. 27. Evaluation of antibody titer and cross-reactivity of antibodies to immunogens by antibody capture immunoassay. (A) 30 kDa immunogen-coated plate; (B) 48 kDa immunogen-coated plate; (C) 60 kDa immunogen-coated plate.

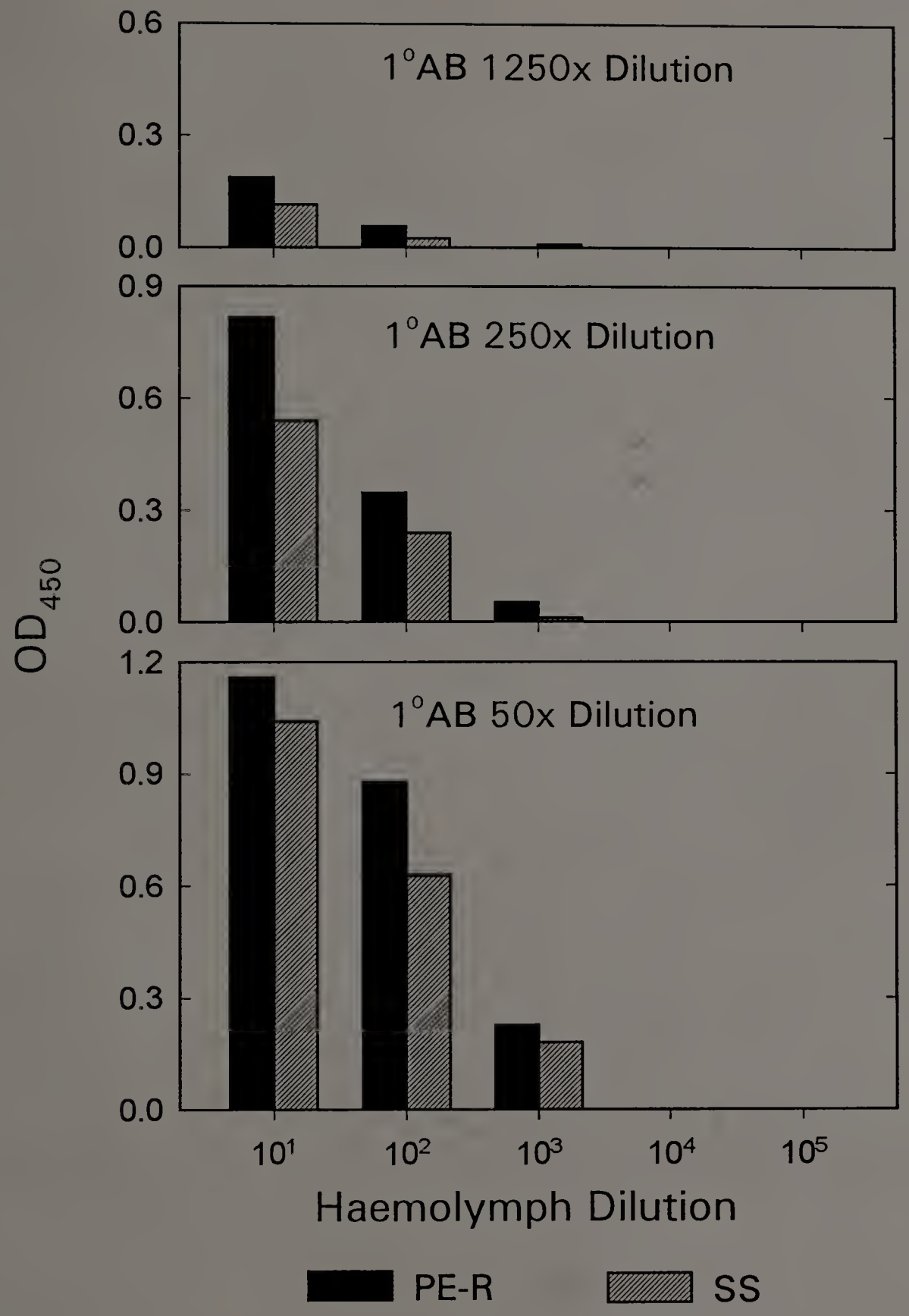

Fig. 28. Determination of the optimum conditions for antibody capture immunoassay.

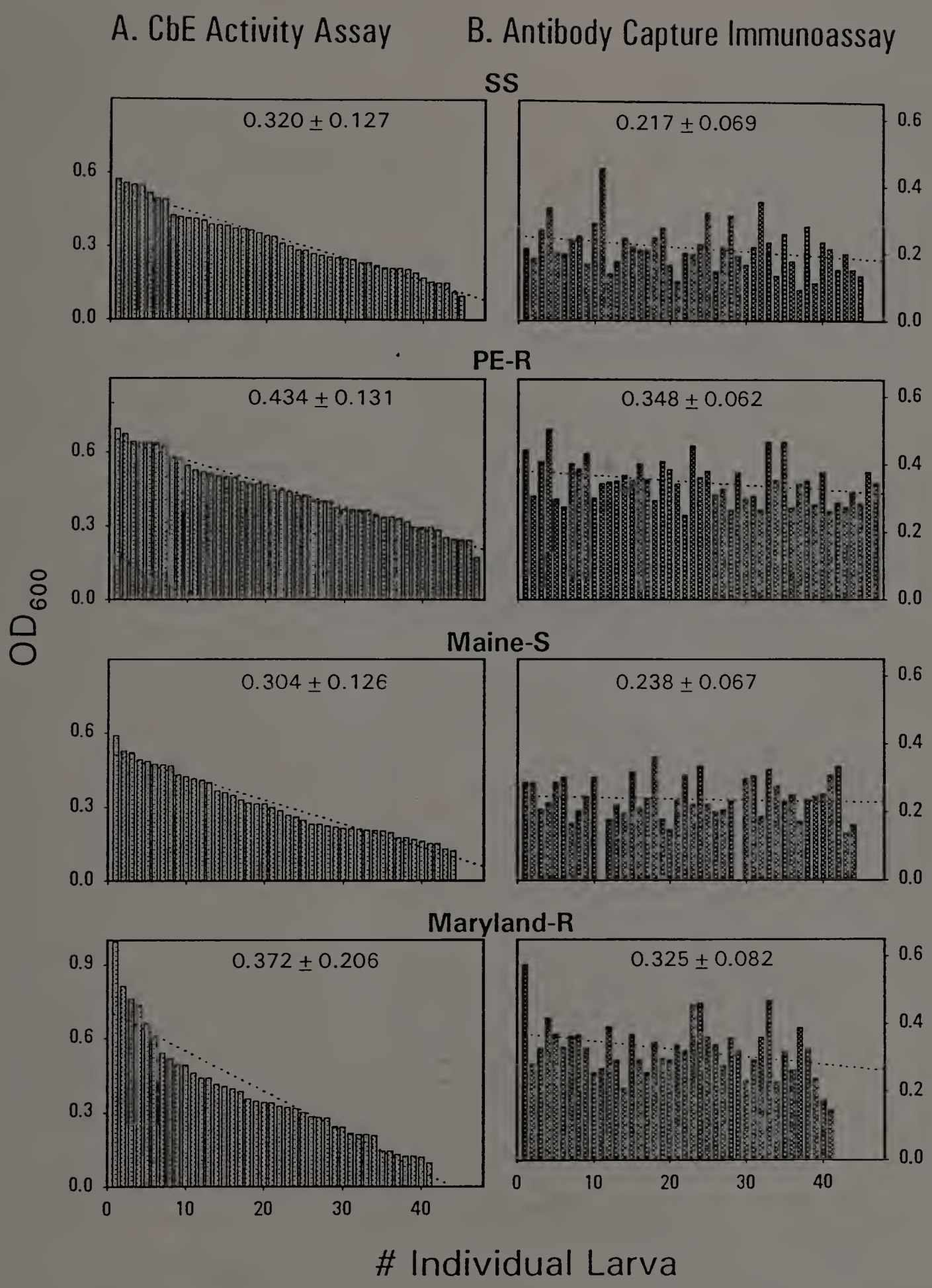

Fig. 29. CbE activity assay (A) and antibody capture immunoassay (B) of the individual hemolymphs from 4 different strains of CPB.

CHAPTER IV

DISCUSSION

A. Tissue Distribution and Identification of Permethrin CbE

An enhanced level of CbE activity that was detected from a whole body preparation has been reported to be associated with permethrin resistance in the PE-R strain of CPB (10, 60). When the tissue distribution of the CbE in CPB was examined in detail, the majority of permethrin hydrolytic activity was found to be associated with the HAE and SOL fractions (Fig. 1). The increased level of permethrin hydrolysis in the HAE and SOL fractions from the PE-R strain correlated well with increased hydrolyzing activity toward αNB, a general CbE substrate (Fig. 1). Although the SOL fraction was prepared from the hemolymph-depleted body, it is likely to be contaminated with hemolymph CbEs because complete removal of hemolymph from CPB body is virtually impossible. It is likely, therefore, that the actual amount of CbEs associated with hemolymph may be more than initially estimated.

Several negatively charged forms of CbEs (i.e., p*I* 4.2-4.8 CbEs) were determined to constitute the major portion of CbE activity in hemolymph and to be associated with resistance through electrophoresis analyses and chromatofocusing (Fig. 3 and 4). The p*I* 4.2-4.8 CbEs had elevated levels of permethrin hydrolysis (i.e., 1.6-6.0 times) in the PE-R strain when compared to the near isogenic SS strain. Since the pH of CPB hemolymph is nearly neutral (i.e., pH 7.4, unpublished observation), the p*I* 4.2-4.8 CbEs are highly negative-charged in hemolymph and accordingly highly soluble. Soluble CbEs implicated in insecticide resistance have also been reported in other insect species (23-25, 34, 41, 68). However, it is not clear whether those soluble CbEs are primarily associated with hemolymph since no information on their tissue

distribution is available. In contrast, pyrethroid-hydrolyzing CbEs that are membrane-associated have been identified in resistant strains of the southern armyworm, *S. eridania* (30), and the cattle tick, *B. microplus* (69).

The p*I* 4.2-4.8 CbEs, particularly p*I* 4.5-4.8 CbEs, were demonstrated to be overproduced in the PE-R strain through electrophoretic comparison and kinetic analysis. According to the densitometric comparison of the CbE protein content, the PE-R strain produces 2.2-3.3 times higher level of the p*I* 4.2-4.8 CbEs compared with the SS strain (Fig. 5). In the comparison of the kinetic constants (i.e., V_{max} and K_m) of the p*I* 4.2-4.8 CbEs from the PE-R and SS strains, the V_{max} values for all three p*I* CbEs from the PE-R strain were higher (i.e., 5.1 to 17.6-times) than the corresponding p*I* CbEs from the SS strain (Table 2). In contrast, the affinity constants (i.e., $1/K_m$) of all three p*I* CbEs from the PE-R strain were slightly lower (i.e., 0.4 to 0.6-times) than those from the SS strain (Table 2). These results corroborate that the enhanced hydrolysis of naphthyl substrates and permethrin by the p*I* 4.2-4.8 CbEs (particularly p*I* 4.5-4.8 CbEs) from the PE-R strain is due to the increased amount of the CbE rather than due to any qualitative change in the enzyme, itself. Overproduced esterases associated with insecticide resistance are well documented in several insects including *M. persicae* (23, 31), *C. quinquefasciatus* (43), and *C. pipiens* (41). However, it is not clear whether the overproduced p*I* 4.2-4.8 CbEs in the PE-R strain are due to gene amplification. Other possible mechanisms for overexpression of protein may be transcriptional regulation, such as increased rate of transcription, increased stability of mRNA, or increased efficiency in 3' end processing of the primary transcript (70-72).

The presence of large amounts of permethrin-hydrolyzing CbEs (i.e., p*I* 4.2-4.8 CbEs) in hemolymph implies a crucial role of hemolymph as the first barrier against the insecticides that have been absorbed and further implicates hemolymph CbEs as a major resistance mechanism in general. However, the overall rate of permethrin hydrolysis by hemolymph CbEs from CPB was very low (i.e., 3.6 pmole/hr/mg

protein) when compared to the pyrethroid-hydrolyzing esterases from other insect species. Abdel-Aal and Soderlund (30) reported that the rates of *trans*-permethrin hydrolysis by the homogenates of cuticle, gut, and fat body from *S. eridania* were in the range of 2.6-3.6 nmole/min/mg protein. The rates of permethrin hydrolysis by soluble esterases from the midguts of the five phytophagous and one entomophagous insects were 0.14-7.85 nmole/min/mg protein (73). In comparison, the rate of permethrin hydrolysis by the hemolymph CbE of CPB are ca. 2,300-130,000 times lower than those by the esterases from the insects described above.

With the above discussion in mind, it is questionable whether the permethrin CbE in the CPB hemolymph can provide sufficient protection from permethrin by simply hydrolyzing it. Topical application of a discriminating dose of permethrin (i.e., 0.5 μg/larvae, 1.4 nmole permethrin/larva) to 4th instars of the PE-R strain usually does not cause any lethality. The same treatment applied to the SS strain, however, results in 100% knockdown in 1 hr and ultimately causes mortality without any recovery (60). If it is assumed that ca. 76% of topically-applied permethrin penetrates through the cuticle in 6 hr (60), the estimated amount of internal permethrin will be ca. 1.1 nmoles. The rate of permethrin hydrolysis by the p*I* 4.2-4.8 CbEs in a single larva was estimated as ca. 18.9 and 4.1 pmole/hr/larva for the PE-R and SS strains, respectively (calculated from Fig. 4). The difference in the permethrin hydrolysis rate of individual larva of the PE-R and SS strains is calculated as ca. 88.8 pmole/6 hrs/larva (i.e., 14.8 pmole/hr/larva). This amount accounts for only 8.1% of the total permethrin penetrated into the CPB body. Thus, the level of permethrin hydrolysis does not appear to be sufficient to explain the prominent differences in the toxicological response between strains. Although this assumption did not take into account the actual toxicokinetic and metabolic processes, it is still meaningful in evaluating the nature of permethrin resistance mediated by the hemolymph CbEs (e.g., p*I* 4.2-4.8 CbEs). The

hemolymph CbEs in CPB are not likely to function as true permethrin hydrolases given the above scenario.

Permethrin inhibits the hemolymph CbEs in a reversible manner, possibly, through high affinity binding to the hydrophobic catalytic site(s) and/or other hydrophobic non-catalytic site(s) (e.g., hydrophobic site) on the CbEs (Fig. 6). Similar reversible interactions between hydrophobic compounds and proteins have been widely documented elsewhere. For example, human serum albumin transports lipophilic drugs through reversible binding in aqueous plasma by doing so regulates the distribution of drugs in serum (74). The E4 esterase from *M. persicae* is known to interact reversibly with pyrethroids through its hydrophobic catalytic center (75).

The obvious differences in the permethrin inhibition patterns between the SS and PE-R strains can be explained by the different amounts of CbEs associated with the hemolymph of each strain (Fig. 6). The higher levels of specific CbEs (i.e., mainly p*I* 4.2-4.8 CbEs as shown in Fig. 4) in the PE-R hemolymph resulted in the continuous dose-dependent inhibition pattern that did not show the inhibition saturation phenomena observed with the SS hemolymph CbE. If the binding of permethrin to specific hemolymph CbEs (i.e., p*I* 4.2-4.8 CbEs) through hydrophobic interaction is more favored than the partitioning and adsorption onto the target site in the nervous system, such an interaction would provide an efficient protection mechanism from permethrin neurotoxicity. Once permethrin bound to the CbE, the CbE-permethrin complex could be freely but preferentially transported to a site(s) for detoxification (e.g., fat body) and/or elimination (e.g., Malpighian tubule). As a result, the overproduced p*I* 4.2-4.8 CbEs in the PE-R strain of CPB appear to confer resistance by sequestration rather than rapid hydrolysis of permethrin. Furthermore, the freely-circulating nature of the p*I* 4.2-4.8 CbEs in hemolymph is likely to ensure an efficient sequestration of lipophilic insecticides such as permethrin.

B. Purification of Permethrin CbE

The purification factor (i.e., 51- and 77-fold purification as judged by αNC and permethrin hydrolysis, respectively, Table 3) obtained in the purification of the permethrin CbE from hemolymph is relatively low when compared to enzymes with high substrate specificities. However, this level of purification is not unusual when compared with the purifications of other CbEs. The CbEs from the rice brown planthopper *Nilaparvata lugens*, rat, and house mouse were purified to homogenous states with the purification factors of ca. 24-, 70-, and 50-fold, respectively (76-78). Although αNC hydrolysis activity was best correlated with the permethrin hydrolysis activity, αNC can be still hydrolyzed by other non-specific esterases. Therefore, the true purification factor in the purification of the permethrin CbE was likely underestimated due, in part, to calculating the purification factor based on the hydrolysis activity of nonspecific substrates, such as naphthyl esters. The low level of purification is also likely a result of the endogenously high abundance of the permethrin CbEs in CPB hemolymph (ca. 1.8% of the total protein in the hemolymph of the PE-R strain), which is essential for efficient sequestration. An esterase whose primary function is sequestration typically constitutes large portion of total proteins in an insect body. The sequestration esterases from the aphid *M. persicae* and the mosquito *C. quinquefasciatus* account for as much as 3% and 12% of total protein, respectively, in highly resistant strains (31, 41).

C. Biochemical Properties of Permethrin CbE

In kinetic analysis of various naphthyl substrates, K_m values for the charged forms of permethrin CbE (i.e., pI 4.8, 4.5, and 4.2 CbEs) were similar to those for other

purified CbEs (23, 29, 76, 79, 80). However, the V_{max} values for the charged forms of permethrin CbE using naphthyl substrates were approximately 120-440, 53, and 50 times lower than those from C. *quinquefasciatus* (79), *N. lugens* (76), and *L. cuprina* (29), respectively, but 16 times higher than that from *L. striatellus* (80). Therefore, the permethrin CbE of CPB appears to be a relatively poor hydrolase when compared with other insect CbEs.

The consistent tendency of increased affinities for all three p*I* CbEs as the hydrophobicity of naphthyl substrate increase implies that the catalytic sites of all the p*I* CbEs have hydrophobic properties (Fig. 15). A similar property of the catalytic site of the rat plasma esterase, ES-1A, was reported, where the K_m value decreased with increasing length of the acyl chain of substrates (81). A hydrophobic catalytic site was also associated with the E4 esterase from *M. persicae* (75). The K_m values of the E4 esterase for αNA, α-naphthyl propionate (αNP), and αNB were 131, 62, and 35 μ*M*, respectively. The hydrophobicity level of substrate was an important factor in the hydrolysis of phosphorothionate substrates by the esterase from *Triatoma infestans* (82). Interestingly, several hydrophobic amino residues in the 10-residue segment surrounding the catalytic site, which are proposed as a hydrophobic lipid binding site, are conserved in all known lipase sequences (83).

The hydrophobicity of the catalytic site of the p*I* 4.8 and 4.5 CbEs, however, was determined not to be associated with overall surface hydrophobicity of the permethrin CbE, as judged from the HIC behavior of the p*I* 4.8 and 4.5 CbE (Fig.). The separate nature of the hydrophobicity of the catalytic site from the overall surface hydrophobicity allows the possibility that the catalytic site of the permethrin CbE is concealed from the surface of enzyme, as proposed in several lipases (84-86). In this model, the hydrophobic catalytic site of the lipase is buried under a short α-helical fragment of a surface loop to ensure water-solubility of the lipase and to protect the catalytic site from aggregation with itself or any other hydrophobic surface.

The hydrolytic efficiency of the permethrin CbE decreases with increasing hydrophobicity of the substrate in spite of an increase in affinity (Fig. 15). The decreasing hydrolytic efficiencies toward the substrates with increasing acyl carbon chain indicates that the permethrin CbE prefers to hydrolyze substrates with short acyl chain. It is also in keeping with the low hydrolysis rate of permethrin, a (2,2-dichlorovinyl)-2,2-dimethyl cyclopropanecarboxylate. This finding is contrary to the kinetics shown by rat plasma esterases, however, where an increase in the length of acyl carbon chain from 2 to 10 in the nitrophenyl and naphthyl substrates results in a progressive increase in the V_{max} values (81, 87).

The less negatively charged forms of the permethrin CbE (e.g., p*I* 4.8 CbE) showed higher affinity and catalytic efficiency toward all three naphthyl substrates tested, regardless of their levels of hydrophobicity (Fig. 15). Similar trends of increases in the affinity and catalytic efficiency among the less negatively charged forms of CbE were reported for the CbE from the rice brown planthopper (76).

The relative differences in the affinity (i.e., $1/K_m$) of the p*I* 4.2-4.8 CbEs for the three naphthyl substrates were in the ranges of ca. 2.9-4.2 times. The relative differences in catalytic efficiency (i.e., V_{max}) of the p*I* 4.2-4.8 CbEs for the three naphthyl substrates were in the range of 3.1-3.7 times. Because the overall differences in the kinetic constants do not differ substantially, it is likely that the catalytic sites are not very different in their primary structure and/or their conformation. The close similarity of the pH-αNC hydrolysis profiles of the p*I* 4.8 and 4.5 CbEs supports this contention (Fig. 19).

Both p*I* 4.8 and 4.5 CbEs were inhibited by serine hydroxyl group esterase inhibitors including DFP, DEF, and PMSF, indicating that they are all serine-type esterases (Table 5). Based on the high degree of DFP sensitivity, both CbEs appear to be B-type esterases. The p*I* 4.8 and 4.5 CbEs are not likely juvenile hormone esterases since juvenile hormone esterase from the CPB hemolymph was reported to be

insensitive to 10^{-3} *M* DFP (88). The lack of inhibition by eserine indicates that the p*I* 4.8 and 4.5 CbEs are not cholinesterases and is in contrast to the CbE from *C. quinquefasciatus* that is quite sensitive to inhibition by eserine (i.e., 95% by 10 μM eserine)(89). The significant difference in the sensitivity to PMSF inhibition between the p*I* 4.8 and 4.5 CbEs (i.e., 232 μM I_{50} for the p*I* 4.8 CbE *vs.* 80 μM I_{50} for the p*I* 4.5 CbE, respectively), however, suggests that their catalytic site structures and/or conformations are not identical. Both p*I* 4.8 and 4.5 CbEs were also inhibited by PHMB, which indicates that they also possess a characteristic of arylesterase (EC 3.1.1.2)(90). However, the p*I* 4.8 CbE was 3-17 times more sensitive to PHMB inhibition compared to the p*I* 4.5 CbE. This finding is again suggestive of the differences in the catalytic site structure and/or conformation of the p*I* 4.8 and 4.5 CbEs. The malathion CbE from the sheep blowfly, *Lucilia cuprina*, also showed a property of arylesterase in terms of inhibition by PCMB, an analogue of PHMB (29).

The allosteric nature of PHMB-inhibition is indicative of the existence of a hydrophobic non-catalytic site on the permethrin CbE (Fig. 16). The presence of the hydrophobic non-catalytic site on the permethrin CbE was demonstrated by the analyses of inhibition kinetics of permethrin and DDT (Fig. 24 and 25). Both the hydrophobic non-catalytic site(s) and hydrophobic catalytic site appear to also play a crucial role in the sequestration of hydrophobic compounds by permethrin CbE. Reversible inhibition of butyrylcholinesterase by various aromatic hydrocarbons is primarily due to hydrophobic interaction (91). Lipophilic drugs are also known to bind to albumin through hydrophobic interaction and hydrogen bonding (74). An anti-flammatory drug, fenoprofen, which shares a phenoxybenzyl alcohol moiety in common with permethrin and a number of other pyrethroids, was reported to strongly bind onto 4-5 sites of albumin (74). Thus, hydrophobic interaction-based equilibrium processes between the CbE and hydrophobic ester compounds, such as permethrin, at

both catalytic and non-catalytic sites are likely responsible for the sequestration of permethrin and, in part, for permethrin resistance in CPB.

Hydrophobic insecticides that contain no ester moieties, such as DDT, abamectin, etc., appear to be sequestered by the permethrin CbE through an interactions with the hydrophobic non-catalytic site of the permethrin CbE. The binding strength of these insecticides to the permethrin CbE, as judged by degree of inhibition, was proportional to their hydrophobicity. Similar findings were reported for serum proteins from rat and cockroach, *P. americana*, in which the strength of hydrophobic interaction between serum proteins and various ligands was directly related to the hydrophobicity of the compounds (92). Therefore, the permethrin CbE seems to function as a nonspecific sequestration protein against various hydrophobic insecticides. This nonspecific sequestration by the permethrin CbE appears to be a mechanism underlying the cross-resistance of the PE-R strain to other pyrethroids, DDT, and abamectin (cross-resistance to abamectin, unpublished observation, S. H. Lee). Cross-resistance of fenitrothion and deltamethrin was reported in the Guatemalan mosquito *A. albimanus*. The cross-resistance seems to be associated with the non-specific sequestration of fenitrothion and deltamethrin by the esterase (36).

The optimum pH of the permethrin CbE (i.e., pH 7) is similar to the typical optimum pH range of other CbEs (i.e., pH 6.5-8.5)(77, 78, 81). The optimum temperature of the permethrin CbE for the hydrolysis of naphthyl substrates (i.e., ca. 50°C for both the p*I* 4.8 and 4.5 CbEs) is somewhat high considering the optimum developmental condition of CPB (i.e., 25-33°C)(93). However, high optimum temperatures for esterase (i.e., 45-60°C) have been reported in other species including mammals and insects (81, 82, 94-96). The p*I* 4.8 CbE elicited a higher thermal stability than the p*I* 4.5 CbE. Besides enhanced thermal stability, the p*I* 4.8 CbE is more resistant to SDS-denaturation as suggested from the renaturation experiments, where only the p*I* 4.8 CbE was renatured and resumed hydrolysis activity (Fig. 11).

The p*I* 4.8 and 4.5 CbEs are functionally similar to each other in that they are the major forms of the permethrin-hydrolyzing and sequestrating CbEs associated with permethrin resistance. Additionally, the p*I* 4.8, 4.5, and 4.2 CbEs are immunologically related, indicating close similarities in their primary protein structure (Fig. 27). Although the p*I* 4.8 and 4.5 CbEs share a number of biochemical properties, including substrate specificity and inhibition properties, their molecular properties appear to be quite distinct from each other. The p*I* 4.8 CbE is 49-50 kDa monomer while the p*I* 4.5 and 4.2 CbEs are likely ca. 57-59 kDa noncovalent dimers. The native *Mr*s of the permethrin CbE are similar to those from other insects, which range from 59-110 kDa (23, 29, 41, 68, 76-82). However, dimeric association of small subunits (i.e., 25-31 kDa), as proposed for the p*I* 4.5 and 4.2 CbEs, has not been previously reported in animal species. One similar case has been reported for a CbE from an aerobic bacterium *Pseudomonas fluorescens,* which was composed of two identical subunits, each with a *Mr* of 23 kDa (97).

These distinct molecular features of the p*I* 4.8 and 4.5 CbEs imply that the different forms of CbE are likely expressed from separate genes rather than generated by post-translational modifications of the products from a single gene or a similar gene family. A similar case has been reported in OP-resistant Culex mosquitoes, where two groups of esterases with different molecular properties [i.e., a 110-120 kDa homodimer (or possibly 67 kDa monomer, see Ref. 89) designated as esterase A and a 62-67 kDa monomer designated as esterase B] are equally involved in OP resistance and share a number of biochemical properties (41, 68, 79, 89). The A and B esterases are encoded by two distinct genes with closely linked loci (98). Since the overproduced A2 and B2 esterases, both isoenzymes of A and B esterases, respectively, from *Culex* have always been found together in field resistant strains throughout at least three continents, it has been proposed that they arose initially from a single gene duplication initial event (99).

Each charged form of permethrin CbE (i.e., p*I* 4.8, 4.5, and 4.2 CbE) is composed of 2-7 proteins with slightly different p*I* values (i.e., charged isomers), as determined from 2-DGE (Fig. 13). Charged isomers of a CbE have been also reported in *N. lugens* (100), *L. striatellus* (80), and in some tissues of vertebrates including rat liver (101) and bird sera (102). Thompson et al. (102) have further suggested that different forms of esterases in bird serum might vary in their binding capacity for pesticides. However, the functional significance of the charged isomers of each p*I* CbE in permethrin resistance is not completely resolved at this point.

The permethrin CbE is *N*-glycosylated, as demonstrated by ConA-Sepharose chromatography (Fig. 20). Glycosylation nature of the CbE can be also found in other insects, such as *M. persicae* and *C. quinquefasciatus* (89, 103). The *N*-glycan moieties are not associated with the charge heterogeneity of the permethrin CbE as demonstrated by *N*-deglycosylation experiments (Fig. 21). Thus, the charge heterogeneity is likely associated with polypeptide moieties and/or possibly with *O*-glycans although it is unknown whether the permethrin CbE has *O*-glycan moieties. If the charge heterogeneity is associated with the polypeptide make-up, substitution of amino acids would then be a possible mechanism. As shown in the IEF and 2-DGE experiments, the charge difference between adjacent charge forms of the p*I* 4.8, 4.5, and 4.2 CbEs is uniformly 0.1-0.15 unit (Fig. 13). These slight differences in p*I* values can arise by the substitution of one histidine residue with any neutral amino acid (i.e., protonation) or *vice versa* (i.e., deprotonation), as demonstrated in the *E. coli* carboxylesterase B polymorphism (104). In addition, post-translational modifications, such as phosphorylation/dephosphorylation, amidation/deamidation, sulfation/desulfation, etc., are also possible means resulting in the charge heterogeneity of the permethrin CbE (105, 106).

The intrinsic physiological function of the permethrin CbE is still not known. The high affinity of the permethrin CbE to various hydrophobic compounds suggests that

perhaps it participates in transport of hydrophobic (or lipophilic) materials in the hemolymph. The CbE associated with resistance in *C. quinquefasciatus* was proposed to have an endogenous lipase function (89). However, the permethrin CbE is not likely involved in lipid hydrolysis because its catalytic efficiency toward naphthyl substrates with longer acyl chain lengths was diminished. To address this question more accurately, an evaluation of substrate specificity toward various lipids such as mono-, di-, and tri-acyl glycerols would be required.

CbEs from vertebrates have been shown to be mainly associated with detoxification of xenobiotics (107). The permethrin CbE also appears to participate in the detoxification of xenobiotics, largely derived from the solanaceous plants, such as potato that serves as the host plant for CPB. However, the interaction of permethrin CbE with steroidal glycoalkaloids (e.g., solanine, chaconine, tomatine, etc.), one major group of toxic secondary compounds originated from the host solanaceous plants, was poor as judged by inhibition experiments (data not shown). This finding suggests that the permethrin CbE, itself, is not likely to be directly involved in the detoxification or sequestration of the steroidal glycoalkaloids. The permethrin CbE may have evolved from a group of esterase initially involved in endogenous detoxification of plant derived esters to have the sequestration functions for hydrophobic insecticides including permethrin under the selection pressure by those insecticides.

The PE-R strain has been continuously selected by permethrin every 3-4 months since 1991 (see 'Insect Strains' in Materials and Methods), during which the overall permethrin resistance level of the PE-R strain increased slightly [i.e., 19-fold resistance (see Ref. 9) to 23-fold resistance in Fall 1994, data not shown]. However, the overall differences in the levels of CbE activity between the PE-R and SS strain have been considerably decreased during the selection period (i.e., from 2.4-fold difference in Dec. 1992 to 1.4-fold difference in Aug. 1995, Fig. 30). This result suggests that other resistance mechanisms, such as nervous system site insensitivity, associated with

permethrin resistance has been more selectively exploited by the selection scheme than the mechanism mediated by the permethrin CbE. This phenomenon may be due to the nature of the permethrin CbE that functions as general sequestration protein for a broad range of hydrophobic insecticides rather than as a specific sequestration protein against permethrin, itself, and due to the selection scheme where only permethrin was used.

D. Immunoassay

The cross-reactivities of the antisera to the three immunogens (i.e., 30-31, 46-48, and 57-60 kDa denatured CbE proteins) indicate that all three proteins must share structural similarities (Fig. 27). Immunochemical characterization has established that the denatured 57-60 kDa protein, which could not be clearly categorized in the previous molecular characterization, is closely related with the permethrin CbE. Also, the immunological relation between the 46-48 kDa protein (i.e., denatured form of p*I* 4.8 CbE) and the 30-31 kDa protein (i.e., denatured form of p*I* 4.5 CbE) suggest that the p*I* 4.8 and 4.5 CbEs are structurally related in spite of the distinct molecular properties.

The initial attempt to develop antigen capture immunoassay was not successful due to the fact that the immunoglobulin generated against the denatured permethrin CbE immunogens could not recognize the native permethrin CbE. Apparently, the denaturation of the permethrin CbE (i.e., pI 4.8, 4.5, and 4.2 CbEs) caused a dramatic change in the native protein conformation so that the epitopic domain of the denatured CbE is not available when the permethrin CbE is in the native conformation.

The antibody capture immunoassay that used denatured hemolymph as the antigen was more accurate and specific in predicting overall permethrin resistance levels of CPB populations than CbE activity assay (Fig. 29). However, subtle differences in the

levels of permethrin CbE among individual hemolymphs could not be distinguished clearly by the antibody capture immunoassay, probably due to excessive handling of hemolymph sample. The procedural step most likely responsible for inter-sample variance appeared to be the denaturation procedure when handling multiple hemolymph samples. High concentration of SDS (i.e., >1%) was required for the complete denaturation of hemolymph and solubilization of denatured hemolymph protein. This level of SDS, however, increased nonspecific signal in the subsequent immunoassay and necessitated the reduction of SDS concentration (i.e., 0.045% final) by dilution following denaturation. The precipitation of protein in some samples at the 0.045% SDS concentration is likely to be one of major causes for the low correlation between the level of the permethrin CbE and the αNC CbE activity in each individual within a strain. If pooled hemolymph sample from several individuals (e.g., 10-20 individual hemolymphs per sample) is used for antibody capture immunoassay instead of the hemolymph from single individual, it would greatly reduce the handling errors. Using this strategy, the antibody capture immunoassay is expected to be an effective and sensitive means to detect the different levels of permethrin CbE in resistant and susceptible CPB populations.

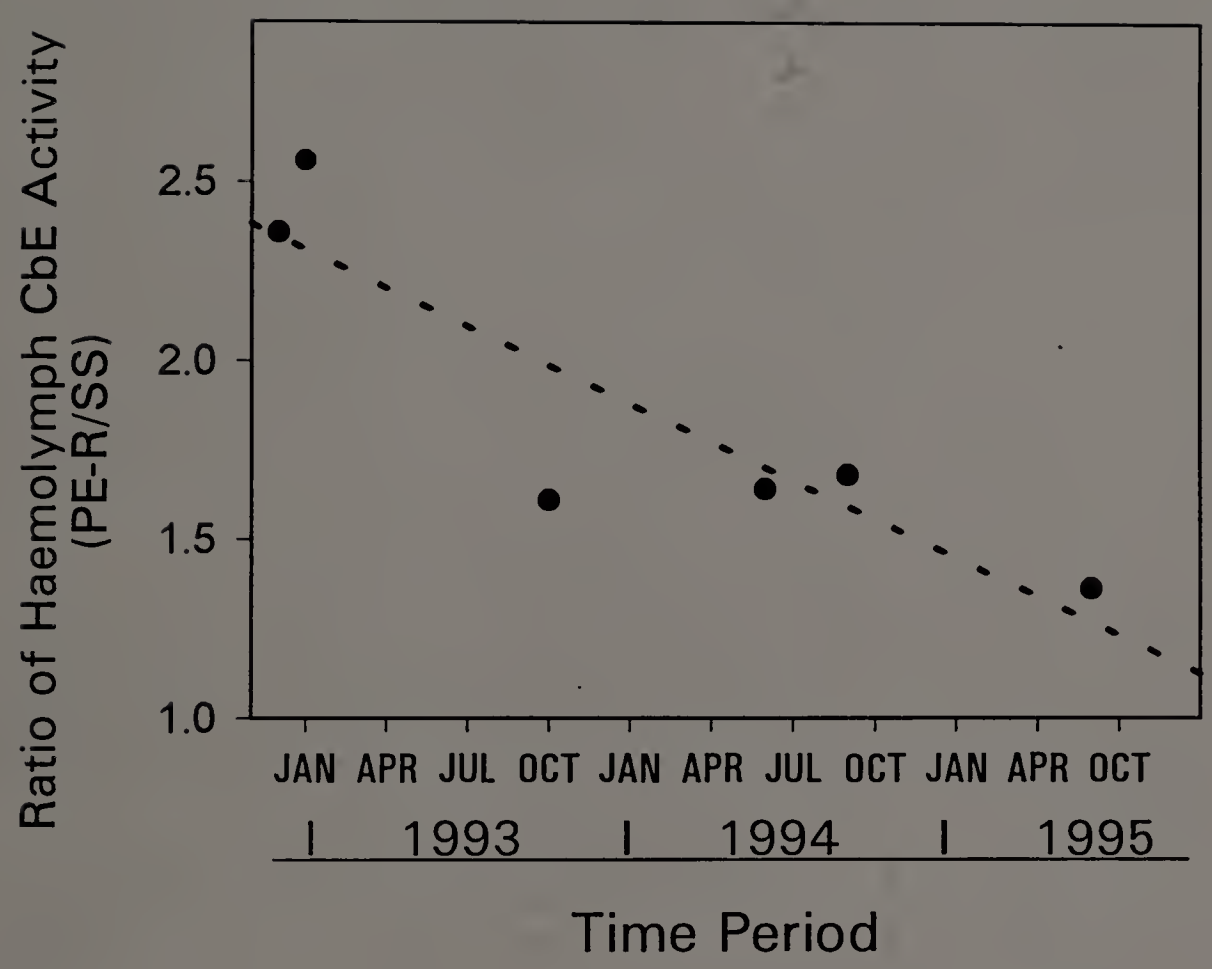

Fig. 30. Change in the relative activity of hemolymph CbEs of the PE-R and SS strains of CPB over 3 years. The data points on Dec. 1992, and Jan. and Oct. 1993 were determined by αNB hydrolysis while other data points were determined by αNC hydrolysis. The dotted line represents the regression line.

APPENDIX A

CHEMICAL STRUCTURE OF NAPHTHYL SUBSTRATES

Common Name	IUPAC Name	Structure
α-Naphthyl acetate	1-Naphthyl acetate	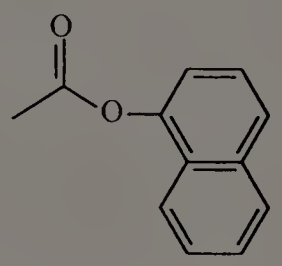
α-Naphthyl butyrate	1-Naphthyl butanoate	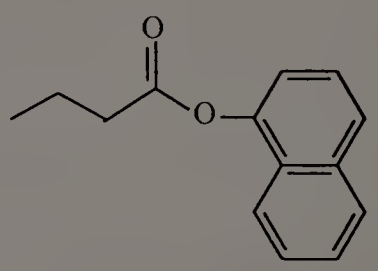
α-Naphthyl caproate	1-Naphthyl hexanoate	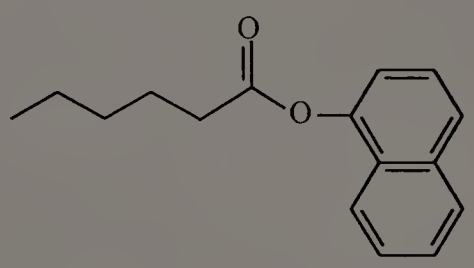
α-Naphthyl caprylate	1-Naphthyl octanoate	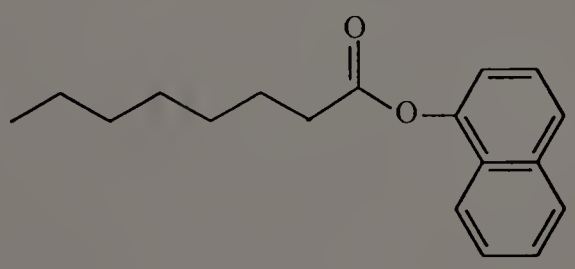

APPENDIX B

CHEMICAL STRUCTURE OF SELECTIVE INHIBITORS

Inhibitors	Structure
ρ-Hydroxymercuribenzoate (PHMB)	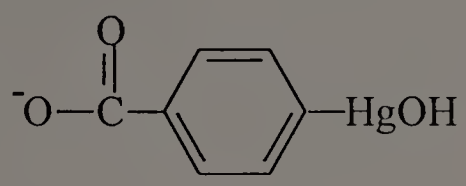
Phenylmethylsulfonyl fluoride (PMSF)	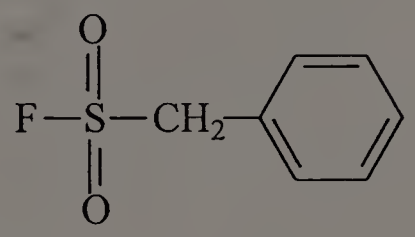

APPENDIX C

CHEMICAL STRUCTURE OF INSECTICIDES AND ESERINE

Compound	Structure
Permethrin	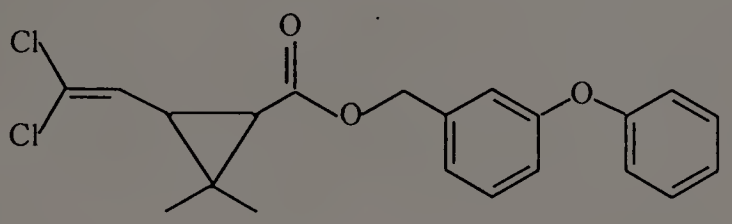
Cypermethrin	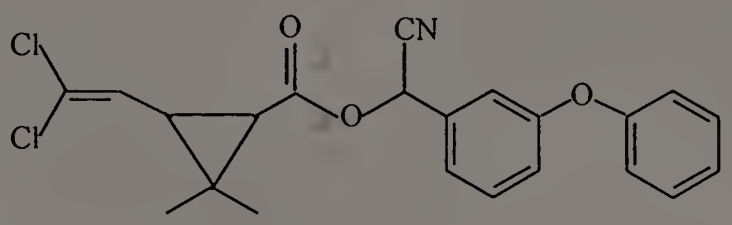
DDT	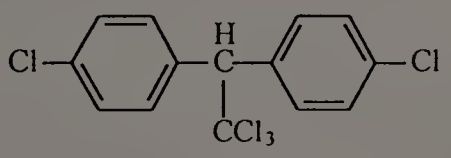
Abamectin	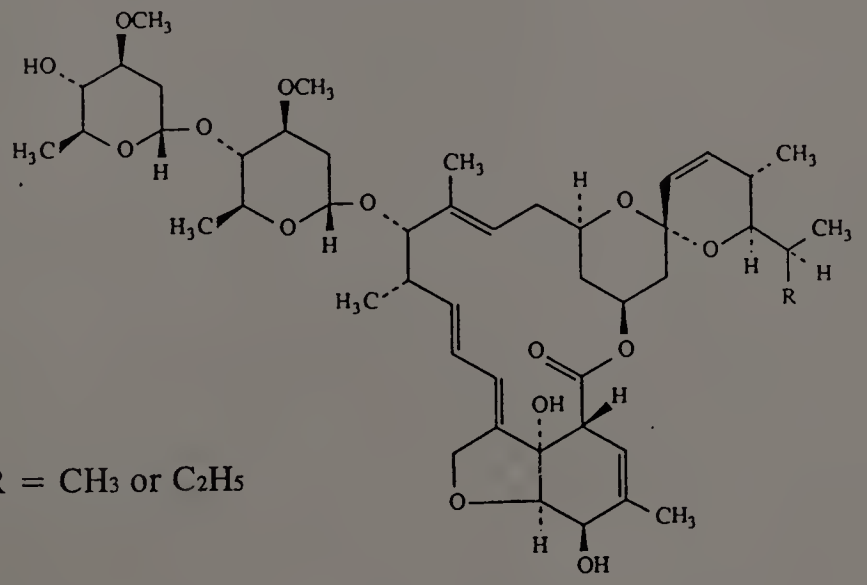
Azinphos-methyl	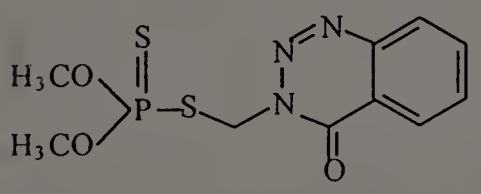
Eserine (Physostigmine)	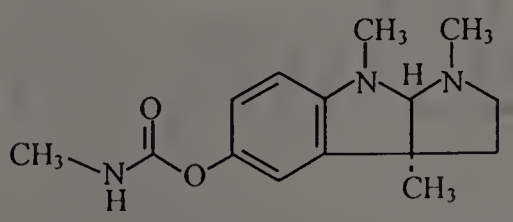

R = CH_3 or C_2H_5

BIBLIOGRAPHY

1. Lashomb J. Potato pest management: a decade of progress, *in* "Advances in Potato Pest Biology and Management" (G. W. Zehnder, M. L. Powelson, R. K. Jansson, and K. V. Raman, Eds.), pp. 3-5, APS Press, St. Paul, MN, 1994.

2. Morrow E. A., E. Grafius, and R. Pax, Potato insect control, 1984, *Insectic. Acaric. Tests* **10**, 138 (1985).

3. Johnston R. L. and L. E. Sandvol, Susceptibility of Idaho populations of Colorado potato beetle to four classes of insecticides, *Am. Potato J.* **63**, 81 (1986).

4. Gauthier N. L., R. N. Hofmaster, and M. Semel, History of Colorado potato beetle control, *in* "Advances in Potato Pest Management" (J. H. Lashomb and H. Casagrande, Eds.), pp. 13-33, Hutchinson Ross, Stroudsburg, 1981.

5. Forgash A. J. Insecticide resistance of the Colorado potato beetle, Leptinotarsa decemlineata (Say), *in* "Advances in Potato Pest Management" (J. H. Lashomb and H. Casagrande, Eds.), pp. 34-46, Hutchinson Ross, Stroudsburg, PA, 1981.

6. Heim D. C., G. G. Kennedy, and J. W. Van Duyn, Survey of insecticide resistance among North Carolina potato beetle (Coleoptera: Chrysomelidae) populations, *J. Econ. Entomol.* **83**, 1229 (1990).

7. Argentine J. A., J. M. Clark, and D. N. Ferro, Genetics and synergism of azinphosmethyl and permethrin resistance in the Colorado potato beetle (Coleoptera: Chrysomelidae), *J. Econ. Entomol.* **82**, 698 (1989).

8. Forgash A. J. History, evolution, and consequences of insecticide resistance, *Pestic. Biochem. Physiol.* **22**, 178 (1985).

9. Argentine J. A. Biochemistry and genetics of insecticide resistance in the Colorado potato beetle, Ph.D. Dissertation, Dept. of Entomol., U. Massachusetts, pp. 113, 1991.

10. Clark J. M. and J. A. Argentine, Biochemical mechanisms of insecticide resistance in the Colorado potato beetle, *in* "Advances in Potato Pest Biology and Management" (G.W. Zehnder, M. L. Powelson, R. K. Jansson, and K. V. Raman, Eds.), pp. 294-308, APS Press, St. Paul, MN, 1994.

11. Argentine J. A. Population genetics of resistance management for the Colorado potato beetle, M. S. Thesis, Dept. of Entomol., U. Massachusetts, pp. 162, 1987.

12. Follett P. A., F. Gould, and G. G. Kennedy, Comparative fitness of three strains of Colorado potato beetle (Coleoptera: Chrysomelidae) in the field: spatial and temporal variation in insecticide selection, *J. Econ. Entomol.* **86**, 1324 (1993).

13. Roush R. T. and J. A. McKenzie, Ecological genetics of insecticide and acaricide resistance, *Annu. Rev. Entomol.* **32**, 361 (1987).

14. Mullin C. A., B. A. Croft, K. Strickler, F. Matsmura, and M. Miller, Detoxification enzyme difference between an herbivorous and predacious mite, *Science* **217**, 1270 (1982).

15. Murdock L. L., G. Brookhart, P. E. Dunn, D. E. Foard, S. Kelly, L. Kitch, R. E. Shade, R. H. Skukle, and J. L. Wolfson, Cysteine digestive proteinase in Coleoptera, *Comp. Biochem. Physiol.* **87**, 783 (1987).

16. Eldefrawi A. T. Acetylcholinesterases and antiacetylcholinesterase, *in* "Comprehensive Insect Biochemistry Physiology and Pharmacology" (G. A. Kerkut and L. I. Gilbert, Eds.), Vol. 12, pp. 115-130, Pergamon Press, New York, NY, 1985.

17. Hammock B. D. Juvenile hormone degradation, *in* "Comprehensive Insect Biochemistry Physiology and Pharmacology" (G. A. Kerkut and L. I. Gilbert, Eds), Vol. 7, pp. 431-472, Pergamon Press, New York, NY, 1985.

18. Yu S. J. Age variation in insecticide susceptibility and detoxification capacity of fall armyworm (Lepidoptera: Noctuidae) larvae, *J. Econ. Entomol.* **76**, 219 (1983).

19. Welling W. and P. Blaakmeer, Metabolism of malathion in a resistant and a susceptible strain of houseflies, in "Proceedings of the 2nd International IUPAC Congress of Pesticide Chemistry (A. S. Tahori Ed.), Vol. II, pp. 61-75, Cordon & Breach, New York, NY, 1971.

20. Needham P. H. and R. M. Sawicki, Diagnosis of resistance to organophosphorus insecticides in *Myzus persicae* Sulz., *Nature* (London) **230**, 125 (1971).

21. Beranek A. P. Stable and non-stable resistance to dimethoate in the peach-potato aphid, (*Myzus persicae*), *Entomol. Exp. Appl.* **17**, 129 (1974).

22. Beranek A. P. and F. J. Oppenoorth, Evidence that the elevated carboxylesterase (esterase 2) in organophosphorus-resistant *Myzus persicae* (Sulz.) is identical with the organophosphate-hydrolyzing enzyme, *Pestic. Biochem. Physiol.* **7**, 16 (1977).

23. Devonshire A. L. The properties of a carboxylesterase from thr peach-potato aphid, *Myzus persicae* (Sulz.), and its role in confering insecticide resistance, *Biochem. J.* **167**, 675 (1977).

24. Hemingway J. The biochemical nature of malathion resistance in *Anopheles stephensi* from Pakistan, *Pestic. Biochem. Physiol.* **17**, 149 (1982).

25. Hemingway J. Malathion carboxylesterase enzymes in *Anopheles arabiensis* from Sudan, *Pestic. Biochem. Physiol.* **23**, 309 (1985).

26. Ziegler R., S. Whyard, A. E. R. Downe, G. R. Wyatt, and V. K. Walker, General esterase, malathion carboxylesterase, and malathion resistance in *Culex tarsalis*, *Pestic. Biochem. Physiol.* **28**, 279 (1987).

27. Ashour M-B. A., L. G. Harshman, and B. D. Hammock, Malathion toxicity and carboxylesterase activity in *Drosophila melanogaster, Pestic. Biochem. Physiol.* **29**, 97 (1987).

28. Konno T., I. Kasai, R. L. Rose, E. Hodgson, and W. C. Dauterman, Purification and characterization of a phosphorotriester hydrolase from methyl parathion-resistant *Heliothis virescens, Pestic. Biochem. Physiol.* **36**, 1 (1990).

29. Whyard S. and V. K. Walker, Characterization of malathion carboxylesterase in the sheep blowfly Lucilia cuprina, *Pestic. Biochem. Physiol.* **50**, 198 (1994).

30. Abdel-Aal Y. A. I. and D. M. Soderlund, Pyretroid-hydrolyzing esterases in southern armyworm larvae: tissue distribution, kinetic properties, and selective inhibition, *Pestic. Biochem. Physiol.* **14**, 282 (1980).

31. Devonshire A. L. and G. D. Moores, A carboxylesterase with broad substrate specificity causes organophosphorous, carbamate and pyrethroid resistance in peach-potato aphids (*Myzus persicae*), *Pestic. Biochem. Physiol.* **18**, 235 (1982).

32. Riskalla M. R. Esterase and resistance to synthetic pyrethroids in the Egyptian cotton leafworm, *Pestic. Biochem. Physiol.* **19**, 184 (1983).

33. de Jersey J., J. Nolan, P. A. Davey, and P. W. Riddles, Seperation and characterization of the pyrethroid-hydrolyzing esterases of the cattle tick, *Boophilus microplus, Pestic. Biochem. Physiol.* **23**, 349 (1985).

34. Chang C. K. and M. E. Whalon, Hydrolysis of permethrin by pyrethroid esterases from resistant and susceptible strains of *Amblyseius fallacis* (Acari: Phytoseiidae), *Pestic. Biochem. Physiol.* **25**, 446 (1986).

35. Delorme R. D., Fournier, J. Chaufaux, A. Cuany, J. M. Bride, D. Auge, and B. Berge, Esterase metabolism and reduced penetration are causes of resistance to deltamethrin in *Spodoptera exigua* Hub (Noctuidea: Lepidoptera), *Pestic. Biochem. Physiol.* **32**, 240 (1988).

36. Brogdon, W. G. and A. M. Barber, Fentrothion-deltamethrin cross-resistance confered by esterases in Guatemalan Anopeles albimanus, *Pestic. Biochem. Physiol.* **37**, 130 (1990).

37. Dowd P. F. and T. C. Sparks, A comparison of properties of *trans*-permethrin hydrolase and leucine aminopeptidase from the midgut of *Pseudoplusia includens* (Walker), *Pestic. Biochem. Physiol.* **31**, 195 (1988).

38. Kao L. R., N. Motoyama, and W. C. Dauterman, The purification and charaterization of esterase from insecticide-resistant and susceptible house flies, *Pestic. Biochem. Physiol.* **23**, 228 (1985).

39. Anber H. A. and F. J. Oppenoorth, A mutant esterases degrading organophosphate in a resistant strain of the predacious mites, *amblyseius pontentillae* (German), *Pestic. Biochem. Physiol*. **33**, 283 (1989).

40. Cuany A., J. Handani, J. Berge, D. Fournier, M. Raymond, G. P. Georghiou, and N. Pasteur, Action of esterase B1 on chlorpyrifos in organophosphate-resistant *Culex* mosquitoes, *Pestic. Biochem. Physiol.* **45**, 1 (1993).

41. Fournier D., J.-M. Bride, C. Mouches, M. Raymond, M. Magnin, J.-B. Berge, N. Pasteur, and G. P. Georghiou, Biochemical characterization of the esterases A1 and B1 associated with organophosphate resistance in the *Culex pipiens* L. complex, *Pestic. Biochem. Physiol.* **27**, 211 (1987).

42. Field L. M., A. L. Devonshire, and B. G. Forde, Molecular evidence that insecticide resistance in peach-potato aphids (*Myzus persicae* Sulz.) results from amplification of an eaterase gene, *Biochem. J*. **251**, 309 (1988).

43. Mouches C., N. Pasteur, J. B. Berge, O. Hyrien, M. Raymond, B. R. de Saint Vincent, M. de Silvestri, and G. P. Georghiou, Amplification of an esterase gene is responsible for insecticide resistance in a Califonia *Culex* mosquito, *Science* **233**, 778 (1986).

44. Raymond M., V. Beyssat-Arnaouty, N. Sivasubramanian, C. Mouches, G. P. Georghiou, and N. Pasteur, Diversity of the amplification of various esterase B responsible for organophosphate resistance in *Culex* mosquitoes, *Biochem. Genet*. **27**, 417 (1989).

45. Field L. M., A. L. Devonshire, and B. G. Forde, The combined use of immunoassay and DNA diagnostic technique to identify insecticide-resistant genotypes in the peach-potato aphids, *Myzus persicae* (Sulz.), *Pestic. Biochem. Physiol.* **34**, 174 (1989).

46. Leeper J. R., R. T. Roush, and H. T. Reynolds, Preventing or managing resistance in arthropods, *in* "Pesticide Resistance: Strategies and Tatics for Management" (National Research Council, Ed.), pp 335-346, National Academy Press, Washington DC, 1986.

47. Devonshire A. L., G. D. Moores, and R. H. Ffrench-Constant, Detection of insecticide resistance by immunological estimation of carboxylesterase activity in *Myzus persicae* (sulzer) and cross reaction of the antiserum with *Phorodon humuli* (Schrank)(Hemiptera: Aphididae), *Bull. Entomol. Res.* **76**, 97 (1986).

48. Ffrench-Constant R. H. and A. L. Devonshire, Monitoring Frequencies of insecticide resistance in *Myzus persicae* Sulzer (Hemiptera: Aphididae) in England during 1985-86 by immunoassay, *Bull. Entomol. Res.* **78**, 163 (1988).

49. Argentine J. A., J. M. Clark, and D. N. Ferro, Relative fitness of insecticide-resistant Colorado potato beetle strains (Coleoptera: Chrysomelidae), *Environ. Entomol.* **18**, 705 (1989).

50. Fleuriet A. Influence of the population size on the frequency of flies infected by sigma virus in populations of *Drosophila mlanogaster*. *J. Invert. Pathol.* **42**, 177 (1983).

51. Mouches C., Y. Pauplin, M. Agarwal, L. Lemieux, M.Herzog, M.Abadon, V. Beyssat-Arnaouty, O. Hyrien, B. R. de Saint Vincent, G. P. Georghiou, and N. Pasteur, Characterization of amplification core and esterase B1 gene responsible for insecticide resistance in *Culex*. *Proc. Natl. Acad. Sci.* **87**, 2574 (1990).

52. Field L. M., M. S. Williamson, G. D. Moores, and A. L. Devonshire, Cloning and analysis of the esterase genes conferring insecticide resistance in the peach-potato aphid, *Myzus persicae* (Sulzer), *Biochem. J.* **294**, 569 (1993).

53. van Asperen K. A study of house fly esterase by means of a sensitive colorimetric method, *J. Insect Physiol.* **8**, 401 (1962).

54. Smith P. K., R. I. Krohn, G. T. Hermanson, A. K. Mallia, F. H. Gartner, M. D. Provenzano, E. K. Fujimoto, N. M. Goeke, B. J. Olson, and D. C. Klenk, Measurement of protein using bicinchoninic acid, *Anal. Biochem.* **150**, 76 (1985).

55. O'Farrell P. H. High resolution two-dimensional electrophoresis of proteins, *J. Biol. Chem.* **250**, 4007 (1975).

56. Switzer R. C., C. R. Merril, and S. Shifrin, A highly sensitive silver stain for detecting proteins and peptides in polyacrylamide gels, *Anal. Biochem.* **98**, 231 (1979).

57. Lacks S. A. and S. S. Springhorn, Renaturation of enzymes after polyacrylamide gel electrophoresis in the presence of sodium dodecyl sulfate, *J. Biol. Chem.* **255**, 7467 (1980).

58. Lee C. A., A. Levin, and D. Branton, copper staining: a five-minute protein stain for sodium dodecyl sulfate-polyacrylamide gels, *Anal. Biochem.* **166**, 308 (1987).

59. Harlow E. and D. Lane, Antibodies, a Laboratory Mannual, pp 726, Cold Spring Harbor Laboratories, New York, NY, 1988.

60. Argentine J. A., S. H. Lee, M. A. Sos, S. R. Barry, and J. M. Clark, Permethrin resistance in a near isogenic strain of Colorado potato beetle, *Pestic. Biochem. Physiol.* **53**, 97 (1995).

61. Ecobichon D. J. Carboxylesterase isozymes in the rabbit liver: physicochemical properties *in* "Isozyme, I Molecular Structure" (C. L. Markert, Ed.), pp. 389-402, Academic Press, New York, 1975.

62. Scott K. and B. Zerner, Carboxylesterases from chicken, sheep, and horse liver, *Methods Enzymol.* **35**, 208 (1975).

63. Dowd P. K. and T. C. Sparks, Inhibition of *trans*-permethrin hydrolysis in Pseudoplusia includens (Walker) and use of inhibitors as pyrethroid synergists, *Pestic. Biochem. Physiol.* **27**, 237 (1987).

64. Aldridge W. N. and E. Reiner, "Enzyme Inhibitors as Substrates. Interaction of Esterases with Esters of Organophosphorus and Carbamic Acids", North-Holland, Amsterdam, 1972.

65. Boehringer Mannheim, Protease Inhibitor Technical Guide, 1156 144, 1995.

66. Pharmacia LKB Biotechnology, "Affinity Chromatography: Principles and Methods", Uppsala, Sweden, 1988.

67. Rademacher T. W., R. B. Parekh, and R. A. Dwek, Glycobiology, *Ann. Rev. Biochem.* **57**, 785 (1988).

68. Callaghan A., C. A. Malcolm, and J. Hemingway, Biochemical studies of A and B carboxylesterases from organophosphate resistant strains of an Italian *Culex pipiens* (Diptera: Culicidae), *Pestic. Biochem. Physiol.* **41**, 198 (1991).

69. Riddles P. W., P. A. Davey, and J. Nolan, Carboxylesterases from *Boophilus microplus* hydrolyze *trans*-permethrin, *Pestic. Biochem. Physiol.* **20**, 133 (1983).

70. Dubik D. and R. P. C. Shiu, Transcriptional regulation of c-*myc* oncogene expression by estrogen in hormone-responsive human breast cancer cell, *J. Biol. Chem.* **263**, 12705 (1988).

71. Liu T.-J., B. J. Levine, A. I. Skoultchi, and W. F. Marzluff, The efficiency of 3'-end formation contributes to the relative levels of different histone mRNA, *Mol. Cell. Biol.* **9**, 3499 (1989).

72. Maniatis T. Mechanisms of alternative pre-mRNA splicing, *Science* **251**, 33 (1991).

73. Yu S. J. Liquid chromatographic determination of permethrin eaterase activity in six phytophagous and entomophagous insects, *Pestic. Biochem. Physiol.* **36**, 237 (1990).

74. Vallner J. J. Binding of drugs by albumin and plasma protein, *J. Pharm. Sci.* **66**, 447 (1977).

75. Devonshire A. L. and G. D. Moores, Detoxification of insecticides by esterases from Myzus persicae-is hydrolysis important? *in* "Enzymes Hydrolysing Organophosphorus Compounds" (E. Reiner, W. N. Aldridge, and F. C. G. Hoskin, Eds.), pp.180-192, Wiley, Chichester, England, 1989.

76. Chen W.-L. and C.-M. Sun, Purification and characterization of carboxylesterases of a rice brown planthopper, *Nilaparvata lugens* Stal, *Insect Biochem. Molec.Biol.* **24**, 347 (1994).

77. Tsujita T., T. Miyada, and H. Okuda, Purification of rat kidney carboxylesterase and its comparison with other tissue esterases, *J. Biochem.* **103**, 327 (1988).

78. Otto J., A. Ronai, and O. Von Deimling, Purification and characterization of esterase 1F, the albumin esterase of the house mouse (*Mus musculus*), *Eur. J. Biochem.* **116**, 285 (1981).

79. Karunaratne S. H. P. P., K. G. I. Jayawardena, J. Hemingway, and A. J. Ketterman, Charaterization of a B-type esterase involved in insecticide resistance from mosquito *Culex quinquefasciatus*, *Biochem. J.* **294**, 575 (1993).

80. Sakata K. and T. Miyata, Biochemical charaterization of carboxylesterase in the small brown planthopper Laodelphax striatellus (Fallen), *Pestic. Biochem. Physiol.* **50**, 247 (1994).

81. van Lith H. A., M. Haller, I, J. M. van Hoof, M. J. A. van Der Wouw, B. F. M. van Zutphen, and A. C. Beynen, Characterization of rat plasma esterase ES-1A concerning its molecular and catalytic properties, *Arch. Biochem. Biophys*. **301**, 265 (1993).

82. de Malkenson N. C., E. J. Wood, and E. N. Zebra, Isolation and chracterization of an esrerase of *Triatoma infestans* with a critical role in the degradation of organophosphorus esters, *Insect Biochem*. **14**, 481 (1984).

83. Persson B., G. Bengtsson-Olivecrona, S. Enerback, T. Olivecrona, and H. Jornvall, Structural features of lipoprotein lipase: lipase family relationship, binding interaction, non-equivalence of lipase cofactors, vitellogenin similarities and functional subdivision of lipoprotein lipase, *Eur. J. Biochem*. **179**, 39 (1989).

84. Brady L., A. M. Brzozowski, Z. S. Derewenda, E. Dodson, G. Dodson, S. Tolly, J. P. Turkenburg, L. Christiansen, B. Huge-jensen, L. Norskov, L. Thim, and U. Menge, A serine protease triad forms the catalytic centre of a triacylglycerol lipase, *Nature* (London) **343**, 767 (1990).

85. Winkler F. K., A. D'Arcy, and W. Hunziker, Structure of human pancreatic lipase, *Nature* (London) **343**, 771 (1990).

86. Blow D. Lipases reach the surface, *Nature* (London) **351**, 444 (1991).

87. Choudhury S. R. Isolation and properties of an esterase isoenzyme of rat serum, *Histochem. J*. **6**, 369 (1974).

88. Kramer S. J. and C. A. D. de Kort, Some properties of haemolymph esterases from *Leptinotarsa decemlineata* Say, *Life Sciences* **19**, 211 (1976).

89. Ketterman A. J., K. G. I. Jayawardena, and J. Hemingway, Purification and charaterization of a carboxylesterase involved in insecticide resistance from the mosquito *Culex quinquefasciatus, Biochem. J*. **287**, 355 (1992).

90. Holmes R. S. and C. J. Masters, The developmental multiplicity and isozyme status of cavian esterases, *Biochim. Biophys. Acta* **132**, 379 (1967).

91. Jarv J. and M. Speek, Reversible inhibition of butyrylcholinesterase with aromatic hydrocarbons, *Biochim. Biophys. Acta*, **706**, 174 (1982).

92. Skalsky H. L. and F. E. Guthrie, Affinities of parathion, DDT, dieldrin, and carbaryl for macromolecules in the blood of the rat and American cockroach and the competitive interaction of steroids, *Pestic. Biochem. Physiol.* **7**, 289 (1977).

93. Hare J. D. Ecology and management of the Colorado potato beetle, *Annu. Rev. Entomol.* **35**, 81 (1990).

94. Zhu K. Y. and W. A. Brindley, Properties of esterases from *Lygus hesperus* Kinght (Hemiptera: Miridae) and the role of the esterase in insecticide resistance, *J. Econ. Entomol.* **83**, 90 (1990).

95. Hipps P. P. and D. R. Nelson, Esterases from the midgut and gastric caecum of the American cockroack, *Perplaneata americana* (L), isolation and characterization, *Biochim. Biophys. Acta* **341**, 421 (1974).

96. Kapin M. A. and S. Ahmad, Esterases in laval tissues of gypsy moth, *Lymantria dispar* (L): optimum assay conditions, quantitification and characterization, *Insect Bichem.* **10**, 331 (1980).

97. Hong K. H., W. H. Jang, K. D. Choi, and O. J. Yoo, Characterization of *Pseudomonas fluorescens* carboxylesterase: cloning and expression of the esterase gene in *Escherichia coli*, *Agric. Biol. Chem.* **55**, 2839 (1991).

98. Pasteur N., A. Iseki, and G. P. Georghiou, Genetic and biochemical studies of the highly active esterase A' and B associated with organophosphate resistance in mosquitoes of the *Culex pipiens* complex, *Biochem. Genet.* **19**, 909 (1981).

99. Raymond M., A. Callaghan, P. Fort, and N. Pasteur, Worldwide migration of amplified insecticide resistant genes in mosquitoes, *Nature* (London) **350**, 151 (1991).

100. Chang C. K. and M. E. Whalon, Substrate specificities and multiple forms of esterases in the brown planthopper, *Nilaparvata lugens* (Stal), *Pestic. Biochem. Physiol.* **27**, 30 (1987).

101. Mentlein R., A. Ronai, M. Robbi, E. Heymann, and O. V. Deimling, Genetic identification of rat liver carboxylesterases isolated in different laboratories, *Biochimica et Biophysica Acta*, **913**, 27 (1987).

102. Thompson H. M., M. I. Mackness, C. H. Walker, and A. R. Hardy, Species differences in avian serum B esterases revealed by chromatofocusing and possible relationships of esterase activity to pesticide toxicity, *Biochem. Pharmacol.* **41**, 1235 (1991).

103. Devonshire A. L., L. M. Searle, and G. D. Moores, Quantitative and qualitative variation in the mRNA for carboxylesterases in insecticide-susceptible and resistant *Myzus persicae* (Sulz), *Insect Biochem.* **16**, 659 (1986).

104. Picard B., P. Goullet, and R. Krishnamoorthy, A novel approach to study of the structural basis of enzyme polymorphism; Analysis of carboxylesterase B of *Escherichia coli* as model, *Biochem. J.* **241**, 877 (1987).

105. Wold F. In vivo chemical modification of protein (Post-translational modification), *Ann. Rev. Biochem.* **50**, 787 (1981).

106. Huttner W. B., Protein tyrosine sulfation, *TIBS* **12**, 361 (1987).

107. Heymann E. Hydrolysis of carboxylic esters and amides, *in* "Metabolic Basis of Detoxification. Metabolism of Functional Groups" (W. B. Jakoby, J. R. Bend, and J. Caldwell, Eds.), pp. 229-245, Academic Press, New York, 1982.